A

Averaging and Bounding of Anisotropic Elastic Constants

By

Guoyu Yang

A dissertation submitted to the Graduate Faculty in Engineering in fulfillment of the requirements for the degree of Doctor of Philosophy, The City University of New York.

1999

UMI Number: 9917717

UMI
300 North Zeeb Road
Ann Arbor, MI 48103

This manuscript has been read and accepted for the Graduate Faculty in Engineering in satisfaction of the dissertation requirement for the degree of Doctor of Philosophy.

12/29/98 — S C Cowin

Date — Chair of Examining Committee

12/30/1998 — Mumtaz K. Kassir

Date — Executive Officer

Prof. Stephen C. Cowin

Prof. Feridun Delale

Prof. Susannah Fritton

Prof. Edward Guo

Prof. Ali M. Sadegh

Supervisory Committee

THE CITY UNIVERSITY OF NEW YORK

Abstract

Averaging and bounding of anisotropic elastic constants

By

Guoyu Yang

Adviser: Stephen C. Cowin

Many materials are anisotropic and inhomogeneous due to the varying composition of their constituents. The analysis of the elastic constant measurements for these materials is difficult because the problem of the identification of the type of elastic symmetry is complicated by the varying composition of the material and vice versa. These two factors are intertwined and each complicates the other. A solution to this problem in which these two aspects are separated and analyzed independently is presented here.

This solution is illustrated here by application to human cancellous bone, hardwoods and softwoods. The solid volume fraction (or apparent density) is the compositional variable for the elastic constants of these natural materials. The solid volume fraction-dependent anisotropic Hooke's law for cancellous bone and a density-dependent one for hardwoods and softwoods are established. The analysis leading to this form of Hooke's law shows that human cancellous bone has orthotropic elastic symmetry at the 95% confidence level and it provides expressions for all elastic constants as functions of the bone solid volume fraction (or apparent density) and orientation only; no measures of trabecular structural architecture are involved. The squared correlation coefficients between

model and data are in a range that is about one-third higher than those obtained with previous models based upon volume fraction only, and are approximately the same or higher than those obtained with models involving volume fraction plus the measures of architecture.

The identification of the best elastic symmetry representation for these natural materials is accomplished by measuring the closeness of two symmetries. Bounds on the effective elastic constants of a material with any anisotropic elastic symmetry in terms of lower symmetry elastic coefficients are constructed to measure the closeness. An interesting result obtained from the applications of this bounding method shows that cancellous bone, generally considered to have orthotropic symmetry, may be considered to have transversely isotropic symmetry with a small error. A similar conclusion applies for hardwoods and softwoods. It is also shown that human cancellous bone has lesser degrees of anisotropy than hardwoods and softwoods.

Acknowledgements

I greatly appreciate the generous support of my mentor, Prof. Stephen C. Cowin. I learned a great deal from him in doing this dissertation research under his guidance.

I am also grateful to Prof. Fritton who answered my questions and gave me many good suggestions. Thanks!

Ms. Liyun Wang, Mr. Tomi Beno, and Mr. Yoon helped me a great deal through discussions and suggestions.

The staff in the Department of Mechanical Engineering and the Center for Biomedical Engineering (Carol Bamberger) are always helpful. To them I am sincerely grateful.

My thanks also go to Prof. Delale, Prof. Guo and Prof. Sadegh for taking time to be members of my examination committee.

Contents

Lists of Tables

Lists of Figures

I. Introduction

Many materials are anisotropic and inhomogeneous due to the varying composition of their constituents. The analysis of the elastic constant measurements for these materials is difficult because the problem of the identification of the type of elastic symmetry is complicated by the varying composition of the material. A solution to this problem in which these two aspects are separated and analyzed independently is presented in this dissertation. This solution is illustrated here by application to an extraordinary data base of cancellous bone elastic constants and woods. The solid volume fraction (or apparent density) is the compositional variable for the elastic constants of these natural materials.

As a primary structural element of the human body, bone supports the gravitational load on the body and allows skeletal motions necessary for survival. The ability of a bone element to carry loads and transmit stress depends on the mechanical properties of its material. Bone tissue consists of two distinct structural types, cortical and cancellous bone. The material properties of cortical bone tissue are determined by the organization and arrangement of its components, including mineral crystallite, collagen fibers, blood vessels, lamellae and Haversian systems (Katz, 1984). Cancellous (or trabecular) bone is the spongy, open celled and porous material consisting of an interconnected lattice of bony plates and columns. Variability in pore size contributes to the differences in volume fraction, and variability in pore shape and orientation contribute to the differences in structural anisotropy. The main objective of this dissertation is to study the mechanical properties of human cancellous bone.

During the lifetime of a human being, there are gradual changes in bone structure and bone mass after the age of 30, especially for women. This condition of bone loss, combined with deteriorated bone structure, called osteoporosis, results in over a million fractures in the US alone annually (Phillips *et al.*, 1988). With osteoporosis, it is widely agreed that there are reductions in trabecular apparent density, average trabecular width and connectivity and these are associated with major reductions in modulus and strength (Carter and Hayes, 1976 and 1977; Gibson, 1985; Rice *et al.*, 1988).

It has long been known that bone adapts its structure in response to loading (Wolff, 1892; Currey, 1984), although the mechanism is not yet completely understood. When an implant is placed in bone, there are significant changes in the local mechanical properties of cancellous bone. Since most of the bone replaced by an implant is cancellous, an improved understanding of the parameter-property relationship for cancellous bone helps the design of artificial bone with properties close to the bone it replaces.

The precise relationships between mechanical properties and morphological parameters of cancellous bone are in the process of being developed. In most of the early studies, the only parameter used to determine the mechanical properties of cancellous bone was apparent density. Lumping bovine and human data for both cancellous and cortical bone together, Carter and Hayes (1976) proposed a relationship in which the effective isotropic Young's modulus was proportional to the cube of volume fraction. Rice *et al.* (1988) showed that there was species dependence in the data on the relationship between the Young's modulus and volume fraction and, more importantly, the inclusion of the data on cortical bone was the source of the cubic dependence. When the data for cortical bone were removed, the dependence of the Young's modulus of cancellous bone was upon the square of the volume fraction. Recent work has assumed a dependence of the anisotropic elastic constants upon the square of the volume fraction as well as measures of the local architecture of the cancellous bone (Turner *et al.*, 1990; van Rietbergen *et al.*, 1996,1997). The architecture (or fabric) measurements (Harrigan and Mann, 1984; Whitehouse, 1974) have been considered as a method to approach the anisotropic properties of cancellous bone. Mean intercept length (MIL) is commonly used to measure the fabric tensor, based on the number of bone-marrow intersection measures in a linear grid of parallel lines, as a function of the grid orientation (Whitehouse, 1974; Harrigan and Mann, 1984; Odgaard *et al.*, 1996). A mathematical model, which relates the anisotropic mechanical properties to volume fraction and fabric tensor was proposed by Cowin (1985). The model implies a polynomial relationship between the compliance tensor on the one hand and a fabric tensor and nine functions of volume fraction on the other.

The mechanical properties of an anisotropic material, such as cancellous bone and wood, are reflected in the anisotropic elastic constant matrices. In chapter two a new method of averaging the data on the anisotropic elastic constants of a material is first presented. The anisotropic elastic constants are represented by the elasticity tensor which is expressed as a second rank tensor in a space of six dimensions. The method consists of averaging eigenbases of different measurements of the elasticity tensor, then averaging the eigenvalues referred to the average eigenbasis. The eigenvalues and eigenvectors are obtained by using a representation of the stress-strain relations due, in principle, to Thomson (1856,1878). The formulas for the representation of the averaged elasticity tensor are simple and concise. The applications of these formulas are illustrated using previously reported data, and contrasted with the traditional analysis of the same data by Hearmon (1952). An interesting result that emerges from this analysis is a method dealing with variable composition anisotropic elastic materials whose elastic constants depend upon the particular composition. In the case of porous isotropic materials, for example, it is customary to regress the Young's modulus against porosity. The result of this chapter suggests a structure or paradigm for extending to anisotropic materials this empirical method of regressing elastic constant data against composition or porosity. That result is extended here to three natural materials, cancellous bone, hardwoods and softwoods. Solid volume fraction (or apparent density) is the compositional variable for the elastic constants of these materials. The solid volume fraction-dependent anisotropic Hooke's law for cancellous bone and a density-dependent one for hardwoods and softwoods are obtained in chapter three. The method of analysis in chapter three also identifies the type of elastic symmetry possessed by the material. No assumption as to the type of elastic symmetry is made. The type of symmetry is identified from the character of the eigenvectors that are calculated. For example, the analysis shows that human cancellous bone has orthotropic symmetry at the 95% confidence level. However the database we employ for wood incorporated the assumption of orthotropic material symmetry so this feature is not illustrated by the analysis of wood data.

In chapter four the implications of a new, anisotropic, volume fraction-dependent form of Hooke's law for human cancellous bone are explored. The law provides expressions for all the orthotropic elastic constants as functions of bone solid volume fraction (or apparent density) only.This form of Hooke's law is obtained from the analysis of a database consisting of 141 human cancellous bone specimens. This data base, reported by van Rietbergen *et al.* (1996 and 1998) and Kabel *et al.* (1997a), is superior to previous data bases because the authors provide the entire set of anisotropic elastic constants without an *a priori* assumption of a particular material symmetry and without an assumption of the direction in which the maximum Young's modulus occurs. This data base is unique in many different ways, the most important of which is the large number of specimens and its method of construction, but particularly because it is not based entirely on measurements of real specimens. The data base of elastic constants of 141 human cancellous bone specimens employed here was constructed by imaging real specimens, then computationally determining their elastic constants. We believe that this cyberspace method of construction is more accurate than the conventional mechanical testing procedures for evaluating the elastic constants of human cancellous bone. The determination of the elastic constants of cancellous bone by conventional mechanical test procedures is very difficult.

The basic problem is that, due to the size of the human body, it is difficult to obtain specimens of cancellous bone that are more than a 5mm cube. The logical way to test small cubes such as these is compression testing. However compression testing is highly inaccurate for cancellous bone because of (1) the frictional end effects of the platens, (2) it is almost impossible to identify, *a priori*, the grain directions in a bone specimen and it is therefore almost impossible to cut a specimen in the grain directions, (3) the stiffening effect of the platens on the bone near the platens and (4) the unpredictable inhomogeneity of the specimen. These and other difficulties in the mechanical testing of cancellous bone are described in Keaveny (1997).

The construction of the data base of elastic constants of 141 human cancellous bone specimens employed here was a breakthrough because it provided a relatively inexpensive method of determining the full set of anisotropic elastic constants for a small specimen of cancellous bone by a combination of imaging the specimen (Odgaard *et al.*, 1997; Kabel *et al.*, 1999a) and subsequent evaluation of the effective elastic constants using computational techniques based on the finite element method (van Rietbergen *et al.*, 1996, 1998; Hollister et al.,1991). This method makes no assumption concerning the type of elastic symmetry characterizing the material. In this method the actual matrix material of the trabeculae comprising the bone specimen is assumed to have a axial Young's modulus E_t. The tissue modulus E_t is a scale factor that magnifies or reduces all the elastic constants. The inverse of the tissue modulus $1/ E_t$ multiplies each component in the elastic compliance matrix. The value of E_t

may be fixed from a knowledge of the axial Young's modulus E_t itself. The elastic constant results are presented here as multiples of E_t. For purposes of numerical calculation E_t was taken to be 1 GPa (van Rietbergen *et al.*, 1996, 1998; Odgaard *et al.*, 1997).

Once the image of the specimen was in the computer and a finite element mesh was generated, a sequence of loadings were applied to the specimen and the responses determined. The loadings were sufficient in number to determine all 21 elastic constants. Thus no material symmetry assumptions were made in the determination of the constants. Quantitative stereological programs were used to determine the solid volume fraction ϕ of each specimen. These are the data employed in the analysis reported here.

The squared correlation coefficients (R^2) between model and data are in a range that is about one-third higher than those obtained with previous models based upon volume fraction only. In fact, the squared correlation coefficients (R^2) are approximately the same or higher than those obtained with models involving volume fraction plus quantitative stereological measures of architecture. Since architecture measures require either invasive techniques or very expensive non-invasive techniques, this model provides the basis for the development of a superior cancellous bone stress analysis and superior non-invasive inexpensive clinical quantification of cancellous bone fracture risk for osteoporosis. This latter end might be accomplished by employing the new representation of Hooke's law for evaluation of local cancellous bone stiffness and strength from a knowledge of the local volume fraction of bone (determined for example, by DXA) and a knowledge of the trabecular grain of the local bone structure.

In chapters five and six the best elastic symmetry representations for natural materials, such as human cancellous bone and woods, are accomplished by measuring the closeness between the symmetry of a material and any higher symmetry.

Hill (1952, 1963) showed that it was possible to construct bounds on the effective isotropic elastic coefficients of a material with triclinic or greater symmetry. In Hill (1952) the material with triclinic or greater symmetry is a polycrystalline material and in Hill (1963) it is a composite material. Hill noted that the triclinic symmetry coefficients appearing in the bounds could be specialized to those of greater symmetry, yielding the effective isotropic elastic coefficients for a material with any elastic symmetry. We show in chapter four that it is possible to construct bounds on the effective elastic constants of a material with any anisotropic elastic symmetry in terms of higher or equal anisotropic elastic symmetry. These results are obtained by combining the approach of Hill (1952, 1963) with a representation of the stress-strain relations due, in principle, to Kelvin (1856, 1878), as well as extensions of the uniform strain and uniform stress bounds of Voigt (1928) and Reuss (1929) from the isotropic case to the case of the crystalline symmetries characterized by finite symmetry groups. In this chapter specific bounds are given for the effective elastic coefficients of cubic, hexagonal, tetragonal and trigonal symmetries in terms of the elastic coefficients of triclinic symmetry (or any higher symmetry). By using these results we can determine the effective symmetry of natural materials.

One application of the results described in chapter five is to determine the best elastic symmetry representation for non-crystalline or textured anisotropic materials, such as cancellous bone and woods. Given the values of the components of a fourth rank elasticity tensor of a material relative to a known, but arbitrary, coordinate system, Cowin and Mehrabadi (1987) showed how to determine the elastic symmetry using the techniques of linear algebra. However, this method is not robust with respect to the input values of the components of a fourth rank elasticity tensor; slight errors in the data could cause a misidentification of the symmetry. The method only works well when the data were exact. For example, cubic symmetry is characterized by three distinct elastic constants, say c_{11}-c_{12} and c_{44}; however if $2c_{44}=c_{11}+c_{12}$, the material is isotropic. Thus if the data for an isotropic material have a value of $2c_{44}$ given by $2c_{44}=c_{11}+c_{12}+$ a small error term, the material will be mistakenly identified as cubic.

For human and whale cancellous bone, hardwoods and softwoods, the effective isotropic and transversely isotropic elastic constants are determined from orthotropic symmetry data in chapter six. For the effective Voigt and Reuss isotropic bounds on the eigenvalues or bulk and shear moduli of human and whale cancellous bones, the biggest percentages in differences are 27% for human cancellous bone and 9.6% for whale cancellous bone. The Voigt and Reuss isotropic bounds on the elastic constants of hardwoods and softwoods are much larger, 115% for hardwoods and 150% for softwoods. These results show that human and whale cancellous bone has lesser degrees of anisotropy than hardwoods and softwoods because the differences of Voigt and Reuss bounds for human cancellous bone are much smaller than those for hardwoods and softwoods. The differences of Voigt and Reuss transversely isotropic bounds on eigenvalues for these three materials are much smaller than those for isotropic bounds: 8% for human cancellous bone, and 20% for hardwoods and softwoods. The results show that human and whale cancellous bone, although generally considered to be orthotropic, is in fact very close to transversely isotropic in their material symmetry. A similar conclusion applies for hardwoods and softwoods.

Chapter seven contains a summary of results.

II. Averaging anisotropic elastic constant data

II – 1. Introduction

A method of averaging the data on the anisotropic elastic constants of a material is presented in this chapter. The method is based on the idea of averaging the eigenbases of different measurements of the elasticity tensor, then averaging the eigenvalues referred to the average eigenbases. The elasticity tensor may be expressed either as a fourth rank tensor, with components C_{ijkm}, in a space of three dimensions or as a second rank tensor, with components $\hat{c}_{km}$, in a space of six dimensions. The averaging processes are applied here to the six eigenvalues of the matrix $\hat{\mathbf{c}}$ and to the eigenbases of $\hat{\mathbf{c}}$; or, equivalently, to the inverse of $\hat{\mathbf{c}}$, the compliance tensor $\hat{\mathbf{s}}$. This averaging process is, basically, an averaging process for the simultaneous invariants of $\hat{\mathbf{c}}$ and $\hat{\mathbf{s}}$.

The second rank tensor $\hat{\mathbf{c}}$ in the six dimensions whose components are $\hat{c}_{km}$ appears in a representation of the stress-strain relations due, in principle, to Kelvin (1856, 1878), but expressed by Rychlewski (1984) and Mehrabadi and Cowin (1990) in contemporary linear algebra notation. In the next section the Kelvin formulation of the generalized Hooke's law is summarized.

The method proposed here for the averaging of elastic constant data treats the individual measurement as a measurement of a tensor instead of as a collection of individual elastic constants or matrix element measurements, recognizing that the measurements by different authors will reflect the systematic invariant tensorial properties of a material, like eigenmodes and eigenvalues. This proposed method for averaging different measurements of the anisotropic elastic constants for a special material has advantages over the traditional method of averaging the individual matrix components of the elasticity or compliance matrices. Averaging invariants removes the effect of the reference coordinate system in the measurements (Wu *et al.*, 1973), while the traditional method of averaging the components may induce errors due to the various reference coordinate systems and may distort the nature of the symmetry. Our averaging process explicitly retains the orthonormality of the eigenbases. In application of the method we have employed statistical methods to exclude some measurements from a measurement set by establishing confidence intervals.

Over a period of several decades R.F.S. Hearmon constructed an extensive data base of the anistropic elastic coefficients of many materials. Significant parts of the data base are Hearmon (1946, 1948 and 1961); the most encompassing and inclusive summary of these data by Hearmon appears in the reference work 'Zahlenwerte und Funktionen aus Naturwissenchaften und Technik', edited by Landolt and Bornstein (1979). We have selected the data in the brief work of Hearmon (1952) on crystals exhibiting piezoelectricity to initially illustrate the theoretical results described above because in this work Hearmon discussed his criteria for the inclusion or exclusion of data in the averaging process.

A result of great interest was the discovery of materials (softwoods, feldspar) for which the eigenvectors, but not the eigenvalues, were relatively independent of material composition. This result suggests a paradigm for extending the empirical method of regressing Young's modulus data against composition or porosity in an isotropic material to anisotropic materials. Recall, for example that in the case of porous isotropic materials it is customary to regress the Young's modulus against porosity. Our results suggest that one may be hopeful that the eigenvectors of a material of varied composition will not depend upon the varied composition, permitting all the compositional dependence to be represented by the eigenvalues.

II – 2. A Tensorial Presentation of the Kelvin Formulation

The anisotropic form of Hooke's law is often written in indicial notation as $T_{ij} = C_{ijkm} E_{km}$, where the C_{ijkm} are the components of the elasticity tensor. Written as a linear transformations in six dimensions, Hooke's law has the representation $\mathbf{T} = \mathbf{c}\,\mathbf{E}$ or

$$\begin{bmatrix} T_{11} \\ T_{22} \\ T_{33} \\ T_{23} \\ T_{13} \\ T_{12} \end{bmatrix} = \begin{bmatrix} c_{11} & c_{12} & c_{13} & c_{14} & c_{15} & c_{16} \\ c_{12} & c_{22} & c_{23} & c_{24} & c_{25} & c_{26} \\ c_{13} & c_{23} & c_{33} & c_{34} & c_{35} & c_{36} \\ c_{14} & c_{24} & c_{34} & c_{44} & c_{45} & c_{46} \\ c_{15} & c_{25} & c_{35} & c_{45} & c_{55} & c_{56} \\ c_{16} & c_{26} & c_{36} & c_{46} & c_{56} & c_{66} \end{bmatrix} \begin{bmatrix} E_{11} \\ E_{22} \\ E_{33} \\ 2E_{23} \\ 2E_{13} \\ 2E_{12} \end{bmatrix} \qquad (II\text{-}1)$$

in the notation of Voigt (1928). The relationships of the components of C_{ijkm} to the components of the symmetric matrix $\mathbf{c}$ are given in Table II -1. Introducing new notation, $(II\text{-}1)$ can be rewritten in the form $\hat{\mathbf{T}} = \hat{\mathbf{c}}\hat{\mathbf{E}}$ where the shearing components of these new six-dimensional stress and strain vectors, denoted by $\hat{\mathbf{T}}$ and $\hat{\mathbf{E}}$ respectively, are multiplied by $\sqrt{2}$, and $\hat{\mathbf{c}}$ is a new six-by-six matrix (Mehrabadi and Cowin, 1990). The matrix form of $\hat{\mathbf{T}} = \hat{\mathbf{c}}\hat{\mathbf{E}}$ is given by

$$\begin{bmatrix} T_{11} \\ T_{22} \\ T_{33} \\ \sqrt{2}T_{23} \\ \sqrt{2}T_{13} \\ \sqrt{2}T_{12} \end{bmatrix} = \begin{bmatrix} c_{11} & c_{12} & c_{13} & \sqrt{2}c_{14} & \sqrt{2}c_{15} & \sqrt{2}c_{16} \\ c_{12} & c_{22} & c_{23} & \sqrt{2}c_{24} & \sqrt{2}c_{25} & \sqrt{2}c_{26} \\ c_{13} & c_{23} & c_{33} & \sqrt{2}c_{34} & \sqrt{2}c_{35} & \sqrt{2}c_{36} \\ \sqrt{2}c_{14} & \sqrt{2}c_{24} & \sqrt{2}c_{34} & c_{44} & c_{45} & c_{46} \\ \sqrt{2}c_{15} & \sqrt{2}c_{25} & \sqrt{2}c_{35} & c_{45} & c_{55} & c_{56} \\ \sqrt{2}c_{16} & \sqrt{2}c_{26} & \sqrt{2}c_{36} & c_{46} & c_{56} & c_{66} \end{bmatrix} \begin{bmatrix} E_{11} \\ E_{22} \\ E_{33} \\ \sqrt{2}E_{23} \\ \sqrt{2}E_{13} \\ \sqrt{2}E_{12} \end{bmatrix} \qquad (II\text{-}2)$$

The matrix $\hat{\mathbf{c}}$ is called the matrix of *elastic coefficients* and its inverse $\hat{\mathbf{s}}$, $\hat{\mathbf{E}} = \hat{\mathbf{s}}\hat{\mathbf{T}}, \hat{\mathbf{s}} = \hat{\mathbf{c}}^{-1}$ is called the *compliance* matrix. A chart relating these various notations for the specific elastic coefficients is given in Table II -1. The symmetric matrices $\hat{\mathbf{c}}$ and $\hat{\mathbf{s}}$ can be shown to represent the components of a second rank tensor in a six-dimensional space, whereas the components of the matrix **c** appearing in (II-1) do not form a tensor (Mehrabadi and Cowin, 1990). The orthogonal transformation in six dimensions is represented by $\hat{\mathbf{Q}}$, which is a second rank tensor in six dimensions that is directly related to an associated orthogonal second rank tensor in three dimensions (Mehrabadi and Cowin, 1990; Cowin and Mehrabadi, 1995); thus the tensor transformation law for $\hat{\mathbf{c}}$ and $\hat{\mathbf{s}}$ to a new or primed. coordinate system is

$$\hat{\mathbf{c}}' = \hat{\mathbf{Q}}\hat{\mathbf{c}}\hat{\mathbf{Q}}^T \ , \ \hat{\mathbf{s}}' = \hat{\mathbf{Q}}\hat{\mathbf{s}}\hat{\mathbf{Q}}^T \ . \qquad (II\text{-}3)$$

Table II - 1. The elasticity and compliance components in different notations. Row 1 illustrates the Voigt notation of these quantities as fourth rank tensor components in a three-dimensional Cartesian space. Row 2 represents the Voigt matrix or double index notation. Row 3 illustrates the Kelvin-inspired notation for these quantities as second rank tensor components in a six-dimensional cartesian space.

1	C_{1111}	C_{2222}	C_{3333}	C_{1122}	C_{1133}	C_{2233}	C_{2323}	C_{1313}	C_{1212}	C_{1323}	C_{1312}
2	c_{11}	c_{22}	c_{33}	c_{12}	c_{13}	c_{23}	c_{44}	c_{55}	c_{66}	c_{54}	c_{56}
3	c_{11}	c_{22}	c_{33}	c_{12}	c_{13}	c_{23}	$c_{44}/2$	$c_{55}/2$	$c_{66}/2$	$c_{54}/2$	$c_{56}/2$
1	S_{1111}	S_{2222}	S_{3333}	S_{1122}	S_{1133}	S_{2233}	S_{2323}	S_{1313}	S_{1212}	S_{1323}	S_{1312}
2	s_{11}	s_{22}	s_{33}	s_{12}	s_{13}	s_{23}	s_{44}	s_{55}	s_{66}	s_{54}	s_{56}
3	s_{11}	s_{22}	s_{33}	s_{12}	s_{13}	s_{23}	$s_{44}/2$	$s_{55}/2$	$s_{66}/2$	$s_{54}/2$	$s_{56}/2$

1	C_{1223}	C_{2311}	C_{1311}	C_{1211}	C_{2322}	C_{1322}	C_{1222}	C_{2333}	C_{1333}	C_{1233}
2	c_{64}	c_{41}	c_{51}	c_{61}	c_{42}	c_{52}	c_{62}	c_{43}	c_{53}	c_{63}
3	$c_{64}/2$	$c_{41}/\sqrt{2}$	$c_{51}/\sqrt{2}$	$c_{61}/\sqrt{2}$	$c_{42}/\sqrt{2}$	$c_{52}/\sqrt{2}$	$c_{62}/\sqrt{2}$	$c_{43}/\sqrt{2}$	$c_{53}/\sqrt{2}$	$c_{63}/\sqrt{2}$
1	S_{1223}	S_{2311}	S_{1311}	S_{1211}	S_{2322}	S_{1322}	S_{1222}	S_{2333}	S_{1333}	S_{1233}
2	s_{64}	s_{41}	s_{51}	s_{61}	s_{42}	s_{52}	s_{62}	s_{43}	s_{53}	s_{63}
3	$s_{64}/2$	$s_{41}/\sqrt{2}$	$s_{51}/\sqrt{2}$	$s_{61}/\sqrt{2}$	$s_{42}/\sqrt{2}$	$s_{52}/\sqrt{2}$	$s_{62}/\sqrt{2}$	$s_{43}/\sqrt{2}$	$s_{53}/\sqrt{2}$	$s_{63}/\sqrt{2}$

The eigenvalues of the matrix $\hat{\mathbf{c}}(\hat{\mathbf{s}})$ are the six numbers Λ $(1/\Lambda)$ satisfying the equations

$$(\hat{\mathbf{c}} - \Lambda\mathbf{1})\hat{\mathbf{N}} = 0, \quad ((\hat{\mathbf{s}} - (1/\Lambda)\mathbf{1})\hat{\mathbf{N}} = 0), \qquad (II\text{-}4)$$

where the vectors $\hat{\mathbf{N}}$ represent the normalized eigenvectors of $\hat{\mathbf{c}}$ or $\hat{\mathbf{s}}$. The normalized $\hat{\mathbf{N}}$ is expressed in terms of the six-dimensional strain and stress vectors by

$$\hat{\mathbf{E}} = \hat{\mathbf{N}} \,|\, \hat{\mathbf{E}} \,|, \quad \hat{\mathbf{T}} = \hat{\mathbf{N}} \,|\, \hat{\mathbf{T}} \,|, \quad |\, \hat{\mathbf{E}} \,|^2 = \hat{\mathbf{E}} \cdot \hat{\mathbf{E}}, \quad |\, \hat{\mathbf{T}} \,|^2 = \hat{\mathbf{T}} \cdot \hat{\mathbf{T}}, \quad \hat{\mathbf{N}} \cdot \hat{\mathbf{N}} = 1. \qquad (II-5)$$

Since $\hat{\mathbf{c}}$ (or $\hat{\mathbf{s}}$) is positive definite it has six positive eigenvalues. These eigenvalues are called the *Kelvin moduli* and are denoted by Λ_i, i=1, 2, ..., 6, and are ordered (if possible) by the inequalities Λ_1 > =... Λ_6 > 0.

The eigensystems for various anisotropic elastic symmetries are described in Appendix **A**. Since there are, at most, six distinct eigenvalues, and since the number of distinct elastic constants exceeds six for several symmetries, the question of the role played by the other distinct elastic constants arises. These other elastic constants are called *elasticity distributors* (Rychlewsk 1984; Cowin and Mehrabadi 1992). The role they play is to specify the ratio of the components for eigenvectors $\hat{\mathbf{N}}$. Geometrically they represent the ratio of relative extensions in perpendicular directions and/or the amount of shear in an eigenmode. Since Poisson's ratios represent the ratio of relative extensions in perpendicular directions in an axial (tensile or compressive) test situation, there is some similarity between the two concepts. However, distributors are associated with eigenmodes and Poisson's ratios are associated with the axial test situation. If the eigenvector $\hat{\mathbf{N}}$ for a particular symmetry is independent of the particular value of the elastic constants for that symmetry, it is said to be a *simple* eigenmode. Thus simple eigenmodes are independent of the distributors. If an eigenmode is not simple, it is said to be a distributor dependent eigenmode or, simple, a distributor eigenmode.

In the case of triclinic symmetry, the sum of the number of distinct eigenvalues and the number of distributors equals to 18; the other three parameters to make 21 are arbitrary in the sense that they depend upon the choice of the coordinate system selected to express the elasticity tensor, see Feaorov (1968) or Cowin and Mehrabadi (1995). It is known that there are 18 invariants of C_{ijkm} for triclinic symmetry and Rychlewski (1984) identifies one set of these invariants as the six distinct eigenvalues Λ_i, i=1, 2, ..., 6, and the twelve distributors. The twelve distributors consist of $tr[\mathbf{N}^{(k)}]$, k=1, 2, ..., 6, and $tr[\mathbf{N}^{(k)}\mathbf{N}^{(k)}\mathbf{N}^{(k)}]$, k=1, 2, ... 6, where the $\mathbf{N}^{(k)}$, k=1, 2, ..., 6, are subject to the normalized conditions $tr\,[\mathbf{N}^{(k)}\mathbf{N}^{(k)}]=1$, k=1, 2, ..., 6.

The results of the preceding paragraphs above show that there exist six eigentensors of stress, denoted by $\hat{\mathbf{T}}^{(k)}, k=1,2,...,6$, in the six-dimensional space, or by $\mathbf{T}^{(k)}$ in 3-dimensional spaces, and six eigentensors of strain, denoted by $\hat{\mathbf{E}}^{(k)}$ and $\mathbf{E}^{(k)}$, k=1, 2, ..., 6.respectively, which are related by the six equations

$$\hat{\mathbf{T}}^{(k)} = \Lambda_k \hat{\mathbf{E}}^{(k)} \quad or \quad \mathbf{T}^{(k)} = \Lambda_k \mathbf{E}^{(k)}, \quad k=1,...,6. \qquad (II-6)$$

Further, they show that $\hat{\mathbf{T}}, \hat{\mathbf{E}}$, $\hat{\mathbf{c}}$ and $\hat{\mathbf{s}}$ have the representations

$$\hat{\mathbf{T}} = \sum_{k=1}^{6} \hat{\mathbf{T}}^{(k)} = \sum_{k=1}^{6} \Lambda_k \hat{\mathbf{E}}^{(k)} = \sum_{k=1}^{6} \Lambda_k \mathbf{N}_k \mid \hat{\mathbf{E}}^{(k)} \mid,$$

$$\hat{\mathbf{E}} = \sum_{k=1}^{6} \hat{\mathbf{E}}^{(k)} = \sum_{k=1}^{6} \frac{1}{\Lambda_k} \hat{\mathbf{T}}^{(k)} = \sum_{k=1}^{6} \frac{1}{\Lambda_k} \mathbf{N}_k \mid \hat{\mathbf{T}}^{(k)} \mid, \qquad (II-7)$$

and

$$\hat{\mathbf{c}} = \sum_{k=1}^{6} \Lambda_k \hat{\mathbf{N}}_k \otimes \hat{\mathbf{N}}_k, \quad \hat{\mathbf{s}} = \sum_{k=1}^{6} \frac{1}{\Lambda_k} \hat{\mathbf{N}}_k \otimes \hat{\mathbf{N}}_k, \qquad (II-8)$$

where we denote the eigenvectors by $\hat{\mathbf{N}}_k$, $k = 1, 2, ..., 6$, both as quantities with an index (k) and a quantities that have vector character. This notation is customarily employed for the elements of a basis of a vector space, which indeed this set of orthonomal eigenvectors is for the six-dimensional space of interest.

To establish a method of quantifying the difference between the eigenmodes associated with two elasticity matrices, say $\hat{\mathbf{c}}^A$ and $\hat{\mathbf{c}}^B$, we introduce the six-dimensional orthogonal transformation $\hat{\mathbf{Q}}^{AB}$ that carries the eigenvectors of symmetry B, $\hat{\mathbf{N}}_k^B$, into the eigenvectors of symmetry A, $\hat{\mathbf{N}}_k^A$, thus

$$\hat{\mathbf{N}}_k^A = \hat{Q}_{km}^{AB} \hat{\mathbf{N}}_m^B , \qquad (II-9)$$

Where $\hat{Q}_{km}^{AB} = \hat{\mathbf{N}}_k^A \cdot \hat{\mathbf{N}}_m^B$. This is, of course, a change of basis in the six-dimensional space of interest. If the eigenvalues are not distinct, so that more than one eigenvector lies in an eigensubspace, they will be made distinct in the analysis by analyzer.

II – 3. Constructing an Average Elasticity Tensor

Given a set of M measurements of the elastic constants for the same material, or the materials with different compositions, $\hat{\mathbf{c}}^{I}, \hat{\mathbf{c}}^{II}, \ldots, \hat{\mathbf{c}}^{M}$, we wish to construct a tensor $\hat{\mathbf{c}}^{AVG}$ representing the average of the set. The tensor $\hat{\mathbf{c}}^{Y}$ representing the Yth measurement can be expressed in terms of its reference basis as

$$\hat{\mathbf{c}}^{Y} = \hat{c}^{Y}_{ij} \hat{\mathbf{B}}_i \otimes \hat{\mathbf{B}}_j = C^{Y}_{ijkm} \mathbf{b}_i \otimes \mathbf{b}_j \otimes \mathbf{b}_k \otimes \mathbf{b}_m . \qquad (II\text{-}10)$$

where the $\mathbf{b}_i$, i=1,2,3 represent a set of three-dimensional base vectors and the $\hat{\mathbf{B}}_i$, i=1,...,6, represent the corresponding set of six-dimensional base vectors (Mehrabadi and Cowin,1990 ; Cowin and Mehrabadi ,1995),

$$\hat{\mathbf{B}}_1 = \mathbf{b}_1 \otimes \mathbf{b}_1 , \quad \hat{\mathbf{B}}_4 = \frac{1}{\sqrt{2}}(\mathbf{b}_2 \otimes \mathbf{b}_3 + \mathbf{b}_3 \otimes \mathbf{b}_2),$$

$$\hat{\mathbf{B}}_2 = \mathbf{b}_2 \otimes \mathbf{b}_2 , \quad \hat{\mathbf{B}}_5 = \frac{1}{\sqrt{2}}(\mathbf{b}_1 \otimes \mathbf{b}_3 + \mathbf{b}_3 \otimes \mathbf{b}_1),$$

$$\hat{\mathbf{B}}_3 = \mathbf{b}_3 \otimes \mathbf{b}_3 , \quad \hat{\mathbf{B}}_6 = \frac{1}{\sqrt{2}}(\mathbf{b}_1 \otimes \mathbf{b}_2 + \mathbf{b}_2 \otimes \mathbf{b}_1). \qquad (II\text{-}11)$$

One can think of the six-dimensional base vectors $\hat{\mathbf{B}}_i$, i=1, ..., 6, either as vectors in the six-dimensional space (1,0,0,0,0,0), ... , (0,0,0,0,0,1) or as special second rank tensors in three dimensions,

$$\begin{bmatrix} 1 & 0 & 0 \\ 0 & 0 & 0 \\ 0 & 0 & 0 \end{bmatrix}, \ldots, \frac{1}{\sqrt{2}}\begin{bmatrix} 0 & 1 & 0 \\ 1 & 0 & 0 \\ 0 & 0 & 0 \end{bmatrix}. \qquad (II\text{-}12)$$

The eigenvalues Λ_k^Y, $k=1, 2, ..., 6$, $Y=1,2,...,M$ and the eigenvectors $\hat{\mathbf{N}}_k^Y$, k=1, ..., 6, Y= 1,..., M for each measurement are determined from the given elastic constant data. Consistent with (II - 8) above, an invariant representation is then possible for the tensor $\hat{\mathbf{c}}^Y$,

$$\hat{\mathbf{c}}^Y = \sum_{k=1}^{6} \Lambda_k^Y \hat{\mathbf{N}}_k^Y \otimes \hat{\mathbf{N}}_k^Y . \qquad (II\text{-}13)$$

The six-dimensional orthogonal transformation $\hat{\mathbf{Q}}^Y$ that carries $\hat{\mathbf{B}}_i$ into the $\hat{\mathbf{N}}_k^Y$ is given by

$$\hat{\mathbf{N}}_k^Y = \hat{Q}_{km}^Y \hat{\mathbf{B}}_m , \qquad (II\text{-}14)$$

where $\hat{Q}^{Y}_{km} = \hat{\mathbf{N}}^{Y}_{k} \cdot \hat{\mathbf{B}}_{m}$. The typical member of the set of six-dimensional orthogonal transformations $\hat{\mathbf{Q}}^{XY}$ that carry the eigenvector basis $\hat{\mathbf{N}}^{X}_{k}$ into the eigenvector basis $\hat{\mathbf{N}}^{Y}_{k}$ is given by

$$\hat{\mathbf{N}}^{Y}_{k} = \hat{Q}^{YX}_{km} \hat{\mathbf{N}}^{X}_{m}, \qquad (II\text{-}15)$$

where $\hat{Q}^{YX}_{km} = \hat{\mathbf{N}}^{Y}_{k} \cdot \hat{\mathbf{N}}^{X}_{m}$.

The entire set of eigenvalues and eigenbases represent an irreducible set of invariants of the elasticity or compliance tensor. The typical representation (II-13) of the elasticity matrix has the properties that all of the eigenvalues are positive ($\Lambda^{Y}_{k} > 0$ for all Y=1, 2, ..., M and all k=1, 2, ..., 6) and each set of eigenvector $\hat{\mathbf{N}}^{Y}_{k}$, $Y=1, 2, \ldots, M$, forms an orthogonal basis in the six-dimensional space ($\hat{\mathbf{N}}^{Y}_{i} \cdot \hat{\mathbf{N}}^{Y}_{j} = \delta_{ij}$). An average eigenbasis $\hat{\mathbf{N}}^{AVG}_{k}$ is defined for a set of measurement data by

$$\hat{\mathbf{N}}^{AVG}_{k} \equiv \hat{\mathbf{J}}^{NA} \hat{\mathbf{N}}^{NA}_{k}, \qquad (II\text{-}16)$$

where the nominal average, $\hat{\mathbf{N}}^{NA}_{k}$, of the eigenvector bases $\hat{\mathbf{N}}^{Y}_{k}$ and the inverse square root $\hat{\mathbf{J}}^{NA}$ of the positive definite tensor $|\sum_{k=1}^{6} \hat{\mathbf{N}}^{NA}_{k} \otimes \hat{\mathbf{N}}^{NA}_{k}|$, are defined by

$$\hat{\mathbf{N}}^{NA}_{k} \equiv \frac{1}{M} \sum_{Y=1}^{M} \hat{\mathbf{N}}^{Y}_{k}, \qquad \hat{\mathbf{J}}^{NA} = \left(\sum_{k=1}^{6} \hat{\mathbf{N}}^{NA}_{k} \otimes \hat{\mathbf{N}}^{NA}_{k}\right)^{-(1/2)}. \qquad (II-17)$$

The determination of $\hat{\mathbf{N}}_k^{AVG}$, k=1, ..., 6, defined by (II-16) is the first step in understanding this averaging process and, from a practical viewpoint, its determination is the first step in an analysis of a data set. It is shown in Appendix B that $\hat{\mathbf{N}}_k^{AVG}$, k=1, ..., 6, defined by (II-16) is the basis that is, on average, the closest to all the eigenvector bases that are determined from the set of elastic constants measurements $\hat{\mathbf{N}}_k^{I}, \hat{\mathbf{N}}_k^{II}, ..., \hat{\mathbf{N}}_k^{M}$. This basis is the particular basis whose orientation minimizes the square of the distance between itself and the M bases $\hat{\mathbf{N}}_k^{I}, \hat{\mathbf{N}}_k^{II}, ..., \hat{\mathbf{N}}_k^{M}$.

It remains then to average the eigenvalues. Each set of eigenvalues corresponding to each eigenbasis is transformed to the average eigenbasis $\hat{\mathbf{N}}_k^{AVG}$. Thus $\sum_{k=1}^{6} \Lambda_k^{Y} (\hat{\mathbf{N}}_k^{Y} \cdot \hat{\mathbf{N}}_q^{AVG})^2$ represents the eigenvalues transformed to the average eigenbasis and these eigenvalues are then averaged leading to the definition

$$\Lambda_q^{AVG} \equiv \frac{1}{M} \sum_{Y=1}^{M} \sum_{k=1}^{6} \Lambda_k^{Y} (\hat{\mathbf{N}}_k^{Y} \cdot \hat{\mathbf{N}}_q^{AVG})^2 . \qquad (II-18)$$

It is easy to see that this formula for Λ_k^{AVG} satisfies the condition that $\Lambda_k^{AVG} > 0$ for all k=1,..., 6, and that $\Lambda_k^{AVG} \neq \Lambda_k^{NA}$ is the nominal average (NA) of the eigenvalues

$$\Lambda_k^{NA} \equiv \frac{1}{M} \sum_{Y=1}^{M} \Lambda_k^{Y} , \qquad (II-19)$$

defined by

unless $\hat{\mathbf{N}}_q^Y \cdot \hat{\mathbf{N}}_k^{AVG} = \delta_{qk}$ (For all the examples we investigated, either $\hat{\mathbf{N}}_q^Y \cdot \hat{\mathbf{N}}_k^{AVG} = \delta_{qk}$ or $\hat{\mathbf{N}}_q^Y \cdot \hat{\mathbf{N}}_k^{AVG} \approx \delta_{qk}$). The average elasticity matrix $\hat{\mathbf{c}}^{AVG}$ is then defined in a manner that preserves the structure of the spectral decomposition $(II$ - 8),

$$\hat{\mathbf{c}}^{AVG} = \sum_{k=1}^{6} \Lambda_k^{AVG} \hat{\mathbf{N}}_k^{AVG} \otimes \hat{\mathbf{N}}_k^{AVG} \quad . \qquad (II-20)$$

Equations $(II$-16) to $(II$-20) represent the key algebraic results in this averaging process. In the next section it is specialized to isotropic and cubic symmetries and, in the section after next, it is specialized to tetragonal, trigonal and hexagonal (transverse isotropy) symmetries.

II – 4. The Average Eigenvectors for Isotropic and Cubic Symmetry

Recall that if the eigenvector $\hat{\mathbf{N}}$ for a particular symmetry is independent of the particular value of the elastic constants for that symmetry, it is said to be a *simple* eigenmode. Thus for a simple eigenmode $\hat{\mathbf{N}}_k^1 = \hat{\mathbf{N}}_k^2 = \ldots = \hat{\mathbf{N}}_k^M$, and it follows that for isotropic and cubic symmetry, which have only simple eigenmodes as may be seen in Appendix **A**, the nominal average (NA) of the eigenvector basis $\hat{\mathbf{N}}_k^{NA}$ is equal to any and all of the eigenvectors in the data set,

$\hat{\mathbf{N}}_k^Y$, Y=1,2,...,M, associated with the same kth mode. It also follows that, since the eigenbasis for each data set is orthonormal, the nominal average (NA) of the eigenvector basis $\hat{\mathbf{N}}_k^{NA}$ is orthonomal; hence $|\sum_{k=1}^{6} \hat{\mathbf{N}}_k^{NA} \otimes \hat{\mathbf{N}}_k^{NA}| = \hat{\mathbf{1}}$ and thus, from (II-17), $\hat{\mathbf{J}}^{NA} = \hat{\mathbf{1}}$ and from (II-19) and (II-20) it follows that $\hat{\mathbf{N}}_k^{AVG} = \hat{\mathbf{N}}_k^{NA}$ for any simple mode and therefore for isotropic and cubic symmetry,

$$\Lambda_k^{AVG} = \Lambda_k^{NA} \quad \text{and} \quad \hat{\mathbf{N}}_k^{AVG} = \hat{\mathbf{N}}_k^{NA} . \qquad (II\text{-}21)$$

II – 5. The Average Eigenvectors for Tetragonal, Trignal, and Hexagonal (Transversely Isotropic) Symmetry

Consider next tetragonal, trigonal and hexagonal (transversely isotropic) symmetries which have combinations of simple eigenmodes and distributor eigenmodes as may be seen in Appendix **A**. The average eigenvalues and eigenvectors for the simple eigenmodes can be obtained by employing (II - 21). For the simple eigenmodes of tetragonal, trigonal and hexagonal symmetry it may be seen from an inspection of the eigenmodes given in Appendix **A** that $\hat{\mathbf{J}}^{NA} = \hat{\mathbf{1}}$ for these three symmetries. It follows that

$$\hat{\mathbf{N}}_k^{AVG} = \hat{\mathbf{N}}_k^{NA} , \qquad (II\text{-}22)$$

for these symmetries and that Λ_k^{AVG} is given by (II-18).

Table II - 2. Classification of the elastic coefficients for the various anisotropic symmetries

Symmetry	Number of Distinct Constants	Number of Distinct Eigenvalues	Number of Distributors	Number of Simple Eigenmodes	Number of Distributor eigenmodes
Triclinic	18	6	12	0	6
Monoclinic	12	6	6	2	4
Orthotropic	9	6	3	3	3
Tetragonal	6	5	1	3	2
Trigonal	6	4	2	1	4
Hexagonal	5	4	1	2	2
Cubic	3	3	0	3	0
Isotropic	2	2	0	2	0

These results will now be illustrated for tetragonal symmetry. Tetragonal symmetry has four simple eigenmodes and two distributor eigenmodes (the eigenmodes are correlated with the elastic constants). The single distributor α in tetragonal symmetry is associated with the two distributor eigenmodes. The average of the two distributor modes of ($A7$) is given by the first two distributor modes of ($A7$) with the angle α replaced by the angle α^{AVG}, where

$$\alpha^{AVG} \equiv \tan^{-1}\left(\frac{\sum_{Y=1}^{M} \sin\alpha_Y}{\sum_{Y=1}^{M} \cos\alpha_Y}\right). \qquad (II-23)$$

It follows then automatically that the set $\hat{\mathbf{N}}_k^{AVG}$ is orthonormal, thus the average eigenbasis for tetragonal symmetry is orthonormal. Similar results hold for trigonal and hexagonal symmetry. For trigonal symmetry the associated eigenvectors $\hat{\mathbf{N}}^{(1)}$ and $\hat{\mathbf{N}}^{(2)}$ coincide with two distributor eigenmodes of tetragonal symmetry (given by ($A7$)) and the other four are given by ($A11$). The average of eigenvectors for these distributor modes using result (II - 23) is again given by the eigenvectors of the first two distributor modes of ($A7$) with the angle α replaced by the angle α^{AVG}, and the last four distributor modes ($A11$) with the angle β replaced by the angle β^{AVG}, the angle β^{AVG} defined analogously α^{AVG}. The result for hexagonal symmetry is obtained in the same way as the one for tetragonal symmetry since these two symmetries have the same eigenbasis. This illustrates that the result (II - 22) for the average eigenbasis, combined with the definitions for the angles α^{AVG} and β^{AVG}, does indeed yield the average orthonormal eigenbasis for tetragonal, trigonal and hexagonal symmetries.

II – 6. An Application of the Results to the Data Employed by Hearmon

The elastic constants of a material measured by different authors may well differ from each other by a certain amount because of different coordinate systems. Measurements differing greatly from the average of the measurements must be deleted from the averaging process. Hearmon (1952) averaged elastic constant tensor components referred to a convenient coordinate system, $C_{ijkm}^{AVG} = \frac{1}{M}\sum_{Y=1}^{M} C_{ijkm}^{Y}$, and excluded particular measurements from the data set on the basis that they influenced the coefficient of variation (which is 100 times the standard deviation divided by the mean).

In contrast to this traditional method, we suggested above an invariant averaging procedure consisting of two steps. First, an averaging process of the orthonormal eigenvector bases (II-16) in which a confidence interval criterion is used rejects measurements in the data base. Second, an averaging process of the Kelvin moduli (Kelvin, 1878), referred to the average eigenbasis constructed in the first step, is accomplished and a second confidence interval criterion is applied. The results are then reassembled using formula (II-20). In this section we employ the same data employed by Hearmon (1952), the data given in Table II - 3. The surnames in Table II - 3, and the text below, refer to the authors of the articles, cited by Hearmon, reporting the data.

For materials with some simple eigenmodes like tetragonal, trigonal and hexagonal symmetries or all simple eigenmodes like isotropic and cubic symmetries, the averaging process consists only of averaging the eigenvalues, which is described in the following paragraph. For distributor eigenmodes, the eigenbases must also be averaged, and this is the first step in the data analysis. Confidence intervals (Blank, 1980; Daniel, 1978) are employed to determine the admissibility of measurements for the averaging process. Specifically, we employ a criterion of failed eigenbasis coincidence, for the elimination of measurements in the process of averaging the eigenbasis. To measure the coincidence of the eigenbases of different measurements we employ the method described in section I-3 to establish the average eigenbasis. From Equation ($B1$) of Appendix **B**, note that the matrix $\hat{\mathbf{Q}}^{AI}$ is just the components of $\hat{\mathbf{N}}_k^{AVG}$ referred to the basis $\hat{\mathbf{N}}_m^I$, $\hat{\mathbf{N}}_k^{AVG} = \hat{Q}_{km}^{AI}\hat{\mathbf{N}}_m^I$. The criterion for the coincidence of the eigenbasis of the Yth individual measurement and the average eigenbasis is that the six-dimensional orthogonal tensor $\hat{\mathbf{Q}}^{AVG-Y}$, $\hat{Q}_{km}^{AVG-Y} = \hat{\mathbf{N}}_k^{AVG} \cdot \hat{\mathbf{N}}_m^Y$, representing the transformation

Table II - 3. The elastic constant data from Hearmon (1952) (units are 10^{11}dynes/cm^2)

Rochelle salt (orthotropic)	c_{11}	c_{22}	c_{33}	c_{44}	c_{55}	c_{66}	c_{12}	c_{13}	c_{23}
Mandell	3.46	4.73	8.01	1.64	0.327	1.25	-0.78	3.14	-3.42
Hinz	6.28	10.31	9.66	1.01	0.297	0.848	6.83	6.38	7.83
Mason	4.25	5.15	6.29	1.25	0.304	0.996	2.96	3.57	3.42
Sundara Rao	4.06	5.2	6.4	1.22	0.3	0.95	2.56	3.46	3.2
Hutington	2.55	3.81	3.71	1.34	0.321	0.979	1.41	1.16	1.46

ADP (Tetragonal)	c_{11}	c_{33}	c_{44}	c_{66}	c_{12}	c_{13}
Mason	7.58	2.96	0.87	0.614	-2.43	1.3
Zwicker	6.17	3.28	0.85	0.592	0.72	1.94
Price & Huntington	6.89	3.35	0.856	0.595	0.4	1.89
Bechmann	6.77	3.38	0.868	0.608	0.59	1.99

KDP (Tetragonal)	c_{11}	c_{33}	c_{44}	c_{66}	c_{12}	c_{13}
Mason	7.8	7.7	1.27	0.61	3.23	3.48
Zwicker	6.91	5.56	1.29	0.6	-0.6	1.22
Bantle	7.08	5.84	1.28	0.633	-0.383	1.55
Price & Huntington	7.14	5.61	1.27	0.628	-0.49	1.29

Quartz(Trigonal)	c_{11}	c_{33}	c_{44}	c_{12}	c_{13}	c_{14}
Voigt	8.51	10.55	5.7	0.7	1.41	-1.69
Atanasoff & Hart	8.67	10.68	5.79	0.69	1.13	-1.8
Mason	8.61	10.71	5.87	0.51	1.05	-1.83
Bhagavantam	8.69	10.68	5.76	0.69	1.56	-1.74
Bechmann	8.67	10.72	5.8	0.71	1.19	-1.78
Nomoto	8.64	10.46	5.66	0.79	1.36	-1.73

between the eigenbasis of Yth individual measurement and the average eigenbasis, must differ from the unit tensor $\hat{\mathbf{1}}$ in six dimensions by a very small amount. In Appendix **C** it is shown that this condition is satisfied if $\xi^{AVG\text{-}Y}$ is small, where

$$(\xi^{AVG-Y})^2 = 2(6 - tr\hat{\mathbf{Q}}^{AVG-Y}). \qquad (II\text{-}24)$$

Table II - 4. The confidence coefficients at the probability level 5%

N, the number of measurements	1	2	3	4	5	6	7	8	9	10
$t_{\alpha/2}$	12.7	4.3	3.18	2.78	2.57	2.45	2.37	2.31	2.26	2.23

Table II - 5. Analysis of the data on the measure ξ^{AVG-Y} of the difference of $\hat{\mathbf{Q}}^{AVG-Y}$ from the unit tensor $\hat{\mathbf{1}}$ in six dimensions. The boxes with star indicate data excluded by the confidence interval criterion for the measure ξ^{AVG-Y}

Rochelle salt

Author	Mandell	Hinz	Mason	Sundara Rao	Huntington	μ_ξ
$(\xi^{AVG-Y})^2$	0.675	0.078	0.124	0.25	0.065	0.552

ADP

Author	Mason	Zwicker	Price	Bechmann	μ_ξ
$(\xi^{AVG-Y})^2$	0.002	0.0007	0.002	0.009	0.103

KDP

Author	Mason	Zwicker	Bantle	Price	μ_ξ
$(\xi^{AVG-Y})^2$	0.002	0.001	0.002	0.001	0.108

Quartz

Author	Voigt	Hart	Mason	Bhagavantam	Bechmann	Nomoto	μ_ξ
$(\xi^{AVG-Y})^2$	0.003	0.004	0.012	0.006	0.003	0.007	0.0763

The standard deviation in ξ^{AVG-Y} is $s_\xi = \sqrt{\frac{1}{M-1}\sum_{Y=1}^{M}(\xi^{AVG-Y})^2}$. The confidence interval is given by $\mu_\xi = t_{\alpha/2} s_\xi / \sqrt{M}$, here $t_{\alpha/2}$ is a value of the Student's t distribution and α is the significance level. The value $t_{\alpha/2}$ as a function of M, the number of measurements, is given in Table II - 4. The analysis of the data for Rohcelle salt and quartz (Table II - 5) that the measurements of Mandell in Rochelle salt should be excluded. This completes the first averaging process.

In the second averaging process we also employ confidence intervals to determine the admissibility of measurements for calculating Λ_k^{AVG}. From the remaining M measurements Λ_k^Y, $Y=1, 2, \ldots, M$, the average Λ_k^{AVG} is determined by (II-18), the standard deviation from $s_{\Lambda_k} = \sqrt{\frac{1}{M-1}\sum_{Y=1}^{M}(\Lambda^Y - \Lambda^{AVG})^2}$ and the half-width of the confidence interval is given by $\mu_\xi = t_{\alpha/2} s_\xi / \sqrt{M}$, where $t_{\alpha/2}$ is a value of the Student's t distribution and α is the significance level. The value $t_{\alpha/2}$ as a function of M, the number of measurements, are given in Table II - 4. The interval between the individual measurement and the averaged one is defined as $L_{\Lambda k}^Y = | \Lambda_k^Y - \Lambda_k^{AVG} |$. The following criterion is then applied: all of the M measurements Λ_k^Y, $Y=1, 2, \ldots, M$, satisfying $\mu_{\Lambda k} \geq L_{\Lambda k}^Y$ are retained and those that do not are deleted from the set of measurements. Examples of the application of this criterion are presented for Rochelle salt, ammonium dihydrogen phosphate (ADP), potassium dihydrogen phosphate (KDP) in Tables II - 6, II - 7, II - 8 and II - 9, respectively. Application of the criterion for the eigenvalues excluded Mason's measurements for ADP and KDP, shown with stars in Table II - 7 and II - 8.

For the anisotropic materials for which the elastic constant data are contained in Hearmon (1952), the averaged elastic constants data are found by using Equation (II - 20) with Λ_k^{AVG} and $\hat{N}_k^{AVG}$ given by (II-18) and (II-16). Table II

-10 shows the average elastic constants determined by the method proposed in this chapter as well as the one used by Hearmon (1952). We return to this in the discussion.

Table II - 6 Analysis of Rochelle salt eigenvalue data (orthorhombic symmetry)

The data of $L^{Y}_{\Lambda_k}$ for each Λ_k, k=1,2,3, are shown with parentheses. The data with stars indicate the measurement excluded by the confidence interval criterion for eigenvalues

	Mandell	Hinz	Mason	Sundara Rao	Huntington	Average	Standard Deviation	Confidence interval
Λ_1	1.458	1.432	1.435	1.558	1.579	1.501	0.078	0.126
	(0.047)	(0.069)	(0.066)	(0.057)	(0.078)			
Λ_2	3.368	2.124	2.181	2.46	2.151	2.248	0.148	0.237
	(0.828)*	(0.125)	(0.067)	(0.212)	(0.022)			
Λ_3	11.374	23.025	11.898	11.447	6.097	13.117	7.112	11.415
	(1.463)	(9.908)	(1.218)	(1.67)	(7.02)			

Table II - 7. Analysis of ammonium dihydrogen phosphate (ADP) eigenvalue data (tetragonal symmetry). The data of $L^{Y}_{\Lambda_k}$ for each Λ_k, k=1,2,3, are shown with parentheses. The data with stars indicate the measurement excluded by the confidence interval criterion for eigenvalues

	Mason	Zwicker	Price Huntington	Bechmann	Average	Standard Deviation	Confidence Interval
Λ_1	10.01	5.45	6.49	6.18	7.032	2.033	2.826
	(2.978)*	(1.583)	(0.543)	(0.853)			
Λ_2	6.188	8.367	8.633	8.813	8.00	1.265	1.759
	(1.88)*	(0.361)	(0.636)	(0.857)			
Λ_3	1.913	1.8	1.998	1.922	1.908	0.085	0.119
	(0.003)	(0.11)	(0.098)	(0.012)			

Table II - 8. Analysis of potassium dihydrogen phosphate (KDP) eigenvalue data (tetragonal symmetry). The data of $L^{Y}_{\Lambda_k}$ for each Λ_k, k=1,2,3, are shown with parentheses. The data with stars indicate the measurement excluded by the confidence interval criterion for eigenvalues

	Mason	Zwicker	Bantle	Price and Huntington	Average	Standard Deviation	Confidence Interval
Λ_1	4.57	7.51	7.463	7.63	6.793	1.484	2.06
	(2.223)*	(0.717)	(0.67)	(0.837)			
Λ_2	14.531	7.692	8.489	8.02	9.683	3.249	4.515
	(4.848)*	(1.991)	(1.194)	(1.663)			
Λ_3	4.161	4.165	4.029	4.229	4.146	0.083	0.118
	(0.015)	(0.019)	(0.117)	(0.093)			

Table II - 9. Analysis of the quartz eigenvalue data (trigonal symmertry). The data of $L^{Y}_{\Lambda_k}$ for each Λ_k, k=1,2,3, are shown with parentheses. No data has been excluded by the confidence interval criterion for eigenvalues (AVG: Average; SD: Standard; DV: Deviation)

	Voigt	Hart	Mason	Bhaga-Vantam	Bech-mann	Nom-oto	AVG	SD DV	Confidence interval
Λ_1	7.763	8.276	8.181	7.71	8.226	7.954	8.013	0.246	0.494
	(0.25)	(0.263)	(0.167)	(0.304)	(0.212)	(0.089)			
Λ_2	11.963	11.728	11.529	12.297	11.843	11.892	11.88	0.256	0.512
	(0.088)	(0.147)	(0.346)	(0.422)	(0.033)	(0.017)			
Λ_3	9.36	9.565	9.8	9.583	9.619	9.435	9.577	0.159	0.318
	(0.217)	(0.079)	(0.226)	(0.006)	(0.042)	(0.142)			
Λ_4	4.139	4.114	4.167	4.176	4.141	4.074	4.136	0.037	0.085
	(0.003)	(0.022)	(0.031)	(0.04)	(0.005)	(0.061)			

Table II -10. Comparison of the present data analysis with the analysis of Hearmon (1952)

Rochelle salt

Rochelle salt	c_{11}	c_{22}	c_{33}	c_{44}	c_{55}	c_{66}	c_{12}	c_{13}	c_{23}
The present analysis	4.269	5.941	6.472	1.21	0.305	0.945	3.418	3.623	4.042
Hearmon's analysis	4.42	6.117	6.515	1.21	0.305	0.945	3.44	3.463	3.978

ADP

ADP	c_{11}	c_{33}	c_{44}	c_{66}	c_{12}	c_{13}
The present analysis	6.609	3.335	0.585	0.598	0.569	1.94
Hearmon's analysis	6.61	3.34	0.585	0.598	0.57	1.94

KDP

KDP	c_{11}	c_{33}	c_{44}	c_{66}	c_{12}	c_{13}
The present analysis	7.042	5.661	1.28	0.62	-0.492	1.352
Hearmon's analysis	7.043	5.67	1.28	0.62	-0.491	1.353

Quartz

Quartz	c_{11}	c_{33}	c_{44}	c_{12}	c_{13}	c_{14}
The present analysis	8.604	10.601	5.763	0.654	1.278	-1.762
Hearmon's analysis	8.632	10.633	5.763	0.682	1.283	-1.762

II – 7. An Application of the Results to Composition-Dependent Data

In this section we undertake the analysis of elastic constant data in which the variation in composition of the material causes variation in the elastic constants. The two examples are soft wood data, which have been reported as functions of material density, and feldspar.

We begin with the data on feldspar as a function of composition, compiled by Hearmon and reported in Landolt and Bornstein (1979). Hearmon did not attempt to average these elastic constant data due to the scatter that their compositional dependence creates in the elastic constants. Fortunately for us he reported all the individual measurements and the associated composition of the specimens. Feldspar is a material with monoclinic symmetry, a constituent of crystalline rocks that forms much of the earth's crust. It is composed of potassium-, sodium-, and calcium-aluminum silicate minerals (orthoclase, albite, and anorthite) and their isomorphic mixtures. The compositions of the specimens tested are given in Table II -11 where the numbers in curly brackets refer to the reference citation in Landolt and Bornstein (1979). The eignvalues of the seven feldspar specimens are given in Table II -12 and show a strong dependence on composition. An analysis of these data in the manner described in previous section shows, not surprisingly, that the varied composition of the specimens causes many of the data to lie outside the confidence intervals. For the eigenvectors, the opposite pattern emerged. In spite of the varied composition of the material specimens, none of the eigenvectors were outside of the confidence intervals, suggesting that the eigenvectors were far less dependent on material composition than were the eigenvalues (see Table II -13). The components of the averaged eigenvectors are listed in Table II -12. From this analysis it is possible to construct a representation of the form (II - 20) for the composition-dependent feldspar elasticity tensor once the dependence of the eigenvalues on composition has been accomplished.

Table II -11. Feldspar constituents in the seven specimens. The numbers in curly brackets are the citation in Landolt and Bornstein (1979)

Feldspar constituent (wt%)	1{2}	2{42}	3{43}	4{60}	5{61}	6{209}	7{215}
Orthoclase, $KAlSi_3O_8$	78.5	75	66.6	53.5	64.9	74	60.7
Albite, $NaAlSi_3O_8$	19.4	22	28.6	34.6	26.6	18.9	35.6
Anorthite, $CaAl_2Si_2O_8$	2.1	_	_	9.15	3.6	1.95	1.64

Table II -12. The average eigenvectors of the Feldspar specimens

Mode 1	Mode 2	Mode 3	Mode 4	Mode 5	Mode 6
0.808	-0.548	0.192	-0.045	0	0
0.371	0.223	-0.851	0.287	0	0
0.442	0.791	0.41	0.038	0	0
-0.091	-0.122	0.248	0.945	0	0
0	0	0	0	0.994	-0.112
0	0	0	0	0.112	0.994

Table II -13. eigenvalues of the seven Feldspar specimens, indicated for model 1 to 6, and the measure $\xi^{AVG\text{-}Y}$ of the difference of $\hat{Q}^{AVG\text{-}Y}$ from the unit tensor $\hat{\mathbf{1}}$ in six dimensions. Note that all the values of square of $\xi^{AVG\text{-}Y}$ are well within the confidence interval of μ=0.234. As in the case of Table II -11, the numbers in curly brackets are the criterion in Landolt and Bornstein

Eigenvalues	1{2}	2{42}	3{43}	4{60}	5{61}	6{209}	7{215}
Mode 1	205.049	172.556	172.988	199.650	188.989	187.621	183.112
Mode 2	115.566	101.223	96.992	100.305	98.012	99.746	110.695
Mode 3	40.926	36.996	36.112	32.868	37.449	33.628	46.799
Mode 4	16.986	14.302	15.221	21.629	16.7	17.18	15.442
Mode 5	13.962	13.473	11.989	9.836	13.61	13.858	13.439
Mode 6	37.735	32.61	34.706	35.85	37.281	36.23	34.331
ξ^2	0.06	0.033	0.05	0.111	0.034	0.047	0.075

This result was one of great interest and it was further explored with the objective of discovering whether there were other materials in which the eigenvectors, but not the eigenvalues, were relatively independent of material composition. Strong candidates were the softwoods, particularly spruce for which there is much data in the literature. We found that the same result held, not only for spruce, but for the softwoods for which we could find density dependent data. In fact we found that all the softwoods for which we could find density dependent data shared the feldspar property described above. The very high degree of coincidence of the eigenvectors of the various softwoods is illustrated by the results of the analysis of the eigenbasis rotation data in Table II -15. The components of the averaged eigenvectors for the softwoods are listed in Table II -14.

Table II -14. The average eigenvectors of the softwood specimens

Mode 1	Mode 2	Mode 3	Mode 4	Mode 5	Mode 6
0.035	0.491	-0.865	0	0	0
0.998	-0.057	0.008	0	0	0
0.046	0.864	0.492	0	0	0
0	0	0	1	0	0
0	0	0	0	1	0
0	0	0	0	0	1

Table II -15. Eigenvalues of the seven softwood data sets, indicated for model 1 to 6, and the measure ξ^{AVG-Y} of the difference of $\hat{Q}^{AVG-Y}$ from the unit tensor $\hat{1}$ in six dimensions. Note that all the values of square of ξ^{AVG-Y} are well within the confidence interval of μ=0.302. The numbers following the name of the softwood are the specific gravity for that softwood data set. Data from Landolt and Bornstein (1979)

Eigenvalues	Spruce (0.44)	Spruce (0.43)	Spruce (0.39)	Spruce (0.50)	Douglas -F (0.59)	Douglas -F (0.45)	Pine (0.54)
Mode 1	16.294	14.106	11.993	17.253	17.086	16.13	16.99
Mode 2	0.84	1.214	1.098	1.155	2.181	1.416	1.549
Mode 3	0.356	0.418	0.454	0.513	0.705	0.63	0.494
Mode 4	1.234	1.442	1.498	1.25	2.348	1.767	1.742
Mode 5	0.072	0.064	0.078	0.07	0.16	0.176	0.132
Mode 6	1.52	1.0	1.442	1.706	1.816	1.766	1.344
ξ^2	0.037	0.025	0.038	0.041	0.035	0.045	0.025

II – 8. Discussion

The method proposed in this chapter for the averaging of elastic constant data treats the individual measurement systematically as a tensor instead of as a collection of individual elastic constant or matrix element measurements. This proposed method for averaging different measurements of the anisotropic elastic constants for a specific material has advantages over the traditional method (i. e., Hearmon's) of averaging the individual matrix components of the elasticity or compliance matrices. Averaging invariants removes the effect of the reference coordinate system in the measurements, while the traditional method of averaging the components may induce errors due to the various reference coordinate systems and may distort the nature of the symmetry.

In application of the method we have employed statistical methods to exclude some measurements from a measurement set by establishing confidence intervals. The methods we employ have an advantage over the traditional method in that they provide a rational basis to including or excluding measurement data. Hearmon (1952) excluded particular measurements from the data set on the basis that their inclusion led to coefficients of variation in the average stiffness of over 50% to 100%. Even after the application of this method, Hearmon expressed concern over the size of the coefficients of variation and concluded that he was less confident in the results for the elasticity tensor $\hat{c}$ than the results for the compliance tensor $\hat{s}$, even though these data came from the same authors. A second advantage of the present method, not related to the arguments above, is that we are averaging the joint eigenvalues and eigenbasis of $\hat{c}$ and $\hat{s}$. Hearmon (1952) found that the coefficients of variation were very small for the compliance matrix compared to those for the elasticity matrix. Hearmon employed the six-by-six matrix $\mathbf{c}$ (non-tensorial) notation of Voigt (1928), illustrated by Equation (II-1). He suggested that the coefficients of variation in elasticity matrix components being larger than those in compliance probably came from the inherent variability of the material. This problem does not appear in our method because we are averaging the joint eigenvalues and eigenbases of $\hat{c}$ and $\hat{s}$. Our analysis reflects this result.

The analysis of the data for Rochelle salt and quartz showed (Table II - 5) that the measurements of Mandell in Rochelle salt should be excluded, both by the method of the present analysis and in the judgment of Hearmon (1952).

However, the measurement of the elastic constants of Rochelle salt by Hinz, excluded by Hearmon, cannot be eliminated by our method. Hearmon excluded these measurements of Rochelle salt stiffness from the averaging process observing that their inclusion led to coefficients of variation in the average stiffness of over 50% to 100%. He also noted that he was less confident in these individual measurements because their associated stiffness was quite different from the stiffness of other measurements. The measurements of Mandell and Hinz were determined by a static mechanical testing method. By similar arguments Hearmon excluded the measurements by Mason for ADP and KDP. After excluding the measurements above, Hearmon obtained the results with low coefficients of variation and he considered that the reduced set of measurements provided better results. However, he still expressed concern over the size of the coefficients of variation, especially for Rochelle salt.

The numerical differences in the results produced by our method and the results produced by the method of Hearmon (1952) of the same data are almost insignificant (Table II -10). We believe that the agreement in the values of the average elastic constants determined by the different methods is due to good coincidence in the eigenbasis of the data set employed. Note that the analysis of measure $\xi^{AVG\text{-}Y}$ (of the difference of $\hat{\mathbf{Q}}^{AVG-Y}$ from the unit tensor $\hat{\mathbf{1}}$ in six dimensions) for the materials in Table II - 5 shows that the $\xi^{AVG\text{-}Y}$ values between all the Y individual measurements and the average of the measurements are very small. Since the transformation $\hat{\mathbf{Q}}^{AVG-Y}$ differs from $\hat{\mathbf{1}}$ only by a term proportional to $\xi^{AVG\text{-}Y}$ (Appendix **C**), the transformation law (II - 3) for $\hat{\mathbf{c}}$ and $\hat{\mathbf{s}}$ will produce changes in the elastic constant tensor components that will differ from the original elastic constant tensor component values only by terms multiplied by ξ^{AVG-Y} under the transformation $\hat{Q}^{AVG-Y}$. We conclude that Hearmon's method of averaging the elastic constant data produce almost the same results as the presently proposed method if the eigenbasis of each of the individual measurement is very close to the averaged eigenbasis, as shown in the examples of Rochelle salt, ADP, KDP and quartz (Table II - 5). Our contribution is that of an invariant method of data analysis that employs a rationale process for data exclusion.

A result of great interest was that, for some materials with varied composition (softwoods, feldspar), the eigenvectors, but not the eigenvalues, were relatively independent of material composition. This result suggests a paradigm for extending the empirical method of regressing Young's modulus data against composition or porosity in an isotropic material to anisotropic materials. Recall, for example that in the case of porous isotropic materials it is customary to regress the Young's modulus against porosity. Our results suggest that one may be hopeful that the eigenvectors of a material of varied composition will not depend upon the varied composition, permitting all the compositional dependence to be represented only by the eigenvalues.

III. The anisotropic Hooke's law for cancellous bone and wood

III – 1. Introduction

Many materials are anisotropic and inhomogeneous due to the varying composition of their constituents. The identification of the type of elastic symmetry is complicated by the variable composition of the material. This makes the analysis of the elastic constant measurement data difficult. A solution to this problem in which identification of the type of elastic symmetry and the analysis of variable composition are separated and analyzed independently was described in chapter II. The method consists of averaging eigenbases, that is to say the bases composed of the orthogonal sets of eigenvectors of different measurements of the elasticity tensor, in order to construct an average eigenbasis for the entire data set. This is possible because the eigenbases, composed of eigenvectors, are independent of composition while the eigenvalues are not. The eigenvalues of all the anisotropic elastic coefficient matrices can then be transformed to the average eigenvector bases and regressed against their compositional parameters. This method treats the individual measurement as a measurement of a tensor instead of as a collection of individual elastic constants or matrix element measurements, recognizing that the measurements by different authors will reflect the systematic invariant tensorial properties of a material, like eigenvectors and eigenvalues. This method for averaging different measurements of the anisotropic elastic constants for a specific material has advantages over the traditional method of averaging the individual matrix components of the elasticity or compliance matrices. Averaging invariants removes the effect of the reference coordinate system in the measurements, while the traditional method of averaging the components may induce errors due to the various reference coordinate systems and may distort the nature of the symmetry. This averaging process explicitly retains the orthonormality of the eigenvector basis.

An interesting result that emerged from the analysis in chapter II was a method dealing with variable composition anisotropic elastic materials whose elastic coefficients depend upon the particular composition of the material. In the case of porous isotropic materials, for example, it is customary to regress the Young's modulus against the solid volume fraction and obtain an expression for Young's modulus E as a function of the solid volume fraction ϕ; for example $E = (\text{constant})\ \phi^n$. The results in chapter II provided a means to extend this empirical method to anisotropic materials. In chapter II this method was applied to feldspar and it was discovered that the eigenvectors, but not the eigenvalues, were relatively independent of material composition. That result is extended here to three natural porous materials, cancellous bone, hardwood and softwood. The previous results and the present work establish this method of analysis as a valid approach to the construction of anisotropic stress – strain relations for other compositionally dependent materials.

This new method of analysis also identifies the type of elastic symmetry possessed by the material. No assumption as to the type of elastic symmetry is made. The type of symmetry is identified from the character of the eigenvectors that are calculated. For example, in the present work the analysis shows that human cancellous bone has orthotropic elastic symmetry at the 95% confidence level. However the data base we employ for wood incorporated the assumption of orthotropic material symmetry so this feature is not illustrated by the analysis of the wood data.

III – 2. Trabecular Grain

The anisotropic Hooke's law was described in chapter II. The symmetry of (linearly elastic) materials may be characterized by the number and orientation of the planes of mirror, or reflective, symmetry (Cowin and Mehrabadi, 1987). The material symmetry of wood is an appropriate example; it has three perpendicular planes of mirror symmetry. One plane is generally perpendicular to the long axes of the three trunk, another is perpendicular to the tangent to the growth ring, and the third is perpendicular to the radial direction associated with the growth ring. In colloquial speech, by the "grain of the wood" we mean the direction along the long axis of the wood fibers, fibers that are generally coincident with the long axis of the three trunk. Here we define "wood grain" as a set of three orthogonal, ordered directions, the first of which coincides with the local "colloquial" grain direction, which is locally the stiffest direction; the second and third directions are directions orthogonal to each other in the plane perpendicular to the "colloquial" grain direction and also represent directions of extrema in stiffness in the local region of the wood. These directions are the directions tangent and perpendicular to the growth rings. The existence of these three perpendicular planes of mirror symmetry, and no others, mean that wood has orthotropic material symmetry.

We refer to the symmetry coordinate system for an orthotropic material as the "grain" coordinate system. In the grain coordinate system the compliance matrix may be expressed as

$$\hat{\mathbf{s}} = \begin{bmatrix} 1/E_1 & -\nu_{12}/E_1 & -\nu_{13}/E_1 & 0 & 0 & 0 \\ -\nu_{12}/E_1 & 1/E_2 & -\nu_{23}/E_2 & 0 & 0 & 0 \\ -\nu_{13}/E_1 & -\nu_{23}/E_2 & 1/E_3 & 0 & 0 & 0 \\ 0 & 0 & 0 & 1/(2G_{23}) & 0 & 0 \\ 0 & 0 & 0 & 0 & 1/(2G_{13}) & 0 \\ 0 & 0 & 0 & 0 & 0 & 1/(2G_{12}) \end{bmatrix}. \qquad (III\text{-}1)$$

The orthotropic elastic coefficients in the compliance matrix (*III*-1) may be considered either as the components of a fourth-rank tensor in a space of three dimensions or as a second-rank tensor in a space of six dimensions (Mehrabadi and Cowin, 1990; Cowin and Mehrabadi, 1995).

For cancellous bone we refer to the grain coordinate system as the trabecular grain to distinguish it from the wood grain. By trabecular grain we mean a set of three ordered orthogonal directions, the first one of which lies along the local predominant trabecular direction, which is locally the stiffest direction; the second and the third directions are orthogonal to each other in the plane perpendicular to the first direction and represent directions of extrema in stiffness in the local region of the cancellous bone, see Figure 1. We know that these three directions are orthogonal because it has been shown that cancellous bone has orthotropic elastic symmetry (shown by the present data analysis to be at 95% confidence level for 141 specimens), that is to say, three perpendicular planes (or, alternatively, axes) of mirror or reflective symmetry, in each local region of the bone tissue.

III – 3. The Elastic Constant Data Bases

In this section we describe the source of the elastic constant data we analyze. The results for cancellous bone presented in this work are based upon an analysis of a data base consisting of 141 human cancellous bone specimens. This data base, reported by van Rietbergen *et al.* (1996,1998) and Kabel *et al.* (1999b), is superior to previous data bases because the authors provide the entire set of anisotropic elastic constants without an *a priori* assumption of a particular material symmetry and without an assumption of the direction in which the maximum Young's modulus occurs. This data base is unique in many different ways, the most important of which is the large number of specimens and its method of construction, but particularly because it is not based entirely on measurements of real specimens. The data base of elastic constants of 141 human cancellous bone specimens employed here was constructed by imaging real specimens, then computationally determining their elastic constants. We believe that this cyberspace method of construction is more accurate than the conventional mechanical testing procedures for evaluating the elastic constants of human cancellous bone. The determination of the elastic constants of cancellous bone by conventional mechanical test procedures is very difficult. The basic problem is that, due to the size of the human body, it is difficult to obtain specimens of cancellous bone that are larger than 5mm cube. The logical way to test small cubes such as these is compression testing. However compression testing is highly inaccurate for cancellous bone because of (1) the frictional end effects of the platens, (2) it is almost impossible to identify, a priori, the grain directions in a bone specimen and it is therefore almost impossible to cut a specimen in the grain directions, (3) the stiffening effect of the platens on the bone near the platens and (4) the unpredictable inhomogeneity of the specimen. These and other difficulties in the mechanical testing of cancellous bone are described in Keaveny (1997).

The construction of the data base of elastic constants of 141 human cancellous bone specimens employed here was a breakthrough because it provided a relatively inexpensive method of determining the full set of anisotropic elastic constants for a small specimen of cancellous bone by a combination of imaging the specimen (Odgaard *et al.*, 1997; Kabel *et al.*, 1999a, 1999b) and subsequent evaluation of the effective elastic constants using computational techniques based on the finite element method (van Rietbergen *et al.*, 1996, 1998; Hollister *et al.*,1991). This method makes no assumption concerning the type of elastic symmetry characterizing the material. In this method the actual matrix material of the trabeculae comprising the bone specimen is assumed to have an axial Young's modulus E_t. The tissue modulus E_t is a scale factor that magnifies or reduces all the elastic constants. The inverse of the tissue modulus $1/E_t$ multiplies each component in the elastic compliance matrix. The value of E_t may be fixed from the knowledge of the axial Young's modulus E_t itself. The elastic constant results are presented here as multiples of E_t. For purpose of numerical calculation E_t was taken to be 1 GPa (van Rietbergen *et al.*, 1996, 1998; Odgaard *et al.*; 1997, Kabel *et al.*, 1999a).

Once the image of the specimen was in the computer and a finite element mesh was generated, a sequence of loadings (van Rietbergen *et al.*, 1996, 1998) were applied to the specimen and the responses determined. The sequence of loading was sufficient in number to determine all 21 elastic constants. Thus no material symmetry assumptions were made in the determination of the constants. Quantitative stereological programs were used to determine the solid volume fraction ϕ of each specimen. These are the data employed in the analysis reported here.

The source of the elastic constant data on hardwoods and softwoods is easier to describe; it was taken from Hearmon (1948). These data (Table III-1 & III-2) are relatively unique because they included both the elastic constants and the apparent density of the specimens. Note that the data on cancellous bone are given as function of solid volume fraction ϕ, while those for hardwoods and softwoods are given as function of bulk or apparent density, ρ. These two quantities are related by $\rho = \gamma\phi$ where γ is the density of the actual solid matrix material (γ = 1.9 gram/cc for human bone). γ is considered to be a constant for these materials, so ρ is proportional to ϕ.

Table III - 1. The elastic constants of hardwoods from Hearmon (1948). The units of ρ are g/cc and the units of the elastic constants are GPa = 10^{10} dynes/cm^2.

Species	ρ	$\hat{c}_{11}$	$\hat{c}_{22}$	$\hat{c}_{33}$	$\hat{c}_{12}$	$\hat{c}_{13}$	$\hat{c}_{23}$	$\hat{c}_{44}$	$\hat{c}_{55}$	$\hat{c}_{66}$
Quipo	0.1	0.045	0.251	1.075	0.027	0.033	0.025	0.226	0.118	0.078
Quipo	0.2	0.159	0.427	3.446	0.069	0.131	0.178	0.43	0.28	0.144
White	0.38	0.547	1.192	10.041	0.399	0.360	0.555	1.442	1.344	0.022
Khaya	0.44	0.631	1.381	10.725	0.389	0.520	0.662	1.80	1.196	0.42
Mahogany	0.50	0.952	1.575	11.996	0.571	0.682	0.79	1.96	1.498	0.638
Mahogany	0.53	0.765	1.538	13.01	0.655	0.631	0.841	1.218	0.938	0.3
S.Germ	0.54	0.772	1.772	12.24	0.558	0.53	0.871	2.318	1.582	0.54
Maple	0.58	1.451	2.565	11.492	1.197	1.267	1.818	2.46	2.194	0.584
Walnut	0.59	0.927	1.76	12.432	0.707	0.936	1.312	1.922	1.4	0.46
Birch	0.62	0.898	1.623	17.173	0.671	0.714	1.075	2.346	1.816	0.372
Y.Birch	0.64	1.084	1.697	15.288	0.777	0.883	1.191	2.12	1.942	0.48
Oak	0.67	1.35	2.983	16.678	1.007	1.005	1.463	2.38	1.532	0.784
Ash	0.68	1.135	2.142	16.958	0.827	0.917	1.427	2.684	1.784	0.54
Beech	0.74	1.659	3.301	15.437	1.279	1.433	2.142	3.216	2.112	0.912
Ash	0.80	1.439	2.439	17.0	1.037	1.485	1.968	1.720	1.218	0.50

Table III - 2. The elastic constants of softwoods from Hearmon (1948). The units of ρ are g/cc and the units of the elastic constants are GPa = 10^{10} dynes/cm^2.

Species	ρ	$\hat{c}_{11}$	$\hat{c}_{22}$	$\hat{c}_{33}$	$\hat{c}_{12}$	$\hat{c}_{13}$	$\hat{c}_{23}$	$\hat{c}_{44}$	$\hat{c}_{55}$	$\hat{c}_{66}$
Balsa	0.2	0.127	0.36	6.38	0.086	0.091	0.154	0.624	0.406	0.066
Spruce	0.39	0.572	1.03	11.95	0.262	0.365	0.506	1.498	1.442	0.078
Spruce	0.43	0.594	1.106	14.055	0.346	0.476	0.686	1.442	1.0	0.064
Spruce	0.44	0.443	0.775	16.286	0.192	0.321	0.442	1.234	1.52	0.072
Douglas fir	0.45	0.929	1.173	16.095	0.409	0.539	0.539	1.767	1.766	0.176
Spruce	0.50	0.755	0.963	17.221	0.333	0.549	0.548	1.25	1.706	0.07
Pine	0.54	0.721	1.405	16.929	0.454	0.535	0.857	3.484	1.344	0.132
Douglas fir	0.59	1.226	1.775	17.004	0.753	0.747	0.941	2.348	1.816	0.16

III – 4. Analysis of Data

The data on the elastic constants of cancellous human bone and their volume fraction were analyzed in five steps. A detailed example for a particular human cancellous bone specimen is given in appendix D. First, the eigenvalues and eigenvectors associated with the six-by-six matrix of elastic constant data were determined for each specimen. Second, the average of the 141 eigenbases was determined (see the Appendix D for details). Third, observing that the elements in the averaged eigenbases associated with other than orthotropic symmetry were near zero, the eigenvector basis was statistically tested for the closeness to orthotropic symmetry. It was found that the set of 141 bone specimens had orthotropic symmetry at the 95% confidence level. Fourth, the data for each specimen were referred to the common eigenvector basis. The orthogonal transformation law for Cartesian second rank tensors was employed to transform the elasticity tensor from its original coordinate system which reflected no symmetry to the common average eigenvector basis where it reflected orthotropic symmetry system except for a few small deviations. The elastic constants that were associated with other than orthotropic symmetry were near zero and were neglected. The error associated with the neglect of these near-zero terms was less than 3.5% of the largest eigenvalue and the maximum error was 4.4% for specimen 36. This result demonstrated that the common average eigenvector basis was indeed common and almost independent of the volume fraction, paralleling the result noted by Cowin and Yang (1997) that the eigenvectors for wood and feldspar were independent of the composition of those materials (the proof of that result in Cowin and Yang follows a different numerical argument, however). Fifth, the six compositional invariants were regressed against their volume fractions by using linear log-log relations. The rationale for the selection of log-log relationships is given in Hodgskinson and Currey (1990). The results of this analysis, the dependence of the eigenvalues upon the solid volume fraction, are shown in Table III - 3. In Table III - 3 the squared correlation coefficients (R^2) for the correlation of that eigenvalue with the corresponding set of the eigenvalue of the original data is shown next to the eigenvalue. A plot of the data on the first eigenvalues versus solid volume fraction is presented in Figure 2. Then, using the spectral representation of the matrix of elastic coefficients in terms of its eigenvalues and eigenvectors, where the eigenvalues are compositionally dependent and the eigenvectors are not, the strain-stress relations were constructed. These relations reflect the explicit dependence upon volume fraction ϕ. The elastic constants obtained are given in the second column of Table III - 4 as a function of the solid volume fraction ϕ and a multiple of E_t. E_t has the dimension of stress and other numbers multiplying all ϕ's raised to a power are dimensionless. The squared correlation coefficients (R^2) for the orthotropic elastic coefficients are as follows: for $1/E_1$, $R^2 = 0.934$; for $1/E_2$, $R^2 = 0.917$; for $1/E_3$, $R^2 = 0.879$; for $1/(2G_{23})$, $R^2 = 0.870$; for $1/(2G_{13})$, $R^2 = 0.887$; for $1/(2G_{12})$, $R^2 = 0.876$; for $-\nu_{12}/E_1$, $R^2 = 0.740$; for $-\nu_{13}/E_1$, $R^2 = 0.841$; for $-\nu 12/E_1$, $R^2 = 0.666$.

The elastic coefficient for human bone is quite interesting and contains revealing insights. The Young's modulus of human cancellous bone plotted as a function of direction at the volume fraction $\phi = 0.35$ is shown in Figure 3. This three-dimensional closed, peanut shell shaped surface reflects the three orthogonal planes of mirror symmetry associated with orthotropy. For an isotropic material the surface shown in Figure 3 would be a sphere. As the solid volume fraction of cancellous bone changes, the overall average shape of the surface in Figure 3 stays the same, but the intercept values of the surface with the three principal directions increase or decrease with the volume fraction; that is to say the plot in Figure 3 is simply enlarged or reduced. It is interesting to note that the anisotropy ratios (E_1/E_2, E_1/E_3, E_2/E_3) calculated are mildly decreasing with increasing volume fraction, thus the more dense material is associated with less pronounced anisotropy.

The data on the hardwoods and softwoods were analyzed in a manner similar to that for cancellous bone. The dependence of the eigenvalues for the wood types upon the apparent density is shown Table III - 3. The elastic constants obtained are given in the third and fourth columns of Table III - 4 as functions of the apparent density. The results for woods are not as strong as the results for the cancellous bone. The reason for this difference is the difference in the quality of the original data base. The data set on the cancellous bone is high quality data in that it contains all 21 elastic constants and the solid volume fraction for 141 specimens. The results concerning these data are strong because of the large number of specimens; the central limit theorem states that the difference between the true mean and the estimated mean depends inversely upon the number of specimens. Thus the true mean and the estimated mean

Table III - 3. Results of the linear log-log regression of the eigenvalues against volume fraction ϕ for cancellous bone and the linear log-log regression of the eigenvalues against apparent density ρ for hardwoods and softwoods.

Eigenvalues (R^2)	Cancellous bone	Hardwood (GPa)	Softwood (GPa)
Λ_1 (R^2)	$1460E_t\,\phi^{1.72}$ (0.911)	$28.44\,\rho^{1.34}$ (0.968)	$32.56\,\rho^{0.99}$ (0.941)
Λ_2 (R^2)	$871E_t\,\phi^{1.89}$ (0.905)	$6.11\,\rho^{1.95}$ (0.936)	$3.92\,\rho^{1.46}$ (0.874)
Λ_3 (R^2)	$493E_t\,\phi^{1.92}$ (0.868)	$0.86\,\rho^{0.75}$ (0.684)	$1.79\,\rho^{1.74}$ (0.894)
Λ_4 (R^2)	$533E_t\,\phi^{2.03}$ (0.879)	$3.94\,\rho^{1.23}$ (0.893)	$4.55\,\rho^{1.24}$ (0.704)
Λ_5 (R^2)	$973E_t\,\phi^{1.97}$ (0.902)	$3.14\,\rho^{1.37}$ (0.875)	$4.01\,\rho^{1.36}$ (0.824)
Λ_6 (R^2)	$973E_t\,\phi^{1.98}$ (0.889)	$0.83\,\rho^{1.21}$ (0.453)	$0.166\,\rho^{0.66}$ (0.271)

Table III - 4. The functional dependence of the orthotropic elastic constants of bone upon solid volume fraction, ϕ, and the functional dependence of the orthotropic elastic constants of the hardwoods and softwoods upon apparent density, ρ.

Elastic Constant	Cancellous bone	Hardwood	Softwood
E_1	$1240\ E_t\,\phi^{1.80}$	$1.307\,\rho^{0.89}$ (GPa)	$2.05\,\rho^{1.71}$ (GPa)
E_2	$885\ E_t\,\phi^{1.89}$	$2.97\,\rho^{1.50}$ (GPa)	$3.14\,\rho^{1.59}$ (GPa)
E_3	$528.8\ E_t\,\phi^{1.92}$	$27.63\,\rho^{1.41}$ (GPa)	$32.01\,\rho^{1.01}$ (GPa)
$2\ G_{23}$	$533.3\ E_t\,\phi^{2.04}$	$3.94\,\rho^{1.23}$ (GPa)	$4.56\,\rho^{1.27}$ (GPa)
$2\ G_{13}$	$633.3\ E_t\,\phi^{1.97}$	$3.14\,\rho^{1.37}$ (GPa)	$4.10\,\rho^{1.36}$ (GPa)
$2\ G_{12}$	$972.6\ E_t\,\phi^{1.98}$	$0.825\,\rho^{1.21}$ (GPa)	$0.166\,\rho^{0.66}$ (GPa)
ν_{23}	$0.256\ E_t\,\phi^{-0.09}$	$0.024\,\rho^{-0.73}$	$0.028\,\rho^{+0.18}$
ν_{32}	$0.153\ E_t\,\phi^{-0.05}$	$0.227\,\rho^{-0.82}$	$0.286\,\rho^{-0.40}$
ν_{13}	$0.316\ E_t\,\phi^{-0.19}$	$0.016\,\rho^{-0.76}$	$0.019\,\rho^{+0.10}$
ν_{31}	$0.135\ E_t\,\phi^{-0.07}$	$0.345\,\rho^{-0.23}$	$0.300\,\rho^{-0.60}$
ν_{12}	$0.176\ E_t\,\phi^{-0.25}$	$0.724\,\rho^{+0.90}$	$0.269\,\rho^{-0.17}$
ν_{21}	$0.125\ E_t\,\phi^{-0.16}$	$1.645\,\rho^{+1.50}$	$0.412\,\rho^{-0.29}$

approach each other as the number of specimens increases. The quality of the data on woods, given in Table III - 1 and III - 2, is easily seen to be about onetenth the number of cancellous bone. In addition, the assumption of orthotropic symmetry was incorporated into the data base for wood, while the data base for human cancellous bone is independent of any assumption concerning elastic material symmetry.

III – 5. Discussion

The superiority of this model for representing the volume fraction dependence of the elastic constants is established by comparing it with the results obtained using other models. The widely employed axial Young's modulus model assumes that the axial Young's modulus E is proportional to the solid volume fraction ϕ raised to a power, E = (constant) ϕ^n. When this model is employed (Rice et al., 1988; Cowin, 1989; Hodgskinson and Currey, 1990a,b) the squared correlation coefficients (R^2) are in the range of 0.4 to 0.7; with present model the squared correlation coefficient (R^2) is 0.934 for the largest Young's modulus, about one-third higher. However the reader should keep in mind that the squared correlation coefficients we report were not obtained directly from experimental data as were the earlier ones. By reminding the reader of this fact we do not mean to imply that the method employed to obtain the elastic constants reported in van Rietbergen et al. (1996, 1998) and Kabel et al. (1997a) is any less accurate, only different. In fact, we believe that the data reported by van Rietbergen *et al.* (1996,1997) and Kabel *et al.* (1997a) are superior to previous data because they provide the entire set of anisotropic elastic constants without an *a priori* assumption of a particular symmetry and without an assumption of the direction in which the maximum Young's modulus occurs. The data bases employed by Rice *et al.*(1988) (see also Cowin, 1989) consisted generally of uniaxial compression tests of small cubes of cancellous bone in which only the Young's modulus was reported. In these studies the direction of the maximum Young's modulus was assumed or estimated.

The results presented here establish the method of analysis developed in Cowin and Yang (1997), in which the identification of the type of elastic symmetry to be accomplished independently of the examination of the variable composition of the material, as a valid approach to the construction of anisotropic stress-strain relations for other compositionally dependent materials.

IV. Human Cancellous Bone Elastic Constants Dependence upon Solid Volume Fraction

IV – 1. Introduction

There has been a great deal of study aimed at specifying the relationship between the elastic constants of cancellous bone and volume fraction. Lumping bovine and human data for both cancellous and cortical bone together, Carter and Hayes (1976) proposed a relationship in which the effective isotropic Young's modulus was proportional to the cube of volume fraction. Rice *et al.* (1988) showed that there was species dependence in the data on the relationship between the Young's modulus and volume fraction and, more importantly, the inclusion of the data on cortical bone were the source of the proposed cubic dependence. When the data for cortical bone were removed, the dependence of the Young's modulus of cancellous bone was upon the square of the volume fraction. Recent work has assumed a dependence of the anisotropic elastic constants upon the square of the volume fraction as well as measures of the local architecture of the cancellous bone (Turner *et al.*, 1990; van Rietbergen *et al.*, 1996,1997).

In an anisotropic material such as cancellous bone the value of Young's modulus changes as a function of direction from a fixed material point. It depends not only upon direction but also upon the solid volume fraction of the cancellous bone in the region of the material point. Experimental determination of the Young's modulus for cancellous bone has been hampered in the past by the inability to separate or distinguish the directional dependence from the solid volume fraction dependence. In chapter III it was shown that the solid volume fraction dependence can be separated from the directional dependence, analyzed independently, then re-endowed with its directional character. The representation of the anisotropic Hooke's law for human cancellous bone presented in chapter III could ultimately lead to a method for the evaluation of bone stiffness directly from solid volume fraction (or apparent density) and anatomical location, a method that can be used for a more accurate and non-invasive assessment of the structural integrity of cancellous bone. This representation of the anisotropic Hooke's law provides a relationship between the axial Young's modulus of human cancellous bone and volume fraction that has a squared correlation coefficient (R^2) of 0.924. This means that *the present model can explain all but approximately 8% of the total variation in the axial Young's modulus of the data base*. The highest squared correlation coefficients (R^2) for axial Young's modulus against (only) volume fraction for previous models against other database are generally under 0.70 (Rice *et al.*, 1988; Hodgskinson and Curry, 1990a). Moreover the representation provides all the elastic constants, not just the axial Young's modulus, with similar high squared correlation coefficients (R^2).

This representation is a breakthrough based on several pieces of very recent research and some previously well-established results. The first recent result is the development of a relatively inexpensive method of determining the full set of anisotropic elastic constants for a small specimen of cancellous bone by a combination of imaging the specimen (Odgaard *et al.*, 1997; Kabel *et al.*, 1997a) and subsequent evaluation of the effective elastic constants using computational techniques based on the finite element method (van Rietbergen *et al.*, 1996, 1997; Hollister *et al.*, 1991). The second recent result is a method of averaging the compositionally dependent anisotropic elastic constants (Cowin and Yang, 1997). The important previously established result is the strong correlation between stiffness and strength for cancellous bone (Currey 1969, 1984; Rice *et al.*, 1988).

In the next section we illustrate the implications and features of the anisotropic Hooke's law for cancellous bone. In the two sections that follow, the Hooke's law is compared with the axial Young's modulus model and the fabric model, respectively. The final section is a discussion of the significance of this result against a background of previous work.

IV – 2. The Implications and Features of This Hooke's Law

In the grain coordinate system, based on the results of Chapter III, the anisotropic Hooke's law for human cancellous bone has the representation

$$\varepsilon_{11} = 1/E_t\,[\,1/(1240\,\phi^{1.8})\,\sigma_{11} - 1/(7056\,\phi^{2.048})\,\sigma_{22} - 1/(3929\,\phi^{1.991})\,\sigma_{33}],$$

$$\varepsilon_{22} = 1/E_t\,[-1/(7056\,\phi^{2.048})\,\sigma_{11} + 1/(885\,\phi^{1.886})\,\sigma_{22} - 1/(3456\,\phi^{1.972})\,\sigma_{33}],$$

$$\varepsilon_{33} = 1/E_t\,[\,-1/(3929\,\phi^{1.991})\,\sigma_{11} - 1/(3456\,\phi^{1.972})\,\sigma_{22} + 1/(528.8\,\phi^{1.919})\,\sigma_{33}],$$

$$\varepsilon_{23} = 1/E_t\,[1/(533.25\,\phi^{2.038})\,\sigma_{23},$$

$$\varepsilon_{13} = 1/E_t\,[1/(633.34\,\phi^{1.972})\,\sigma_{13},$$

$$\varepsilon_{12} = 1/E_t\,[1/(972.63\,\phi^{1.984})\,\sigma_{12}. \qquad (IV-1)$$

where ϕ is the (dimensionless) solid volume fraction, E_t (tissue Young's modulus) has the dimension of stress and the other numbers are dimensionless. (Sometimes these elastic constants are presented as functions of the bulk or apparent density, ρ, which is related to by $\rho = \gamma\phi$ where γ is the density of the actual solid matrix material (γ = 1.9 gram/cc for human bone). The squared correlation coefficients (R^2) of this model with the original data are given in Table IV - 1.

The representation (*IV* - 1) of the elastic coefficients for human bone is quite interesting and contains revealing insights. The Young's modulus of human cancellous bone of the average representation (*IV* - 1) plotted as a function of direction at the volume fraction ϕ=0.35 is shown in Figure 3. This three-dimensional closed, peanut shell shaped surface reflects the three orthogonal planes of mirror symmetry associated with orthotropy. For an isotropic material the surface shown in Figure 3 would be a sphere. As the solid volume fraction of cancellous bone changes, the overall average shape of this surface stays the same, but the intercept values of the surface with three principal directions increase or decrease; that is to say the plot in Figure 3 is simply enlarged or reduced. It is interesting to note that anisotropy ratios (E_1/E_2, E_1/E_3 and E_2/E_3) calculated from (*IV* - 1) are mildly decreasing with increasing volume fraction, thus the more dense material is associated with less pronounced anisotropy.

The data on human cancellous bone were from six anatomical sites. The results of the analysis of the data are grouped on the basis of six anatomical sites (the vertebral, the calcaneus, the proximal tibia, the distal femur, the proximal femur and the proximal humerus). For most of the sites the shape of the plot of Young's modulus as a function of direction is similar to that for the average representation (IV - 1) shown in Figure 3, although the values of the intercepts along the axes may change. The site that produces the plot of Young's modulus as a function of direction which is most different from that illustrated in Figure 3 is the distal femur. The plot of Young's modulus as a function of direction for the cancellous bone from the distal femur is shown in Figure 4. Note that the shape of the surface representing the directional dependence of Young's modulus in Figure 4 is slightly different from the average representation (IV - 1) shown in Figure 3, and that both surfaces have a three-dimensional peanut shell shape. The difference between these figures reflects a difference in the directional dependence of the average Young's modulus in the cancellous bone of the distal femur from the anatomically averaged directional dependence of the Young's modulus of cancellous bone model represented by (IV - 1). The purpose of this illustration is to show that these differences in shape exist, but they appear to be minor.

The plot of the 141 specimen average Poisson's ratios against volume fraction for human cancellous bone is shown in Figure 5. Note that the values of these Poisson's ratios are all greater than zero and less than one half, the customary range of the Poisson's ratios for isotropic materials (note that ν_{13} is larger than 0.5 for very low volume fractions). The permitted value range for orthotropic material is much larger than for isotropic materials. Note that, for human bone, there is a consistent trend of decreasing Poisson's ratio as an increasing volume fraction. While anisotropy is reflected in Poisson's ratios, it is not exaggerated as the values of the Poisson's ratios all stay in the range of those for isotropic materials.

IV – 3. Comparison with Other Models

The superiority of this model for representing the volume fraction dependence of the elastic constants by comparing it with the results of axial Young's modulus models were shown in Chapter III.

If we compare the results of the present model with the more sophisticated fabric tensor model, the squared correlation coefficients (R^2) that are slightly higher are obtained, but the fabric model has the cost of additional information that are difficult to obtain. The fabric model employs a representation of the elastic constants that involves a dependence both upon volume fraction and upon a quantitative stereological measure of trabecular architecture called the fabric tensor (Cowin, 1985; Turner *et al.*, 1990; van Rietbergen *et al.*, 1996, 1998; Odgaard, 1997; Odgaard *et al.*, 1997; Kabel *et al.*, 1997a). Four types of fabric tensors are considered by Odgaard *et al.* (1997). Recall that the "trabecular grain" consisted of the ordered set of three principal (orthogonal) axes of orthotropic elastic symmetry, ordered by the magnitude of the elastic constants in the three directions. These grain axes coincide with the principal axes of fabric tensor in the models under consideration. The difference between the trabecular grain and the normalized fabric tensor is two ratios that are part of the fabric tensor, the ratios of the maximum to minimum and maximum to mini-max values of the architectural feature (i. e., the normalized eigenvalues of the fabric tensor).

Regression of the human cancellous bone data against the present model produces the squared correlation coefficients (R^2) shown in Table IV - 1. These data have been regressed against the fabric model by van Rietbergen *et al.* (1996, 1998), and Kabel *et al.* (1997b). Regression of the data against the present model produces slightly higher squared correlation coefficients (R^2) than does a regression against the fabric model employed by van Rietbergen *et al.* (1996, 1998), as shown in Table IV - 1. In the case of Young's moduli of human bone the difference is between 0.924 and 0.85, the present model being more effective.

Table IV – 1. Comparison of the correlations of the data on cancellous human bone with two different models. The table presents the squared correlation coefficients (R^2) for this data base with the present model and with the fabric model. The present model assumes a dependence upon the trabecular grain plus the volume fraction to a variable power in a reference coordinate system. The fabric tensor model assumes a dependence upon the fabric tensor and takes all terms to be proportional to the inverse of volume fraction squared. The squared correlation coefficients (R^2) for the fabric tensor model are taken from work of Kabel *et al.* (1999a).

Elastic Constants	Regression Coefficients	Lumped Elastic Constants	Present Model	Fabric Model
$1/E_1$	0.934			
$1/E_2$	0.917	$1/E_i$	0.924	0.85
$1/E_3$	0.879			
$1/G_{23}$	0.87			
$1/G_{13}$	0.887	$1/G_{ij}$	0.884	0.83
$1/G_{12}$	0.876			
$-\nu_{12}/E_1$	0.74			
$-\nu_{13}/E_1$	0.841	$-\nu_{ij}/E_i$	0.755	0.67
$-\nu_{23}/E_2$	0.666			

The squared correlation coefficients for both the present model and the fabric model are lowest for the correlation of the Poisson's ratios divided by the various Young's modulus as may seen from Table IV - 1. In particular the squared correlation coefficients (R^2) for the present model with the data base for $-\nu_{13}/E_1$ and $-\nu_{23}/E_2$ are significantly lower than that of the other seven squared correlation coefficients (R^2) given in Table IV - 1. We know of no reason why the squared correlation coefficients (R^2) for the present model with the data base for $-\nu_{12}/E_1$ and $-\nu_{23}/E_2$ should be lower than squared correlation coefficients (R^2) for $-\nu_{13}/E_1$, the Young's moduli and the shear moduli.

IV – 4. Discussion

We conclude that, for whale and human cancellous bone data, the volume fraction plus the trabecular grain are slightly better predictors of the elastic moduli than the fabric tensor models currently in use. When taken as independent variables the volume fraction plus the trabecular grain explain all but 8% of the variance in the Young's modulus data, all but 11% of the variance in the shear modulus data, and all but 12% of the variance in the Poisson's ratio divided by Young's modulus data (Tables IV - 1). Considering only Young's modulus data, Hodgskinson and Currey (1990b) reported that when the apparent density, fabric, marrow connectivity and mineral volume fraction are taken as independent variables all but 7% of the variance in the Young's modulus data is explained.

In addition to the assumption of the dependence upon fabric, the current fabric models assume a dependence upon the square of volume fraction (or apparent density). This conclusion of the current superiority of the present model means that a more accurate representation of these cancellous bone data may be possible using both a fabric tensor and allowing the various matrix components to depend upon the volume fraction to different powers. Alternatively it may mean that the only aspect of a fabric measure that is significant for this cancellous bone tissue is the trabecular grain. This latter result would suggest that trabecular architecture is strongly correlated with solid volume fraction or apparent density. There are suggestions in the literature that this might be the case. For example, Hodgskinson and Currey (1990b) and Odgaard (1997) note the dependence of marrow connectivity on apparent density. There have been other reports suggesting a strong dependence of trabecular architecture upon volume fraction. Fyhrie *et al.* (1992) and Fyhrie *et al.* (1993) have demonstrated a linear dependence of the inverse of the fabric tensor upon volume fraction. These two results are consistent and strongly suggest the dependence of the trabecular architecture upon volume fraction. Investigators who have studied cancellous bone samples note that specific specimens can have different architectures but the same apparent density. These data and their observations suggest that cancellous bone specimens can have different architectures with the same volume fraction. Our results suggest the possibility that, in spite of the non-uniqueness of architecture at the same volume fractions, the elastic constants are the same for the differing architectures at the same volume fraction.

From a clinical viewpoint our result suggests that more information concerning cancellous bone competence can be extracted from DXA data and textbook data on local cancellous bone structure (i.e., the primary direction data). From a biomechanics perspective the model provides the most accurate representation of the elastic coefficients of cancellous bone achieved to date.

The proposed enhancement of the evaluation of a person's risk for osteoporosis would be based on a knowledge of the local cancellous bone volume fraction and a knowledge of the anatomically established, and previously recorded, trabecular grain. If it is assumed that the bone structure at the site in question is "normal," the application of the model based on the data analyzed in this chapter is possible. If the bone structure at the site in question is not "normal" (for example, it has bone disease, or has been subjected to significant reorientation of its local trabecular directions due to remodeling) then this method offers no advantage as the trabecular grain would have to be determined as it would have to be for other methods. If the bone at the site is normal, these data would be combined using the method described here to evaluate the fracture risk in a local cancellous bone mass. There are some difficulties with this proposed risk evaluation for osteoporosis. First, the correlation between bone elastic constants and the strength is not 100%, but methods are under study to improve this correlation along the lines of the present study. Second, there is the precision of the DXA to consider. Third, there is the question of how accurately the trabecular grain can be evaluated from an anatomical data basis. Incremental improvement is possible in all these areas, and the combination may well be significant.

The representation of the anisotropic (orthotropic) stress-strain relations as a function of volume fraction (*IV* - 1) contains much interesting information. Recall that this 141 specimen data base for human cancellous bone shows that human cancellous bone has orthotropic elastic symmetry at the 95% confidence level and that this was demonstrated without making an *a priori* assumption of orthotropy. That result, which is incorporated in the representation (*IV*-1), is strong. It is strong because of the large number of specimens; the central limit theorem states that the difference between the true mean and the estimated mean depends inversely upon the number of specimens. Thus the true mean and the estimated mean approach each other as the number of specimens increases.

The results reported here shed light on earlier work. Hodgskinson and Currey (1990a,b) reported data that showed that the mean of the three Young's moduli had high correlation with the apparent density. One would expect that result on the basis of the present work because the mean of the three Young's moduli is an invariant of the compliance tensor, thus independent of coordinate system. Light was also shed by the present work on why certain traditional mechanical tests have been difficult to accomplish for cancellous bone. The high degree of anisotropy in Young's modulus has been the problem with its experimental evaluation using the traditional method of compression testing of small specimens of cancellous bone. One of them is well illustrated by Figure 3. If one desires to measure the largest Young's modulus in a cancellous bone mass, the specimen must be selected so its sides align with the trabecular grain.

If the specimen does not exactly align with the trabecular grain, the error in determining the Young's modulus can be significant as can be seen from Figure 3 (or Figure 4). These Figures show that the curved ends of the peanut shell shape associated with the largest Young's modulus are the most highly curved ends, slight angular deviations of the specimen from alignment with the trabecular grain can cause a significant underestimate of the value of the largest Young's modulus. Those doing this type of mechanical testing (Snyder and Hayes, 1990; Keaveny, 1997b) have observed this fact. It is likely that this alignment feature was the prime difficulty associated with the methodology in the measurement of the cancellous bone elastic constants measured by Snyder (1991).

V. **Bounds on the effective anisotropic elastic constants**

V. – 1. Introduction

Hill (1952,1963) constructed bounds on the effective isotropic coefficients of a material with triclinic symmetry using energy theorems from classical elasticity and the uniform strain and uniform stress isotropic bounds of Voigt (1928) and Reuss (1929). For an extensive review and extension of these bounds to general boundary conditions, see section 2 of Nemat-Naser and Hori (1993) and Balendran and Nemat-Nasser (1995). We present here the bounds on the effective elastic constants of a material with any anisotropic elastic symmetry in terms of triclinic symmetry elastic coefficients. It is then possible to specialize the triclinic symmetry coefficients appearing in the bounds to those of a greater symmetry. These results are obtained by combining the approach of Hill (1952, 1963) with a representation of the stress-strain relations due, in principle, to Kelvin (1856, 1878), as well as extensions of the uniform strain and uniform stress bounds of Voigt (1928) and Reuss (1929) from the isotropic case to the case of the crystalline symmetries characterized by finite symmetry groups.

The proof of these results involves strain energy inequalities cast as inequalities of quadratic forms. There are two key points that permit the analysis presented to be successful. The first is an extension of this well known linear algebra result: Given two symmetry N by N matrices **A** and **B** that satisfy the inequality of quadratic forms, $\mathbf{x}^*\mathbf{A}\mathbf{x} \leq \mathbf{x}^*\mathbf{B}\mathbf{x}$, for all vectors **x** in the N-dimensional space, then the eigenvalues of **A** and **B**, $\Lambda_\alpha^{\mathbf{A}}$ and $\Lambda_\alpha^{\mathbf{B}}$, α=1,...,N, respectively, satisfy the inequalities $\Lambda_\alpha^{\mathbf{A}} \leq \Lambda_\alpha^{\mathbf{B}}$, α=1,...,N if the principle axes (i.e., the orthonormalized eigenvectors) of **B** and **A** coincide. The requirement that the principal axes coincide is referred to as the strong coaxiality requirement. It is shown here that this result also holds under weaker conditions, namely, if the principal axes of **B** are rotated from the principal axes of **A** by a small amount. This is called the weaker coaxiality requirement; it is the first key to our extension of known results. A proof of the weak coaxiality theorem is given in Appendix **E**. The second key point is the demonstration that the principal directions associated with the uniform strain bounds of Voigt differ by a small rotation from the principal directions associated with the uniform stress bounds of Reuss for all real materials considered. Thus all the materials considered, which may well include all materials, allowed the weaker coaxiality requirement.

In the next section the Kelvin formation of the generalization of the Hill inequalities for simple Kelvin eigenmodes are summarized. The Kelvin eigenmodes are two types, *simple* Kelvin eigenmodes of a particular material symmetry contain no coefficients that depend on the elastic constants, while *distributor* Kelvin eigenmodes do. The eigenmode coefficients that depend on the elastic constants are called *distributors* to indicate their role in proportioning an eigenmode. The development of bounds on the effective cubic elastic coefficients of a material triclinic symmetry is presented in V. - 3. Cubic and isotropic symmetries contain only simple Kelvin eigenmodes. In V - 4 a proof that Hill inequalities are also valid for distributor Kelvin eigenmodes is presented. It is then possible to develop all the bounds on the effective coefficients for symmetries other than cubic and isotropy. The development of bounds on the effective tetragonal elastic coefficients of a material with triclinic symmetry is presented in V. - 5 and the development of bounds on effective trigonal (hexagonal) elastic coefficients of a material with triclinic symmetry is presented in V. - 6. For each set of bounds developed, it is possible to specialize the triclinic symmetry coefficients appearing in the bounds to those of a great symmetry. In V. - 7 there is a discussion of the results. The Kelvin eigenmodes and moduli for the crystalline symmetries are recorded in Appendix **A**. The uniform strain and uniform stress bounds of Voigt (1928) and Reuss (1929) for the crystalline symmetries are recorded in Appendix **E**. Appendix **C** contains a representation theorem for N-dimensional orthogonal transformations in the case of small rotation while Appendix **F** contains the proof of the weak coaxiality theorem mentioned above.

V. – 2. Generalized Hill Inequalities

There are two approaches to the generalized Hill inequalities, one is to assume that the averaging processes are being applied to a polycrystalline material (Hill, 1952) and the other is to assume the averaging processes are being applied to a composite material (Hill, 1963). Following Hill (1963) we consider a mixture of two anisotropic phase bonded together into a single solid. There are no restrictions on the shape or concentration of the two phases. Let ν_1 and ν_2 denote the concentrations of the two phases ($\nu_1+\nu_2=1$), $\hat{\mathbf{T}}^{(1)}$ and $\hat{\mathbf{T}}^{(2)}$ the stresses of the phases, and $\hat{\mathbf{E}}^{(1)}$and $\hat{\mathbf{E}}^{(2)}$ the strains of the two phases. Let the superscript *A* stand for averaging over the volume of the indicated phase or the entire volume, whichever is appropriate. By averaging we mean integration over the volume divided by the volume. Thus $\hat{\mathbf{T}}^{A}$ represents the volume average of the stress and $\hat{\mathbf{E}}^{A}$ the volume average of the strain. The stresses and strains in the phases and entire volume are related by the following formulas:

$$\hat{\mathbf{T}}^{A} = \nu_1 \hat{\mathbf{T}}^{(1)A} + \nu_2 \hat{\mathbf{T}}^{(2)A} \ , \quad \hat{\mathbf{E}}^{A} = \nu_1 \hat{\mathbf{E}}^{(1)A} + \nu_2 \hat{\mathbf{E}}^{(2)A} , \qquad (V-1)$$

Within each of the phases the stresses and the strains at each point are related by

$$\hat{\mathbf{T}}^{(1)} = \hat{\mathbf{c}}^{(1)} \hat{\mathbf{E}}^{(1)} , \ \hat{\mathbf{T}}^{(2)} = \hat{\mathbf{c}}^{(2)} \hat{\mathbf{E}}^{(2)} , \ \hat{\mathbf{E}}^{(1)} = \hat{\mathbf{s}}^{(1)} \hat{\mathbf{T}}^{(1)} , \ \hat{\mathbf{E}}^{(2)} = \hat{\mathbf{s}}^{(2)} \hat{\mathbf{T}}^{(2)} . \qquad (V-2)$$

We employ the methods of approximation of Voigt and of Reuss. The Voigt approximation is to assume that the strains is uniform throughout the mixture, thus $\hat{\mathbf{E}}^{(1)A} = \hat{\mathbf{E}}^{(2)A} = \hat{\mathbf{E}}^{A}$ and, from $(V-2)$ and $(V-1)$

$$\hat{\mathbf{T}}^{A,V} = \hat{\mathbf{c}}^{V} \hat{\mathbf{E}}^{A} , \ \hat{\mathbf{c}}^{V} = \nu_1 \hat{\mathbf{c}}^{(1)A} + \nu_2 \hat{\mathbf{c}}^{(2)A} , \qquad (V-3)$$

where the superscript V indicates the uniform strain assumption of Voigt. The Reuss approximation is to assume that the stress is uniform throughout the mixture, thus $\hat{\mathbf{T}}^{(1)A} = \hat{\mathbf{T}}^{(2)A} = \hat{\mathbf{T}}^{A}$ and, from $(V-2)$ and $(V-1)$

$$\hat{\mathbf{E}}^{A,R} = \hat{\mathbf{s}}^R \hat{\mathbf{T}}^A \,, \; \hat{\mathbf{s}}^R = v_1 \hat{\mathbf{s}}^{(1)A} + v_2 \hat{\mathbf{s}}^{(2)A} \,, \qquad (V-4)$$

where the superscript *R* indicates the uniform strain assumption of Reuss.

Hill (1963) noted that the average strain energy in any region can be caculated from the average stress and the average strain when the surface constraints are of a prescribed kind (see Gurtin (1972) and Nemat-Nasser and Hori (1993) for general theorems). Hence, for the prescribed (constant) strain $\hat{\mathbf{E}}^A$, and the prescribed (constant) stress $\hat{\mathbf{T}}^A$, the average strain energy has the dual representation

$$2\Sigma^A = \hat{\mathbf{E}}^A \cdot \hat{\mathbf{c}}^{eff} \hat{\mathbf{E}}^A = \hat{\mathbf{T}}^A \cdot \hat{\mathbf{s}}^{eff} \hat{\mathbf{T}}^A \,, \qquad (V-5)$$

where the definitions of $\hat{\mathbf{c}}^{eff}$ and $\hat{\mathbf{s}}^{eff}$ have been employed,

$$\hat{\mathbf{T}}^A = \hat{\mathbf{c}}^{eff} \hat{\mathbf{E}}^A \,, \; \hat{\mathbf{E}}^A = \hat{\mathbf{s}}^{eff} \hat{\mathbf{T}}^A \,. \qquad (V-6)$$

Now, still following Hill(1963), the principles of minimum potential energy and minimum complementary energy are employed to show that

$$\hat{\mathbf{E}}^A \cdot \hat{\mathbf{c}}^{eff} \hat{\mathbf{E}}^A \le \hat{\mathbf{E}}^A \cdot \hat{\mathbf{c}}^V \hat{\mathbf{E}}^A \text{ and } \hat{\mathbf{T}}^A \cdot \hat{\mathbf{s}}^{eff} \hat{\mathbf{T}}^A \le \hat{\mathbf{T}}^A \cdot \hat{\mathbf{s}}^R \hat{\mathbf{T}}^A \,, \qquad (V-7)$$

respectively. This same result was obtained by Hill (1952) for a polycrystalline material is a simple manner because the material contained only one phase.

In his application of these results Hill (1952,1963) considered the macroscopic symmetry, that of $\hat{\mathbf{c}}^{eff}$ ($\hat{\mathbf{s}}^{eff}$), to be isotropy. Since, in general, the symmetry of $\hat{\mathbf{c}}^{V}$ and $\hat{\mathbf{s}}^{R}$ is not isotropy, Hill employed the Voigt (1928) averaging process over all orientations to obtain the orientational average "isotropic" elastic constants. Voigt (1928) applied this process to the elasticity tensor and Reuss (1929) applied it to the compliance tensor. Since the symmetry group characterizing isotropy is the infinite group, it was necessary to integrate in order to average all orientations; thus the Voigt and Reuss averages for isotropy are integrals given by

$$\hat{\mathbf{c}}^{V,Iso} = \frac{1}{8\pi^2} \iiint \hat{\mathbf{Q}}\hat{\mathbf{c}}^{V}[\hat{\mathbf{Q}}^T]\sin\theta\, d\theta\, d\varphi d\psi,\ \hat{\mathbf{s}}^{R,Iso} = \frac{1}{8\pi^2} \iiint \hat{\mathbf{Q}}\hat{\mathbf{s}}^{V}[\hat{\mathbf{Q}}^T]\sin\theta\, d\theta\, d\varphi d\psi. \quad (V\text{-}8)$$

where $\hat{\mathbf{Q}}$'s are the orthogonal transformations of the infinite isotropic group and θ, φ and ψ are spherical coordinates. The symmetry group of all crystalline elastic symmetries are finite (and also proper), hence the Voigt and Reuss averagees for the crystalline elastic symmetries are averages over the finite set of orthogonal transformations in the crystalline symmetry group. Let the symmetry group be denoted by *Grp*, where *Grp* indicates either the Iso(tropic), Cub(ic), Hex(agonal), Tri(gonal), Tet(ragonal), Ort(hotropic), Mon(oclinic) or T(riclinic) symmetry groups. The average for the isotropic symmetry is given by (V - 8). The average for the finite symmetry groups are given by

$$\hat{\mathbf{c}}^{V,Grp}=\frac{1}{\mathbf{N}}\sum_{n=1}^{\mathbf{N}}\hat{\mathbf{Q}}^{(n)}\hat{\mathbf{c}}^{V}[\hat{\mathbf{Q}}^{(n)}]^{T},\ \hat{\mathbf{s}}^{R,Grp}=\frac{1}{\mathbf{N}}\sum_{n=1}^{\mathbf{N}}\hat{\mathbf{Q}}^{(n)}\hat{\mathbf{s}}^{R}[\hat{\mathbf{Q}}^{(n)}]^{T} \qquad (V-9)$$

where $\hat{\mathbf{Q}}$'s are the orthogonal transformations of the finite symmetry group *Grp* and $\mathbf{N}$ is the order of the group *Grp*. The $\hat{\mathbf{c}}^{V,Grp}$ and $\hat{\mathbf{s}}^{R,Grp}$ for the crystalline elastic symmetries are given in Appendix **E**. The orientational averaging processes (V-8) and (V-9) are applied to $\hat{\mathbf{c}}^{V}$ and $\hat{\mathbf{s}}^{R}$ in (V-7) so that the symmetry of $\hat{\mathbf{c}}^{V}$ and $\hat{\mathbf{s}}^{R}$ coincides with the symmetry of $\hat{\mathbf{c}}^{eff}$ and $\hat{\mathbf{s}}^{eff}$; thus

$$\hat{\mathbf{E}}^{A}\cdot\hat{\mathbf{c}}^{eff,Grp}\hat{\mathbf{E}}^{A}\le\hat{\mathbf{E}}^{A}\cdot\hat{\mathbf{c}}^{V,Grp}\hat{\mathbf{E}}^{A}\ \text{and}\ \hat{\mathbf{T}}^{A}\cdot\hat{\mathbf{s}}^{eff,Grp}\hat{\mathbf{T}}^{A}\le\hat{\mathbf{T}}^{A}\cdot\hat{\mathbf{s}}^{R,Grp}\hat{\mathbf{T}}^{A}, \qquad (V-10)$$

where we have introduced the superscript Grp on $\hat{\mathbf{c}}^{eff}$ and $\hat{\mathbf{s}}^{eff}$ to emphasized that the symmetry groups of $\hat{\mathbf{c}}^{V}$, $\hat{\mathbf{s}}^{R}$, $\hat{\mathbf{c}}^{eff}$ and $\hat{\mathbf{s}}^{eff}$ must be the same.

The strain energy, following by (II - 8), can be expressed in terms of strain, or in terms of stress, as

$$2\Sigma=\sum_{k=1}^{6}\Lambda_k[\hat{\mathbf{E}}\cdot\hat{\mathbf{N}}^{(k)}]^2 \quad \text{and} \quad 2\Sigma=\sum_{k=1}^{6}\frac{1}{\Lambda_k}[\hat{\mathbf{T}}\cdot\hat{\mathbf{N}}^{(k)}]^2 \qquad (V-11)$$

When the representation (V - 11) is used for $\hat{\mathbf{c}}^{V,Grp}$, $\hat{\mathbf{s}}^{R,Grp}$, $\hat{\mathbf{c}}^{eff,Grp}$ and $\hat{\mathbf{s}}^{eff,Grp}$ it follows from (V-10) that

$$\sum_{K=1}^{6} \Lambda_k^{eff,Grp} [\hat{\mathbf{E}}^A \cdot \hat{\mathbf{N}}_{eff}^{(k)}]^2 \leq \sum_{K=1}^{6} \Lambda_k^{V,Grp} [\hat{\mathbf{E}}^A \cdot \hat{\mathbf{N}}_V^{(k)}]^2 ,$$

$$\sum_{K=1}^{6} \frac{1}{\Lambda_k^{eff,Grp}} [\hat{\mathbf{T}}^A \cdot \hat{\mathbf{N}}_{eff}^{(k)}]^2 \leq \sum_{K=1}^{6} \frac{1}{\Lambda_k^{R,Grp}} [\hat{\mathbf{T}}^A \cdot \hat{\mathbf{N}}_R^{(k)}]^2 . \qquad (V-12)$$

If all the modes are simple eigenmodes, $\hat{\mathbf{N}}_V^{(k)}$ and $\hat{\mathbf{N}}_R^{(k)}$ are equal. This is equivalent to noting that the strong coaxiality condition is automatically satisfied for simple eigenmodes. Thus, for simple eigenmodes, we may therefore select $\hat{\mathbf{N}}_{eff}^{(k)}$ to coincide with the equal $\hat{\mathbf{N}}_V^{(k)}$ and $\hat{\mathbf{N}}_R^{(k)}$; thus (V-12) becomes

$$\sum_{K=1}^{6} \Lambda_k^{eff,Grp} [\hat{\mathbf{E}}^A \cdot \hat{\mathbf{N}}_{eff}^{(k)}]^2 \leq \sum_{K=1}^{6} \Lambda_k^{V,Grp} [\hat{\mathbf{E}}^A \cdot \hat{\mathbf{N}}_{eff}^{(k)}]^2 .$$

$$\sum_{K=1}^{6} \frac{1}{\Lambda_k^{eff,Grp}} [\hat{\mathbf{T}}^A \cdot \hat{\mathbf{N}}_{eff}^{(k)}]^2 \leq \sum_{K=1}^{6} \frac{1}{\Lambda_k^{R,Grp}} [\hat{\mathbf{T}}^A \cdot \hat{\mathbf{N}}_{eff}^{(k)}]^2 . \qquad (V-13)$$

Note that, in the special case of isotropic and cubic symmetry, all the modes are simple eigenmodes. The results (V - 13) must hold for each eigenmode, thus

$$\Lambda_k^{eff,Grp} \leq \Lambda_k^{V,Grp} \; . \; \frac{1}{\Lambda_k^{eff,Grp}} \leq \frac{1}{\Lambda_k^{R,Grp}} \text{ , for } k=1,2,\ldots,6. \qquad (V-14)$$

The two inequalities in (V - 14) may be combined in the final result,

$$\Lambda_k^{R,Grp} \leq \Lambda_k^{eff,Grp} \leq \Lambda_k^{V,Grp}, \quad \text{for } k=1,\ldots,6. \qquad (V-15)$$

Nemat-Nasser and Hori (1993) also obtained formulas of the type (V - 15). Their result is more general in one aspect and less general in another. Their result is more general in that they obtain these results for uniform tractions and linear displacement data and ours is less general in that we have assumed uniform strain or uniform stress. However, uniform strain or uniform stress is the situation of our present interest. Their result is less general in that they obtained these results by assuming that $\hat{\mathbf{c}}^{V}$ and $\hat{\mathbf{s}}^{R}$ are coaxial, i.e., that $\hat{\mathbf{N}}_{V}^{(k)}$ and $\hat{\mathbf{N}}_{R}^{(k)}$ are equal; they make the strong coaxiality assumption. As we indicate above, the assumption of strong coaxiality for $\hat{\mathbf{c}}^{V}$ and $\hat{\mathbf{s}}^{R}$ is appropriate for isotropic and cubic symmetry (symmetries whose modes are all simple) as we have known above, but it is too strong for the material symmetries with distributor Kelvin eigenmodes. In V - 4 a proof of the result (V - 15) for distributor Kelvin eigenmodes is given for the situation when the eigenvectors $\hat{\mathbf{N}}_{V}^{(k)}$ and $\hat{\mathbf{N}}_{R}^{(k)}$ are "close" to each other, rather than equal. This weaker coaxiality result of ours is more general than the strong coaxiality assumption for $\hat{\mathbf{c}}^{V}$ and $\hat{\mathbf{s}}^{R}$ employed by Nemat-Nasser and Hori (1993). The weaker coaxiality assumption is the key to permit us to construct bounds on the effective elastic constants of material symmetries with distributor Kelvin eigenmodes, hence for any anisotropic elastic symmetry.

Hill (1952) presented a result that illustrates the theory presented above in the case of isotropy, a result we review in the present notation. In the case of isotropic symmetry there are two distinct eigenvalues of the elasticity or compliance tensor - one has a multiplicity of one and the other has a multiplicity of five (Mehrabadi and Cowin, 990). The eigenvalue with a multiplicity one is three times the bulk modulus K, and the eigenvalue with a multiplicity of five is twice the shear modulus G. Thus, for effective isotropic symmetry, (V-14) takes the form

$$K^R \leq K^{eff} \leq K^V, G^R \leq G^{eff} \leq G^V. \qquad (V\text{-}16)$$

where the values of the Voigt and Reuss bounds on K and G, determined by use of the macroscope orientational averaging process (V-8), are given by

$$K^V = \frac{1}{9}(\hat{c}_{11}^T + \hat{c}_{22}^T + \hat{c}_{33}^T) + \frac{2}{9}(\hat{c}_{12}^T + \hat{c}_{23}^T + \hat{c}_{31}^T),$$

$$K^R = \frac{1}{(\hat{s}_{11}^T + \hat{s}_{22}^T + \hat{s}_{33}^T) + 2(\hat{s}_{12}^T + \hat{s}_{23}^T + \hat{s}_{31}^T)},$$

$$G^V = \frac{1}{15}(\hat{c}_{11}^T + \hat{c}_{22}^T + \hat{c}_{33}^T - \hat{c}_{12}^T - \hat{c}_{23}^T - \hat{c}_{31}^T) + \frac{1}{10}(\hat{c}_{44}^T + \hat{c}_{55}^T + \hat{c}_{66}^T), \qquad (V\text{-}17)$$

and

$$G^R = \frac{1}{\frac{4}{15}(\hat{s}_{11}^T + \hat{s}_{22}^T + \hat{s}_{33}^T - \hat{s}_{12}^T - \hat{s}_{23}^T - \hat{s}_{31}^T) + \frac{2}{5}(\hat{s}_{44}^T + \hat{s}_{55}^T + \hat{s}_{66}^T)},$$

and where the bounds are in terms of a matrix $\hat{\mathbf{c}}^T$ representing the $\hat{\mathbf{c}}$ matrix for a triclinic material. The inequalities (V- 16) appear in the paper of Hill (1952). The inequalities (V- 15) are referred to here the generalized Hill inequalities.

III-3. Bounds for Any Less Symmetry by Cubic Symmetry

In the case of cubic material symmetry there are three distinct eigenvalues: they are of multiplicity one, two and three and are given by (Appendix **A**)

$$\Lambda_{(1)}^{Cub} = \hat{c}_{11} + 2\hat{c}_{12}\,,\ \Lambda_{(2,3)}^{Cub} = \hat{c}_{11} - \hat{c}_{12}\,,\ \Lambda_{(4,5,6)}^{Cub} = \hat{c}_{44}\,, \qquad (V\text{-}18)$$

respectively. The bounds on the eigenvalues of the $\hat{\mathbf{c}}^{eff,Cub}$ matrix,

$$\hat{\mathbf{c}}^{eff,Cub} = \begin{bmatrix} \hat{c}_{11}^{eff,Cub} & \hat{c}_{12}^{eff,Cub} & \hat{c}_{12}^{eff,Cub} & 0 & 0 & 0 \\ \hat{c}_{12}^{eff,Cub} & \hat{c}_{11}^{eff,Cub} & \hat{c}_{12}^{eff,Cub} & 0 & 0 & 0 \\ \hat{c}_{12}^{eff,Cub} & \hat{c}_{12}^{eff,Cub} & \hat{c}_{11}^{eff,Cub} & 0 & 0 & 0 \\ 0 & 0 & 0 & \hat{c}_{44}^{eff,Cub} & 0 & 0 \\ 0 & 0 & 0 & 0 & \hat{c}_{44}^{eff,Cub} & 0 \\ 0 & 0 & 0 & 0 & 0 & \hat{c}_{44}^{eff,Cub} \end{bmatrix}, \qquad (V\text{-}19)$$

follow directly from the generalized Hill inequalities (V- 15); thus

$$\Lambda_1^{R,Cub} \le \Lambda_1^{eff,Cub} \le \Lambda_1^{V,Cub}\,, \Lambda_{(2,3)}^{R,Cub} \le \Lambda_{(2,3)}^{eff,Cub} \le \Lambda_{(2,3)}^{V,Cub}\,, \Lambda_{(4,5,6)}^{R,Cub} \le \Lambda_{(4,5,6)}^{eff,Cub} \le \Lambda_{(4,5,6)}^{V,Cub}\,, \qquad (V\text{-}20)$$

where, from (E2), the elements of $\hat{\mathbf{c}}^{V,Cub}$ and $\hat{\mathbf{s}}^{R,Cub}$ in the Voigt and Reuss eigenvalues are expressed in terms of the elements of the triclinic elastic coefficients $\hat{\mathbf{c}}^{T}$ by

$$\Lambda_1^{V,Cub} = \frac{1}{3}(\hat{c}_{11}^T + \hat{c}_{22}^T + \hat{c}_{33}^T) + \frac{2}{3}(\hat{c}_{12}^T + \hat{c}_{23}^T + \hat{c}_{31}^T),$$

$$\Lambda_{(2,3)}^{V,Cub} = \frac{1}{3}(\hat{c}_{11}^T + \hat{c}_{22}^T + \hat{c}_{33}^T - \hat{c}_{12}^T - \hat{c}_{23}^T - \hat{c}_{31}^T),\ \Lambda_{(4,5,6)}^{V,Cub} = \frac{1}{3}(\hat{c}_{44}^T + \hat{c}_{55}^T + \hat{c}_{66}^T),$$

$$\frac{1}{\Lambda_1^{R,Cub}} = \frac{1}{3}(\hat{s}_{11}^T + \hat{s}_{22}^T + \hat{s}_{33}^T) + \frac{2}{3}(\hat{s}_{12}^T + \hat{s}_{23}^T + \hat{s}_{31}^T),$$

$$\frac{1}{\Lambda_{(2,3)}^{R,Cub}} = \frac{1}{3}(\hat{s}_{11}^T + \hat{s}_{22}^T + \hat{s}_{33}^T - \hat{s}_{12}^T - \hat{s}_{23}^T - \hat{s}_{31}^T),\ \frac{1}{\Lambda_{(4,5,6)}^{R,Cub}} = \frac{1}{3}(\hat{s}_{44}^T + \hat{s}_{55}^T + \hat{s}_{66}^T).$$

$$(V\text{-}21)$$

If $\hat{c}_{44}^{eff,Cub} = \hat{c}_{11}^{eff,Cub} - \hat{c}_{12}^{eff,Cub}$, the matrix ($V$ - 16) becomes the matrix for $\hat{\mathbf{c}}^{eff,Iso}$. In the case of isotropic material symmetry there are two distinct eigenvalues, one with a multiplicity of one and one that has a multiplicity of five. The eigenvalues with a multiplicity of one is three times the bulk modulus K,

$$\Lambda_{(1)}^{Iso} = 3\mathbf{k} = \hat{c}_{11}^{Iso} + 2\hat{c}_{12}^{Iso} = c_{11}^{Iso} + 2c_{12}^{Iso} = 3\lambda + 2\mu, \qquad (V\text{-}22)$$

and the eigenvalue with a multiplicity of five is twice the shear modulus G,

$$\Lambda_{(2,3,4,5,6)}^{Iso} = 2\mathbf{G} = \hat{c}_{44}^{Iso} = 2c_{44}^{Iso} = 2\mu, \qquad (V\text{-}23)$$

where λ and μ are Lame' moduli. The bounds (V - 20) given above for cubic symmetry reduce to the bounds given for isotropic symmetry by Hill (1952) if Voigt and Reuss isotropic eigenvalues are related to the Voigt and Reuss cubic eigenvalues by

$$\Lambda_{(1)}^{V,Iso}=\Lambda_{(1)}^{V,Cub}, \Lambda_{(2,3,4,5,6)}^{V,Iso}=\frac{2}{5}\Lambda_{(2,3)}^{V,Cub}+\frac{3}{5}\Lambda_{(4,5,6)}^{V,Cub},$$

$$\Lambda_{(1)}^{R,Iso}=\Lambda_{(1)}^{R,Cub}, \frac{1}{\Lambda_{(2,3,4,5,6)}^{R,Iso}}=\frac{2}{5}\frac{1}{\Lambda_{(2,3)}^{R,Cub}}+\frac{3}{5}\frac{1}{\Lambda_{(4,5,6)}^{R,Cub}},$$

$$(V-24)$$

respectively. This reduction of the bounds (V - 20) may be used, in conjunction with (V - 22) and (V - 23), to derive the inequalities (V - 16) obtained by Hill (1952).

IV – 4. The Principal Result for Distributor Eigenmodes

As noted, in the case of cubic and isotropic symmetry the bounds on the effective eigenvalues follow in a sample and direct manner from the generalized Hill inequalities (V - 15) because the eigenmodes are simple and the strong coaxiality assumption is appropriate. In this section we show that the principal result, the generalized Hill inequalities of equation (V - 15), also holds for distributor eigenmodes if the eigenmodes associated with $\hat{\mathbf{c}}^{V,Grp}$ differ from those associated with $\hat{\mathbf{s}}^{R,Grp}$ by only a small amount, that is to say under the weaker coaxility requirement. To establish the criterion for this near coincidence of eigenmodes we consider the $\hat{\mathbf{s}}^{R,Grp}$ eigenvectors, $\hat{\mathbf{N}}^{(k)R}$, and the $\hat{\mathbf{c}}^{V,Grp}$ eigenvectors, $\hat{\mathbf{N}}^{(k)V}$, to be basis of the six-dimensional space denoted by $\hat{\mathbf{N}}_k^V$ and $\hat{\mathbf{N}}_k^R$, respectively, and introduce the six-dimensional orthogonal transformation $\hat{\mathbf{Q}}^{VR}$ that carries the $\hat{\mathbf{N}}_k^R$ into $\hat{\mathbf{N}}_k^V$, thus

$$\hat{\mathbf{N}}_k^{V} = \hat{Q}_{km}^{VR}\hat{\mathbf{N}}_m^{R} \,, \tag{V-25}$$

where $\hat{Q}_{km}^{VR} = \hat{\mathbf{N}}_k^{V} \cdot \hat{\mathbf{N}}_m^{R} = \hat{\mathbf{N}}_k^{R} \cdot \hat{\mathbf{N}}_m^{V}$. To formulate a restriction on $\hat{\mathbf{Q}}^{VR}$ for near coincidence of eigenmodes we employ the result of Appendix **C**. If a six-dimensional orthogonal tensor $\hat{\mathbf{Q}}^{VR}$ satisfies the condition that $4\xi^4$ be small compared to $\xi^2/2$, where $\xi^2=2(6-\mathrm{tr}\,\hat{\mathbf{Q}}^{VR})$, then $\hat{\mathbf{Q}}^{VR}$ has the representation in terms of a skew-symmetric tensor,

$$\hat{\mathbf{Q}}^{VR} \approx \hat{\mathbf{1}} + \xi\hat{\mathbf{W}}^{VR} \,. \tag{V-26}$$

where $\hat{\mathbf{W}}^{VR}$ satisfies the conditions

$$\hat{\mathbf{W}}^{VR} + (\hat{\mathbf{W}}^{VR})^T=0 \,,\ \mathrm{tr}[\hat{\mathbf{W}}^{VR}(\hat{\mathbf{W}}^{VR})^T]=1 \,. \tag{V-27}$$

The orthogonal transformations $\hat{\mathbf{Q}}^{eff,R}$ and $\hat{\mathbf{Q}}^{eff,V}$ are defined by

$$\hat{\mathbf{N}}_k^{eff} \equiv \hat{Q}_{km}^{eff,R}\hat{\mathbf{N}}_m^{R} \equiv \hat{Q}_{km}^{eff,V}\hat{\mathbf{N}}_m^{V} \,, \tag{V-28}$$

from which it may be seen that $\hat{\mathbf{N}}_k^{V} = \hat{Q}_{km}^{eff,V}\hat{Q}_{mq}^{eff,R}\hat{\mathbf{N}}_q^{R}$; from (V-25) it follows that

$$\hat{\mathbf{Q}}^{eff,R} = \hat{\mathbf{Q}}^{eff,V}\,\hat{\mathbf{Q}}^{VR}. \qquad (V-29)$$

It follows from (V - 26) that $\hat{\mathbf{Q}}^{eff,R}$ and $\hat{\mathbf{Q}}^{eff,V}$ may be expressed as

$$\hat{\mathbf{Q}}^{eff,R} \cong \hat{\mathbf{1}} + \xi_R \hat{\mathbf{W}}^{VR}\ ,\ \hat{\mathbf{Q}}^{eff,V} \cong \hat{\mathbf{1}} - \xi_V \hat{\mathbf{W}}^{VR} \qquad (V-30)$$

Where both ξ_R and ξ_V are small and $\xi_R + \xi_V = \xi$; thus from (V - 28):

$$\hat{\mathbf{N}}_k^R = \hat{\mathbf{N}}_k^{eff} - \xi_R \hat{\mathbf{W}}^{VR} \hat{\mathbf{N}}_q^{eff}\ ,\ \hat{\mathbf{N}}_k^V = \hat{\mathbf{N}}_k^{eff} + \xi_R \hat{\mathbf{W}}^{VR} \hat{\mathbf{N}}_q^{eff}\ . \qquad (V-31)$$

Due to the fact that $\hat{\mathbf{W}}^{VR}$ is skew-symmetric, and hence $\hat{\mathbf{N}}_k^{eff}\ \hat{\mathbf{W}}_{km}^{VR}\ \hat{\mathbf{N}}_m^{eff} = 0$, it follows that $\hat{\mathbf{W}}_{km}^{VR}\ \hat{\mathbf{N}}_m^{eff}$ is perpendicular $\hat{\mathbf{N}}_k^{eff}$ in the six-dimensional space. To obtain representations of the equations (V - 12) in terms of $\hat{\mathbf{N}}_k^{eff}$ only, (V - 30) is substituted into (V - 12), thus

$$\sum_{k=1}^{6} \Lambda_k^{eff,Grp} [\hat{\mathbf{E}}^A \cdot \hat{\mathbf{N}}_k^{eff}]^2 \le \sum_{k=1}^{6} \Lambda_k^{V,Grp} [\hat{\mathbf{E}}^A \cdot \hat{\mathbf{N}}_k^{eff} + \xi_V \hat{\mathbf{E}}^A \cdot (\hat{\mathbf{W}}_{kq}^{VR} \hat{\mathbf{N}}_q^{eff})]^2, \qquad (V-32)$$

$$\sum_{k=1}^{6} \frac{1}{\Lambda_k^{eff,Grp}} [\hat{\mathbf{T}}^A \cdot \hat{\mathbf{N}}_k^{eff}]^2 \le \sum_{k=1}^{6} \frac{1}{\Lambda_k^{R,Grp}} [\hat{\mathbf{T}}^A \cdot \hat{\mathbf{N}}_k^{eff} + \xi_R \hat{\mathbf{T}}^A \cdot (\hat{\mathbf{W}}_{kq}^{VR} \hat{\mathbf{N}}_q^{eff})]^2. \qquad (V-33)$$

We reconsider now the arguments leading from (V - 13) to (V - 15), using equations (V - 32) and (V - 33) in place of (V - 13). In the passage from (V - 32) and (V - 33) to (V - 14) it is argued that, since (V - 32) and (V - 33) hold for all possible strain states, they must hold for each mode when all other modes are zero. In this case the terms involving $\hat{\mathbf{W}}^{VR}_{kq}$ in (V - 32) and (V - 33) play no role due to the fact that $\hat{\mathbf{W}}^{VR}_{km}\,\hat{\mathbf{N}}^{eff}_{m}$ is perpendicular to $\hat{\mathbf{N}}^{eff}_{k}$ in the six-dimensional space, hence $\hat{\mathbf{W}}^{VR}_{km}\,\hat{\mathbf{N}}^{eff}_{m}$ is zero when all modes except $\hat{\mathbf{N}}^{eff}_{k}$ are zero. Thus the terms involving $\hat{\mathbf{W}}^{VR}_{km}\,\hat{\mathbf{N}}^{eff}_{m}$ in (V - 32) and in (V - 33) do not enter the final argument. (Note that the proof given above is a double application or the weaker coaxiality theorem given in Appendix **C**.) The equation (V - 14) then follows, as does (V -15) by the same arguments that were used in chapter V - 3, and the desired result has been obtained. This result may be summarized as a theorem: *The inequalities (V - 15) also hold when the six-dimensional orthogonal transformation $\hat{\mathbf{Q}}^{VR}$ that carries $\hat{\mathbf{s}}^{R.Grp}$ eigenvectors, $\hat{\mathbf{N}}^{R}_{k}$, into the $\hat{\mathbf{c}}^{V.Grp}$ eigenvectors, $\hat{\mathbf{N}}^{V}_{k}$, satisfies the condition that $4\xi^4$, ξ^2=2(6-tr$\hat{\mathbf{Q}}^{VR}$), be a small quantity compared to $\xi^2/2$, and we select $\hat{\mathbf{N}}^{eff}_{k}$ to be a system intermediate to $\hat{\mathbf{N}}^{R}_{k}$ and $\hat{\mathbf{N}}^{V}_{k}$ in the sense that $4\xi_R^4$, ξ_R^2=2(6-tr($\hat{\mathbf{Q}}^{eff.R}$), and $4\xi_V^4$, ξ_V^2=2(6-tr($\hat{\mathbf{Q}}^{eff.V}$)), are small quantities compared to $\xi_R^2/2$ and $\xi_V^2/2$, respectively.*

V – 5. Bounds for Any Less Symmetry by Tetragonal Symmetry

Tetragonal symmetry is the first symmetry with a distributor that will be dealt with it has one distributor and five distinct eigenvalues. The five distinct eigenvalues are given by (*A*6) and the single distributor is the angle α given by (*A*8). Note that the distributor appears in the expressions for the eigenmodes as shown by the first equations of the set (*A*7). In order to apply the criterion that $4\xi^4$ be small compared to $\xi^2/2$, ξ^2 is calculated for tetragonal symmetry,

$$\xi^2 = 4[1-\cos(\alpha_V-\alpha_R)] \,. \qquad (V-34)$$

The criterion is satisfied if $\alpha_V-\alpha_R$ is small. If $\alpha_R \le \alpha_V$ ($\alpha_V \le \alpha_R$)we select the angle α_{eff} so that

$$\alpha_V \le \alpha_{eff} \le \alpha_R \; (\alpha_R \le \alpha_{eff} \le \alpha_V). \qquad (V-35)$$

Using the expression for α in terms of the elastic coefficients (A8) for tetragonal symmetry, the inequality (V - 35) is written as

$$\tan 2\alpha_R \le \frac{(\hat{c}_{11}^{eff.Tet} + \hat{c}_{12}^{eff.Tet} - \hat{c}_{33}^{eff.Tet})}{2\sqrt{2}\hat{c}_{13}^{eff.Tet}} \le \tan 2\alpha_V$$
$$(\tan 2\alpha_V \le \frac{(\hat{c}_{11}^{eff.Tet} + \hat{c}_{12}^{eff.Tet} - \hat{c}_{33}^{eff.Tet})}{2\sqrt{2}\hat{c}_{13}^{eff.Tet}} \le \tan 2\alpha_R). \qquad (V-36)$$

The generalized Hill inequalities are then

$$\Lambda_1^{R,Tet}(\alpha_R) \le \Lambda_1^{eff,Tet}(\alpha_{eff}) \le \Lambda_1^{V,Tet}(\alpha_V), \Lambda_2^{R,Tet}(\alpha_R) \le \Lambda_2^{eff,Tet}(\alpha_{eff}) \le \Lambda_2^{V,Tet}(\alpha_V) \quad (V\text{-}37)$$

for the distributor eigenmodes and

$$\Lambda_3^{R,Tet} \le \Lambda_3^{eff,Tet} \le \Lambda_3^{V,Tet}, \Lambda_{(4,5)}^{R,Tet} \le \Lambda_{(4,5)}^{eff,Tet} \le \Lambda_{(4,5)}^{V,Tet}, \Lambda_6^{R,Tet} \le \Lambda_6^{eff,Tet} \le \Lambda_6^{V,Tet} \quad (V\text{-}38)$$

for the simple eigenmodes. Using the expression for the eigenvalues in terms of the elastic coefficients (A6) for tetragonal symmetry, it follows from $(V\text{-}37)$ that

$$\begin{aligned}
&\frac{4}{\hat{s}_{11}^T + \hat{s}_{22}^T + 2\hat{s}_{12}^T + 2\hat{s}_{33}^T \pm 2\sqrt{2}(\hat{s}_{13}^T + \hat{s}_{23}^T)\sec(2\alpha_R)} \le \\
&\frac{\hat{c}_{11}^{eff,Tet} + \hat{c}_{12}^{eff,Tet} + \hat{c}_{33}^{eff,Tet} \pm 2\sqrt{2}\hat{c}_{13}^{eff,Tet}\sec(2\alpha_{eff})}{2} \le \\
&\frac{\hat{c}_{11}^T + \hat{c}_{22}^T + 2\hat{c}_{12}^T + 2\hat{c}_{33}^T \pm 2\sqrt{2}(\hat{c}_{13}^T + \hat{c}_{23}^T)\sec(2\alpha_V)}{4}.
\end{aligned} \quad (V\text{-}39)$$

and, from $(V\text{-}34)$ that

$$\begin{aligned}
&\frac{2}{\hat{s}_{11}^T + \hat{s}_{22}^T - 2\hat{s}_{12}^T} \le \hat{c}_{11}^{eff,Tet} - \hat{c}_{12}^{eff,Tet} \le \frac{1}{2}(\hat{c}_{11}^T + \hat{c}_{22}^T - 2\hat{c}_{12}^T) \\
&\frac{1}{\hat{s}_{44}^T + \hat{s}_{55}^T} \le 2\hat{c}_{44}^{eff,Tet} \le \hat{c}_{44}^T + \hat{c}_{55}^T, \frac{1}{\hat{s}_{66}^T} \le \hat{c}_{66}^{eff,Tet} \le \hat{c}_{66}^T.
\end{aligned} \quad (V\text{-}40)$$

Note that the two relations (V - 39) may be summed to yield the inequalities

$$\frac{8(\hat{s}_{11}^{T}+\hat{s}_{22}^{T}-2\hat{s}_{12}^{T}+2\hat{s}_{33}^{T})}{(\hat{s}_{11}^{T}+\hat{s}_{22}^{T}-2\hat{s}_{12}^{T}+2\hat{s}_{33}^{T})^{2}-8(\hat{s}_{13}^{T}+\hat{s}_{23}^{T})^{2}}\leq\hat{c}_{11}^{eff.Tet}+\hat{c}_{12}^{eff.Tet}+\hat{c}_{33}^{eff.Tet}\leq$$

$$\frac{1}{2}(\hat{c}_{11}^{T}+\hat{c}_{22}^{T}+2\hat{c}_{12}^{T}+2\hat{c}_{33}^{T}). \qquad (V-41)$$

Examples of bounds of the effective tetragonal elastic constants are presented in Table V - 1. The bounds of the effective tetragonal eigenvalues, the least and the greatest terms occurring in the inequalities (V - 37) and (V - 38), for the orthotropic woods (spruce, Douglas fir, pine and maple) as well as orthotropic bone are given in the first eight rows of Table V - 1. The wood data are from Kollmann and Cote (1968) and the bone data are from Cowin (1989). The bounds for the effective tetragonal eigenvalues for four materials possessing monoclinic symmetry are presented in the last four rows of Table V - 1. The data for these materials are taken from Hearmon (1956). There are a number of features of Table V - 1 that are worthy of note. First, from the next to last column it may be seen that the condition that $\alpha_V - \alpha_R$ be small is easily satisfied. Second, from the last column the condition that $4\xi^4$ be small compared to $\xi^2/2$ is easily satisfied. Third, note the rightness of the bounds by comparing the value of the upper bound in column 3 with the corresponding lower bound value in column 4.

Table V - 1. Examples of bounds of the effective tetragonal elastic constants.

Material	C_{11}	C_{44}	C_{12}	C_{14}	C_{56}	Λ_1^V	Λ_4^V	Λ_1^R	Λ_4^R	α_V	
	C_{22}	C_{55}	C_{13}	C_{24}		Λ_2^V	Λ_5^V	Λ_2^R	Λ_5^R		ξ^2
	C_{33}	C_{66}	C_{23}	C_{34}		Λ_3^V	Λ_6^V	Λ_3^R	Λ_6^R	α_R	
Spruce	0.443	0.617	0.192	0	0	16.29	1.377	16.27	1.362	-1.501	
	0.775	0.760	0.321	0		0.782	1.377	0.719	1.362		0.000005
	16.28	0.036	0.442	0		0.417	0.072	0.383	0.072	-1.506	
Douglas Fir	1.226	1.174	0.753	0	0	17.096	2.082	17.06	2.048	-1.41	
	1.775	0.900	0.747	0		2.1550	2.082	2.062	2.048		0.000012
	17.00	0.080	0.940	0		0.75	0.16	0.717	0.16	-1.418	
Pine	0.721	1.742	0.454	0	0	16.07	1.205	15.97	0.967	-1.436	
	1.400	0.672	0.535	0		1.447	1.205	1.273	0.967		0.000064
	16.93	0.066	0.857	0		0.606	0.066	0.530	0.066	-1.454	
Maple	1.450	1.220	1.197	0	0	12.03	2.325	11.72	2.317	-1.086	
	2.565	1.100	1.267	0		2.655	2.325	2.403	2.317		0.000072
	11.94	0.292	1.820	0		0.815	0.580	0.719	0.580	-1.146	
Human	17.98	6.230	9.935	0	0	42.99	11.84	42.88	11.81	0.048	
	21.09	5.610	10.14	0		13.02	11.84	13.47	11.81		0.000002
Femur	27.51	4.530	10.70	0		9.108	9.060	9.068	9.36	0.045	
Canine	18.97	6.670	9.678	0	0	46.73	12.35	46.62	12.27	0.017	
	22.09	5.680	11.90	0		13.02	12.35	12.92	12.27		0.000007
Femur	29.58	4.680	11.93	0		10.80	9.36	10.69	9.36	0.011	
Bovine	14.00	6.990	6.327	0	0	32.20	13.78	31.53	13.77	-0.147	
	18.43	6.290	4.830	0		15.33	13.78	15.28	13.77		0.000097
Femur	25.00	5.290	6.97	0		9.870	10.58	9.633	10.58	-0.169	
Human	11.40	4.910	7.726	0	0	30.42	8.56	30.09	8.37	-0.105	
	14.12	3.650	5.986	0		12.38	8.56	12.29	8.37		0.000072
Tibia	22.35	2.410	6.742	0		5.055	4.82	4.965	4.82	-0.124	
Sodium	0.295	0.107	0.181	0.098	-0.027	0.731	0.082	0.722	0.036	0.035	
	0.332	0.057	0.171	0.022		0.222	0.082	0.081	0.036		0.00049
Thiosuphate	0.459	0.060	0.188	-0.068		0.133	0.06	0.074	0.047	-0.015	
Di-Po	0.396	0.110	0.173	0.004	0.005	0.773	0.099	0.715	0.092	-0.036	
	0.307	0.088	0.162	0.032		0.308	0.099	0.294	0.092		0.001
(DKT)	0.558	0.082	0.165	0.076		0.179	0.082	0.170	0.082	0.0001	
Lithim	0.706	0.242	0.263	0.259	-0.026	0.997	0.191	0.939	0.159	0.296	
	0.548	0.139	0.171	0.065		0.512	0.191	0.443	0.159		0.009
Suphate	0.619	0.114	0.269	-0.052		0.364	0.269	0.341	0.264	0.199	
Tartaric	0.193	0.082	0.139	-0.040	0.014	1.163	0.082	0.756	0.066	-0.26	
	0.465	0.081	0.202	-0.004		0.235	0.082	0.208	0.066		0.00013
Acid	0.930	0.106	0.367	-0.12		0.190	0.106	0.132	0.104	-0.273	

V – 6. Bounds for Any Less Symmetry by Trigonal Symmetry

Trigonal symmetry is a symmetry with two distributors and four distinct eigenvalues. The first distributor and the first two eigenvalues are the same as the distributor and the first two eigenvalues of tetragonal symmetry, hence the results (V - 35), (V - 36), (V - 37), (V - 39) and (V - 41) also apply to trigonal symmetry although they were originally obtained for tetragonal symmetry. The new distributor in trigonal symmetry is the angle β given by (A12). The other two distinct eigenvalues are given by (A10). In order to apply the criterion that $4\xi^4$ be small compared to $\xi^2/2$, ξ^2 is calculated for trigonal symmetry:

$$\xi^2 = 4[3-\cos(\alpha_V - \alpha_R) - 2\cos(\beta_V - \beta_R)]. \qquad (V - 42)$$

In the case of trigonal symmetry the criterion is satisfied if $\alpha_V - \alpha_R$ and $\beta_V - \beta_R$ are small, hence (IV - 35) applies for α_{eff} and the angle β_{eff} is selected so that $\beta_V \geq \beta_{eff} \geq \beta_R$ if $\beta_V \geq \beta_R$ or $\beta_R \geq \beta_{eff} \geq \beta_V$ if $\beta_R \geq \beta_V$. Using the expression for the angle β in terms of the elastic coefficients for trigonal symmetry (A12), the inequality $\beta_V \geq \beta_{eff} \geq \beta_R$ ($\beta_R \geq \beta_{eff} \geq \beta_V$) is rewritten as

$$\tan 2\beta_R \leq \frac{2\sqrt{2}\hat{c}_{14}^{eff,Tri}}{\hat{c}_{11}^{eff,Tri} - \hat{c}_{12}^{eff,Tri} - \hat{c}_{44}^{eff,Tri}} \leq \tan 2\beta_V.$$

$$\left(\tan 2\beta_V \leq \frac{2\sqrt{2}\hat{c}_{14}^{eff,Tri}}{\hat{c}_{11}^{eff,Tri} - \hat{c}_{12}^{eff,Tri} - \hat{c}_{44}^{eff,Tri}} \leq \tan 2\beta_R\right). \qquad (V - 43)$$

The generalized Hill inequalities, in addition to (V - 37), are then

$$\Lambda^{R,Tn}_{(3,6)}(\beta_R) \le \Lambda^{eff,Tn}_{(3,6)}(\beta_{eff}) \le \Lambda^{V,Tn}_{(3,6)}(\beta_V), \Lambda^{R,Tn}_{(4,5)}(\beta_R) \le \Lambda^{eff,Tn}_{(4,5)}(\beta_{eff}) \le \Lambda^{V,Tn}_{(4,5)}(\beta_V). \quad (V\text{ - }44)$$

Using the expressions for the eigenvalues in terms of the elastic coefficients (A10) for tetragonal symmetry, it follows from (V - 44) that

$$\frac{8}{\hat{s}^T_{11} + \hat{s}^T_{22} - 2\hat{s}^T_{12} + 2\hat{s}^T_{44} + 2\hat{s}^T_{55} + 2\hat{s}^T_{66} \pm 2\sqrt{2}\,(\hat{s}^T_{14} - \hat{s}^T_{24} - \sqrt{2}\,\hat{s}^T_{56})\csc(2\beta_R)} \le$$
$$\frac{\hat{c}^{eff,Tn}_{11} - \hat{c}^{eff,Tn}_{12} + \hat{c}^{eff,Tn}_{44} \pm 2\sqrt{2}\,\hat{c}^{eff,Tn}_{14}\csc(2\beta_{eff})}{2} \le$$
$$\frac{\hat{c}^T_{11} + \hat{c}^T_{22} - 2\hat{c}^T_{12} + 2\hat{c}^T_{44} + 2\hat{c}^T_{55} + 2\hat{c}^T_{66} \pm 2\sqrt{2}\,(\hat{c}^T_{14} - \hat{c}^T_{24} - \sqrt{2}\,\hat{c}^T_{56})\csc(2\beta_V)}{8}.$$

(V - 45)

Note that the two relations (V - 45) may be summed to yield the inequalities

$$\frac{16(\hat{s}^T_{11} + \hat{s}^T_{22} - 2\hat{s}^T_{12} + 2\hat{s}^T_{44} + 2\hat{s}^T_{55} + 2\hat{s}^T_{66})}{(\hat{s}^T_{11} + \hat{s}^T_{22} - 2\hat{s}^T_{12} + 2\hat{s}^T_{44} + 2\hat{s}^T_{55} + 2\hat{s}^T_{66})^2 - 8(\hat{s}^T_{14} - \hat{s}^T_{24} - \sqrt{2}\hat{s}^T_{56})^2\csc^2(2\beta_R)} \le$$
$$\hat{c}^{eff,Tn}_{11} - \hat{c}^{eff,Tn}_{12} + \hat{c}^{eff,Tn}_{44} \le \frac{\hat{c}^T_{11} + \hat{c}^T_{22} - 2\hat{c}^T_{12} + 2\hat{c}^T_{44} + 2\hat{c}^T_{55} + 2\hat{c}^T_{66}}{4}.$$

(V - 46)

Examples of bounds of the effective trigonal elastic constants are presented in Table V - 2. The bounds of the effective trigonal eigenvalues for materials possessing monoclinic symmetry are given in column 3 and 4. These bounds

Table V - 2. Examples of bounds of the effective trigonal elastic constants.

Material	c_{11} c_{44} c_{12} c_{14} c_{22} c_{55} c_{13} c_{24} c_{33} c_{66} c_{23} c_{34} c_{56}	Λ_1^V Λ_2^V Λ_3^V Λ_4^V	Λ_1^R Λ_2^R Λ_3^R Λ_4^R	α_V α_R	β_V β_R	ξ^2
Sodium Thiosuphate	0.295 0.107 0.181 0.098 0.332 0.570 0.171 0.022 0.459 0.060 0.188 -0.068 -0.027	0.731 0.222 0.13 0.048	0.722 0.081 0.106 0.028	0.035 -0.015	0.698 0.581	0.0055
Tartaric Acid	0.193 0.082 0.139 -0.04 0.465 0.081 0.202 -0.004 0.930 0.106 0.367 -0.12 0.014	1.163 0.235 0.153 0.076	0.756 0.208 0.133 0.062	-0.521 -0.547	-0.535 -0.721	0.0035
Lithim Sophate (Bechmann)	0.542 0.168 0.184 0.062 0.552 0.140 0.153 0.021 0.547 0.277 0.213 -0.027 -0.005	0.914 0.364 0.322 0.152	0.905 0.344 0.313 0.147	0.342 0.312	0.198 0.157	0.00042
Lithim Sophate (Bechmann)	0.706 0.242 0.263 0.159 0.548 0.139 0.114 0.065 0.619 0.269 0.165 -0.052 -0.026	0.997 0.512 0.332 0.175	0.939 0.443 0.315 0.155	0.296 0.19	0.316 0.242	0.0045
Ethylene Diamine Tartrate (Mason)	0.564 0.087 0.503 0.087 0.887 0.053 0.710 0.159 1.960 0.057 1.228 0.227 0.0006	3.013 0.176 0.148 0.062	1.825 0.122 0.078 0.055	-0.261 -0.131	-0.636 -0.409	0.006
Ethylene Diamine Tartrate (Bechmann)	0.397 0.106 0.108 -0.004 0.416 0.052 0.138 0.075 0.175 0.052 0.127 0.040 -0.001	0.598 0.092 0.183 0.072	0.559 0.088 0.088 0.064	0.368 0.393	-0.258 -0.222	0.0005
Di-Po (TDK) (Bechmann)	0.396 0.110 0.173 0.004 0.307 0.088 0.162 0.032 0.558 0.082 0.165 0.076 0.005	0.773 0.309 0.135 0.095	0.715 0.294 0.115 0.089	-0.036 0.00013	-0.335 -0.398	0.002
Di-Po (TDK) (Mason)	0.565 0.135 0.149 0.057 0.305 0.084 0.435 -0.014 0.782 0.096 0.116 0.080 -0.005	1.091 0.285 0.199 0.101	0.85 0.276 0.137 0.097	-0.13 -0.067	0.297 0.293	0.001

correspond to the least and the greatest terms occurring in the equalities (*V* - 37) and (*V* - 44). The data for these materials are taken from Hearmon (1956) and the surnames Mason and Bechmann after the material names refers to the author who reported the indicated values (Hearmon, 1956). There are a number of features of Table V - 2 that are worthy of note. First, from the fifth and sixth columns it may be seen that the conditions that $\alpha_V - \alpha_R$ and $\beta_V - \beta_R$, respectively, be small are easily satisfied. Second, from the last column the condition that $4\xi^4$ be small compared to $\xi^2/2$ is also easily satisfied. Lastly, note the tightness of the bounds by comparing the value of the upper bound in column 3 with the corresponding lower bound value in column 4.

The bounds of the effective transversely isotropic or hexagonal elastic constants are obtained from the trigonal bounds given above by allowing $\hat{c}_{14}^{eff\ Tri}$ to vanish. As in the case of trigonal symmetry, there are four distinct eigenvalues for transversely isotropic or hexagonal symmetry. Since $\hat{c}_{14}^{eff\ Tri}$ and hence the angle β defined by $(A12)$ vanish, the third through sixth eigenvalues of $(A10)$ reduced to those given by $(A13)$. These are simple eigenmodes and the bounds on $\hat{c}_{11}^{eff\ Hex} - \hat{c}_{12}^{eff\ Hex}$ and $\hat{c}_{44}^{eff\ Hex}$ are given by $(V-40)$ if the Tet superscript is replaced by Hex.

Examples of bounds of the effective hexagonal elastic constants are presented in Table V - 3. The remarks concerning the bounds of the effective trigonal elastic constants presented in Table V - 2 apply to the effective hexagonal elastic constants also.

V – 7. Discussion

It has been shown that it is possible to construct bounds on the effective elastic constants of any anisotropic elastic symmetry in terms of triclinic symmetry elastic coefficients. Specific bounds have been presented for the effective elastic coefficients of cubic, hexagonal, tetragonal and trigonal symmetries in terms of the elastic coefficients of triclinic symmetry.

Table V - 3. Examples of bounds of the effective hexagonal elastic constants.

Material	c_{11} c_{44} c_{12} c_{14} c_{22} c_{55} c_{13} c_{24} c_{33} c_{66} c_{23} c_{34} c_{56}	Λ_1^V Λ_2^V Λ_3^V Λ_4^V	Λ_1^R Λ_2^R Λ_3^R Λ_4^R	α_V α_R	ξ^2
Sodium Thiosuphate	0.296 0.107 0.181 0.098 0.333 0.570 0.171 0.022 0.460 0.060 0.188 -0.068 -0.027	0.731 0.222 0.096 0.082	0.722 0.081 0.058 0.036	0.035 -0.015	0.0005
Tartaric Acid	0.194 0.082 0.139 -0.04 0.466 0.081 0.202 -0.004 0.931 0.106 0.367 -0.12 0.014	1.163 0.235 0.148 0.082	0.756 0.208 0.116 0.066	-0.521 -0.547	0.00003
Lithim Sophate (Bechmann)	0.543 0.168 0.184 0.062 0.553 0.140 0.153 0.021 0.549 0.277 0.213 -0.027 -0.005	0.914 0.364 0.32 0.154	0.905 0.344 0.311 0.148	0.342 0.312	0.000045
Lithim Sophate (Bechmann)	0.707 0.242 0.263 0.159 0.550 0.139 0.114 0.065 0.620 0.269 0.165 -0.052 -0.026	0.997 0.512 0.317 0.191	0.939 0.443 0.298 0.159	0.296 0.19	0.002
Ethylene Diamine Tartrate (Mason)	0.566 0.087 0.503 0.087 0.888 0.053 0.710 0.159 1.961 0.057 1.228 0.227 0.0006	3.013 0.176 0.14 0.07	1.825 0.122 0.077 0.056	-0.261 -0.131	0.00084
Ethylene Diamine Tartrate (Bechmann)	0.398 0.106 0.108 -0.004 0.417 0.052 0.138 0.075 0.176 0.052 0.127 0.040 -0.001	0.598 0.092 0.176 0.079	0.559 0.088 0.087 0.065	0.368 0.393	0.00012
Di-Po (TDK) (Bechmann)	0.397 0.110 0.173 0.004 0.308 0.088 0.162 0.032 0.559 0.082 0.165 0.076 0.005	0.773 0.309 0.13 0.099	0.715 0.294 0.11 0.092	-0.036 0.00013	0.000263
Di-Po (TDK) (Mason)	0.567 0.135 0.149 0.057 0.306 0.084 0.435 -0.014 0.783 0.096 0.116 0.080 -0.005	1.091 0.285 0.191 0.11	0.85 0.276 0.132 0.10	-0.13 -0.067	0.0008

The elastic coefficients of triclinic symmetry may be specialized to any greater symmetry, the symmetry as great as the symmetry of the effective coefficients.

The method applies to all the material symmetries of linear elasticity, with necessary modifications for the greatest and least symmetries, but it was only for the cubic, hexagonal, tetragonal and trigonal symmetries that algebraic expressions for the bounds on the effective elastic constants can be easily constructed. In particular the method also applies to materials with orthotropic and monoclinic symmetry, but it is easier to apply the formulas numerically due to the occurrence of solutions to cubic and quadratic equations in the analysis.

VI. On the selection of the anisotropic elastic symmetry representation for a textured material

VI – 1. Introduction

The question of the identification of the best elastic symmetry representation for a non-crystalline or textured anisotropic material occurs frequently for natural materials (Cowin and Mehrabadi, 1989). Cowin and Mehrabadi (1987) presented a solution to the problem given the values of the components of a fourth rank elasticity tensor of a material relative to a known, but arbitrary, coordinate system, they showed how to determine the elastic symmetry using the techniques of linear algebra. However, this method is not robust with respect to the input values of the components of a fourth rank elasticity tensor; slight errors in the data could cause a misidentification of the symmetry. The method only works well when the data was exact. For example, cubic symmetry is characterized by three distinct elastic constants, say c_{11} - c_{12} and c_{44}; however if $2c_{44} = c_{11} - c_{12}$, the material is isotropic. Thus if the data for an isotropic material has a value of $2c_{44}$ given by $2c_{44} = c_{11} - c_{12}$ + a small error term, the material will be mistakenly identified as cubic.

It has been shown in chapter V that it is possible to construct bounds on the effective elastic constants of a material with any anisotropic elastic symmetry in terms of a higher or equal anisotropic elastic symmetry. In that work specific bounds are given for the effective elastic coefficients of cubic, hexagonal, tetragonal and trigonal symmetries in terms of the elastic coefficients of triclinic symmetry (or any higher symmetry). Here we use these results to determine the effective symmetry of natural materials.

Four natural materials, human and whale cancellous bone, hardwoods and softwoods, are considered. These materials were selected for three reasons. First, our long term research concerns cancellous bone, a material whose elastic constants are strongly dependent upon volume fraction. Second, the data on wood provides illustrative contrasts with the cancellous bone data because wood is more strongly anisotropic. Three, the dependence of the elastic constants upon composition, or volume fraction, provides elastic constants that are functions rather than single numerical values to be analyzed. These functions of composition are the basis for stronger results than could be obtained for a material without a compositional dependence. The data on the dependence of the anisotropic elastic constants of human cancellous bone as functions of volume fraction are taken from chapter III. The data on the elastic constant matrices of hardwoods and softwoods, recorded with the specimen density, are taken from Hearmon (1948). Bounds on the effective isotropic and transversely isotropic elastic constants are determined from these orthotropic symmetry data in the present work. It is shown that human and whale cancellous bones, although generally considered to be orthotropic, are in fact very close to transversely isotropic in their material symmetry. A similar conclusion applies for hardwoods and softwoods.

After a section on the notation we employ for the generalized Hooke's law, the previous work on the anisotropic elastic constant bounds is summarized. In the section that follows isotropic and transversely isotropic bounds for human cancellous bone are presented. The isotropic and transversely isotropic bounds for the elastic constants of whale cancellous bone are briefly discussed in section VI - 5. In section VI - 6 some of results for hardwoods and softwoods are presented. In section VI - 5 there is a short discussion of results.

VI – 2. Notation for the Generalized Hooke's Law

Voigt (1928) wrote the anisotropic form of Hooke's law in matrix notation as $\mathbf{T} = \mathbf{c}\,\mathbf{E}$ or

$$\begin{bmatrix} T_{11} \\ T_{22} \\ T_{33} \\ T_{23} \\ T_{13} \\ T_{12} \end{bmatrix} = \begin{bmatrix} c_{11} & c_{12} & c_{13} & c_{14} & c_{15} & c_{16} \\ c_{12} & c_{22} & c_{23} & c_{24} & c_{25} & c_{26} \\ c_{13} & c_{23} & c_{33} & c_{34} & c_{35} & c_{36} \\ c_{14} & c_{24} & c_{34} & c_{44} & c_{45} & c_{46} \\ c_{15} & c_{25} & c_{35} & c_{45} & c_{55} & c_{56} \\ c_{16} & c_{26} & c_{36} & c_{46} & c_{56} & c_{66} \end{bmatrix} \begin{bmatrix} E_{11} \\ E_{22} \\ E_{33} \\ 2E_{23} \\ 2E_{13} \\ 2E_{12} \end{bmatrix} \qquad (VI - 1)$$

where $\mathbf{T}$, $\mathbf{E}$ and $\mathbf{c}$ represent the stress tensor, the strain tensor, and a non-tensorial matrix of elastic coefficients, respectively. Introducing new notation, (*VI* - 1) can be rewritten in the form $\hat{\mathbf{T}} = \hat{\mathbf{c}}\hat{\mathbf{E}}$ where the shearing components of these new six-dimensional stress and strain vectors, denoted by $\hat{\mathbf{T}}$ and $\hat{\mathbf{E}}$ respectively, are multiplied by $\sqrt{2}$, and $\hat{\mathbf{c}}$ is a new six-by-six matrix (Mehrabadi and Cowin, 1990). The matrix form of $\hat{\mathbf{T}} = \hat{\mathbf{c}}\hat{\mathbf{E}}$ is given by

$$\begin{bmatrix} T_{11} \\ T_{22} \\ T_{33} \\ \sqrt{2}T_{23} \\ \sqrt{2}T_{13} \\ \sqrt{2}T_{12} \end{bmatrix} = \begin{bmatrix} c_{11} & c_{12} & c_{13} & \sqrt{2}c_{14} & \sqrt{2}c_{15} & \sqrt{2}c_{16} \\ c_{12} & c_{22} & c_{23} & \sqrt{2}c_{24} & \sqrt{2}c_{25} & \sqrt{2}c_{26} \\ c_{13} & c_{23} & c_{33} & \sqrt{2}c_{34} & \sqrt{2}c_{35} & \sqrt{2}c_{36} \\ \sqrt{2}c_{14} & \sqrt{2}c_{24} & \sqrt{2}c_{34} & c_{44} & c_{45} & c_{46} \\ \sqrt{2}c_{15} & \sqrt{2}c_{25} & \sqrt{2}c_{35} & c_{45} & c_{55} & c_{56} \\ \sqrt{2}c_{16} & \sqrt{2}c_{26} & \sqrt{2}c_{36} & c_{46} & c_{56} & c_{66} \end{bmatrix} \begin{bmatrix} E_{11} \\ E_{22} \\ E_{33} \\ \sqrt{2}E_{23} \\ \sqrt{2}E_{13} \\ \sqrt{2}E_{12} \end{bmatrix} \qquad (VI-2)$$

The matrix $\hat{\mathbf{c}}$ is called the matrix of *elastic coefficients* and its inverse $\hat{\mathbf{s}}$, $\hat{\mathbf{E}} = \hat{\mathbf{s}}\hat{\mathbf{T}},\ \hat{\mathbf{s}} = \hat{\mathbf{c}}^{-1}$ is called the *compliance* matrix. The symmetric matrices $\hat{\mathbf{c}}$ and $\hat{\mathbf{s}}$ can be shown to represent the components of a second rank tensor in a six-dimensional space, whereas the components of the matrix **c** appearing in $(VI-1)$ do not form a tensor (Mehrabadi and Cowin, 1990).

The eigenvalues of the matrix $\hat{\mathbf{c}}(\hat{\mathbf{s}})$ are the six numbers $\Lambda(1/\Lambda)$ satisfying the equations

$$(\hat{\mathbf{c}} - \Lambda\mathbf{1})\hat{\mathbf{N}} = 0, \quad ((\hat{\mathbf{s}} - (1/\Lambda)\mathbf{1})\hat{\mathbf{N}} = 0), \qquad (VI-3)$$

where the vectors $\hat{\mathbf{N}}$ represent the normalized eigenvectors of $\hat{\mathbf{c}}$ or $\hat{\mathbf{s}}$. Since $\hat{\mathbf{c}}$ (or $\hat{\mathbf{s}}$) is positive definite it has six positive eigenvalues. These eigenvalues are called the *Kelvin moduli* and are denoted by Λ_i, i = 1,2, ..., 6, and are ordered (if possible) by the inequalities $\Lambda_1 > = \ldots\ \Lambda_6 > 0$.

The eigensystems for various anisotropic elastic symmetries are described in Mehrabadi and Cowin (1990). There exist six eigentensors of stress, denoted by $\hat{\mathbf{T}}^{(k)}$, $k = 1, 2, \ldots, 6$, in the six-dimensional space, or by $\mathbf{T}^{(k)}$ in 3-dimensional spaces, and six eigentensors of strain, denoted by $\hat{\mathbf{E}}^{(k)}$ and $\mathbf{E}^{(k)}$, $k = 1, 2, \ldots, 6$. respectively, which are related by the six equations

$$\hat{\mathbf{T}}^{(k)} = \Lambda_k \hat{\mathbf{E}}^{(k)} \quad or \quad \mathbf{T}^{(k)} = \Lambda_k \mathbf{E}^{(k)}, \quad k = 1, \ldots, 6. \tag{VI-4}$$

Further, they show that $\hat{\mathbf{T}}, \hat{\mathbf{E}}, \hat{\mathbf{c}}$ and $\hat{\mathbf{s}}$ have the representations

$$\hat{\mathbf{T}} = \sum_{k=1}^{6} \hat{\mathbf{T}}^{(k)} = \sum_{k=1}^{6} \Lambda_k \hat{\mathbf{E}}^{(k)} = \sum_{k=1}^{6} \Lambda_k \mathbf{N}_k \mid \hat{\mathbf{E}}^{(k)} \mid,$$

$$\hat{\mathbf{E}} = \sum_{k=1}^{6} \hat{\mathbf{E}}^{(k)} = \sum_{k=1}^{6} \frac{1}{\Lambda_k} \hat{\mathbf{T}}^{(k)} = \sum_{k=1}^{6} \frac{1}{\Lambda_k} \mathbf{N}_k \mid \hat{\mathbf{T}}^{(k)} \mid. \tag{VI-5}$$

and

$$\hat{\mathbf{c}} = \sum_{k=1}^{6} \Lambda_k \hat{\mathbf{N}}_k \otimes \hat{\mathbf{N}}_k, \quad \hat{\mathbf{s}} = \sum_{k=1}^{6} \frac{1}{\Lambda_k} \hat{\mathbf{N}}_k \otimes \hat{\mathbf{N}}_k, \tag{VI-6}$$

Finally the superscript *Grp* stands for the symmetry group. In this paper we employ the following short notation for the indicated symmetry group: Transversely Isotropy = *TI*, Orthotropic = *Ort*, and Triclinic = *T*. Thus the notation

$\hat{c}^T$ represents the $\hat{c}$ matrix for a triclinic material and $\hat{c}^{TI}$ represents the $\hat{c}$ matrix for a transversely isotropic material in its symmetry coordinate system. Where appropriate, the components of these matrices also carry the superscript *Grp* notation, as do the eigenvalues.

VI – 3. Generalized Formulations of Bounds on Anisotropic Elastic Constants

Hill (1952) showed that it is possible to construct bounds on the effective isotropic elastic constants of a material with triclinic or greater symmetry. Hill noted that triclinic symmetry coefficients appearing in the bounds could be specialized to those of a greater symmetry, yielding the effective isotropic elastic coefficients for a material with any elastic symmetry. It was showed in chapter V that it is possible to construct bounds on the effective elastic constants of a material with any anisotropic elastic symmetry in terms of triclinic symmetry elastic coefficients. In chapter V we noted that it was then possible to specialize the triclinic symmetry coefficients appearing in the bounds to those of a greater symmetry. Specific bounds for the effective elastic coefficients of cubic, hexagonal, tetragonal and trigonal symmetries in terms of the elastic coefficients of triclinic symmetry are also given in chapter V. These results were obtained by combining the approach of Hill (1952) with a representation of the stress-strain relations due, in principle, to Kelvin but recast in the structure of contemporary linear algebra. Hill (1952) employed the Voigt (1928) averaging process over all orientations to obtain the orientational average "isotropic" elastic constants. Voigt

(1928) applied this process to the elasticity tensor and Reuss (1929) applied it to the compliance tensor.

It was showed in chapter V that the six eigenvalues of the Voigt bound elasticity tensor, Λ_k^V, $k = 1, ..., 6$, and the inverse of the six eigenvalues of the Reuss bound compliance tensor Λ_k^R, $k = 1, ..., 6$, constituted upper and lower bounds on the values of the six eigenvalues of the effective elasticity tensor Λ_k^{eff}, $k = 1, ...,6$,

$$\Lambda_k^{R,Grp} \leq \Lambda_k^{eff,Grp} \leq \Lambda_k^{V,Grp}, \quad \text{for } k=1,...,6. \qquad (VI-7)$$

Hill (1952) obtained this result in the case of isotropy; a result we review in the present notation. In the case of isotropic symmetry there are two distinct eigenvalues of the elasticity tensor or compliance tensor - one has a multiplicity of one and the other has a multiplicity of five (Mehrabadi and Cowin, 1990; Appendix A). The eigenvalue of multiplicity of one is three times the bulk modulus K, and the eigenvalue of multiplicity of five is twice the shear modulus G. Thus, the isotropic symmetry, $(VI-7)$ takes the form

$$K^R \leq K^{eff} \leq K^V, \; G^R \leq G^{eff} \leq G^V, \qquad (VI-8)$$

where the values of the Voigt and Reuss bounds on K and G are given by

$$K^V = \frac{1}{9}(\hat{c}_{11}^T + \hat{c}_{22}^T + \hat{c}_{33}^T) + \frac{2}{9}(\hat{c}_{12}^T + \hat{c}_{23}^T + \hat{c}_{31}^T),$$

$$K^R = \frac{1}{(\hat{s}_{11}^T + \hat{s}_{22}^T + \hat{s}_{33}^T) + 2(\hat{s}_{12}^T + \hat{s}_{23}^T + \hat{s}_{31}^T)},$$

$$G^V = \frac{1}{15}(\hat{c}_{11}^T + \hat{c}_{22}^T + \hat{c}_{33}^T - \hat{c}_{12}^T - \hat{c}_{23}^T - \hat{c}_{31}^T) + \frac{1}{10}(\hat{c}_{44}^T + \hat{c}_{55}^T + \hat{c}_{66}^T), \qquad (VI-9)$$

and

$$G^R = \frac{1}{\frac{4}{15}(\hat{s}_{11}^T + \hat{s}_{22}^T + \hat{s}_{33}^T - \hat{s}_{12}^T - \hat{s}_{23}^T - \hat{s}_{31}^T) + \frac{2}{5}(\hat{s}_{44}^T + \hat{s}_{55}^T + \hat{s}_{66}^T)},$$

and where the bounds are in terms of a elasticity matrix $\hat{\mathbf{c}}^T$ representing the $\hat{\mathbf{c}}$ matrix for a triclinic material. The inequalities (VI - 8) appear in the paper of Hill (1952). The inequality (VI - 7) are referred to here as the generalized Hill inequalities.

There are four distinct eigenvalues for transversely isotropic symmetry and one additional parameter called a distributor (Mehrabadi and Cowin, 1990). Before introducing the triclinic bounds associated with this symmetry we introduce the notation

$$\tan 2\alpha_V = \frac{\frac{1}{2}(\hat{c}_{11}^T + \hat{c}_{11}^T) + \hat{c}_{12}^T - \hat{c}_{33}^T}{2\sqrt{2}(\hat{c}_{13}^T + \hat{c}_{23}^T)}, \quad \tan 2\alpha_R = \frac{\frac{1}{2}(\hat{s}_{11}^T + \hat{s}_{11}^T) + \hat{s}_{12}^T - \hat{s}_{33}^T}{2\sqrt{2}(\hat{s}_{13}^T + \hat{s}_{23}^T)},$$

and

$$\tan 2\alpha_{eff} = \frac{(\hat{c}_{11}^{eff.TI} + \hat{c}_{12}^{eff.TI} - \hat{c}_{33}^{eff.TI})}{2\sqrt{2}\hat{c}_{13}^{eff.TI}}. \qquad (VI-10)$$

The expressions for the bounds of the transversely isotropic eigenvalues in terms of the triclinic symmetry coefficients are given by the following inequalities:

$$\frac{4}{\hat{s}_{11}^T + \hat{s}_{22}^T + 2\hat{s}_{12}^T + 2\hat{s}_{33}^T \pm 2\sqrt{2}(\hat{s}_{13}^T + \hat{s}_{23}^T)\sec(2\alpha_R)} \leq$$

$$\frac{\hat{c}_{11}^{eff,TI} + \hat{c}_{12}^{eff,TI} + \hat{c}_{33}^{eff,TI} \pm 2\sqrt{2}\hat{c}_{13}^{eff,TI}\sec(2\alpha_{eff})}{2} \leq \qquad (VI-11)$$

$$\frac{\hat{c}_{11}^T + \hat{c}_{22}^T + 2\hat{c}_{12}^T + 2\hat{c}_{33}^T \pm 2\sqrt{2}(\hat{c}_{13}^T + \hat{c}_{23}^T)\sec(2\alpha_V)}{4},$$

and

$$\frac{2}{\hat{s}_{11}^T + \hat{s}_{22}^T - 2\hat{s}_{12}^T} \leq \hat{c}_{11}^{eff,TI} - \hat{c}_{12}^{eff,TI} \leq \frac{1}{2}(\hat{c}_{11}^T + \hat{c}_{22}^T - 2\hat{c}_{12}^T)$$

$$\frac{1}{\hat{s}_{44}^T + \hat{s}_{55}^T} \leq 2\hat{c}_{44}^{eff,TI} \leq \hat{c}_{44}^T + \hat{c}_{55}^T, \frac{1}{\hat{s}_{66}^T} \leq \hat{c}_{44}^{eff,TI} \leq \hat{c}_{66}^T. \qquad (VI-12)$$

The bounds associated with the additional parameter, the distributor, are either

$$\tan 2\alpha_R \leq \frac{(\hat{c}_{11}^{eff,TI} + \hat{c}_{12}^{eff,TI} - \hat{c}_{33}^{eff,TI})}{2\sqrt{2}\hat{c}_{13}^{eff,Tet}} \leq \tan 2\alpha_V$$

or $\qquad (VI-13)$

$$\tan 2\alpha_V \leq \frac{(\hat{c}_{11}^{eff,TI} + \hat{c}_{12}^{eff,TI} - \hat{c}_{33}^{eff,TI})}{2\sqrt{2}\hat{c}_{13}^{eff,Tet}} \leq \tan 2\alpha_R.$$

VI – 4. Bounds on the Effective Isotropic and Transversely Isotropic Elastic Constants of Human Cancellous Bone

In chapter III we analyzed a 141 specimen data base consisting the elasticity matrices of human cancellous bone as functions of volume fraction. The elastic constants were measured relative to arbitrary coordinate systems; no material symmetry was assumed. The full set of anisotropic constants were obtained by first imaging the specimen (Odgaard *et al.* 1996) and then evaluating the effective elastic constants using a homogenization procedure in a finite element model (van Reitbergen *et al.*, 1996,1997). It was also established in Chapter III that human cancellous bones had orthotropic symmetry at a confidence level of 95% using statistical methods. The elasticity matrices of human cancellous bone were constructed as functions of volume fraction, using the fact that the eigenvalues of the elastic coefficient matrix are strongly dependent upon volume fraction (Table III - 3) and the eigenvectors are almost independent of the solid volume fraction.

The Voigt and Reuss bounds on elastic constants of a material with a certain material symmetry by a higher symmetry (Chapter V) provide a measure of the closeness between the two symmetries of the material. The closeness is represented by the Voigt and Reuss bound differences in the eigenvalues or Young's moduli. For instance, the Voigt and Reuss bounds on eigenvalues of a material are identical if the bounds are calculated for the same symmetry, that is to say the higher and lower symmetries are taken to be the same and to have the same values for the elastic constants. Since orthotropic elastic human cancellous bone data is employed, the bounds on the elastic constants by any higher symmetry are in terms of orthotropic elastic constants. In the application of the results (VI - 9), (VI - 10), (VI - 11), (VI - 12) and (VI - 13) are replaced the elastic constants superscript T by Ort.

The isotropic bounds on the bulk modulus and shear modulus of human cancellous regressed against solid volume fraction were accomplished (Figure 6). The range of the solid volume fraction is from 0.05 to 0.35. Voigt and Reuss bounds on the effective bulk modulus and effective shear modulus have high squared correlation coefficients (over 0.919). The differences between the Voigt and Reuss eigenvalues of human cancellous bone are not very large. The biggest percentage in difference is 17.3% (the difference between the eigenvalues of Voigt and Reuss divided by the mean of Voigt and Reuss).

The Voigt and Reuss bounds on the transversely isotropic eigenvalues of the elasticity matrix of human cancellous bone are plotted against solid volume fraction in Figure 7. These bounds are obtained using the formulas (VI - 10) through (VI - 13) with the set of triclinic elastic constants replaced by the set of orthotropic elastic constants. Although we have demonstrated in Chapter III that human cancellous bone has orthotropic symmetry, the difference between the orthotropic and transversely isotropic symmetries is small (below 7.9% in the Voigt and Reuss bounds of the eigenvalues). Thus, the symmetry of human cancellous bone, although orthotropic, is close to transversely isotropic.

VI – 5. Bounds on the Effective Isotropic and Transversely Isotropic Elastic Constants of Whale Cancellous Bone

The orthotropic elastic coefficient matrices of 29 whale cancellous bone specimens were also obtained by using the same method as that used for human cancellous bone in chapter III. The results of linear log-log regression of the eigenvalue invariants against solid volume fraction for whale cancellous bone are shown in Table VI - 1. The bounds on the isotropic bulk and shear moduli as a function of solid volume fraction are shown in Figure 8, and the bounds on the four transversely isotropic eigenvalues are shown in Figure 9. The results are similar to those for human cancellous bone. The error in the isotropic bounds for the bulk and shear moduli (see Figure 8) is below 9.6%. The error is under 3% in the case of the transversely isotropic eigenvalue bounds (Figure 9). The material symmetry of whale cancellous bone data employed here is much closer to transversely isotropic symmetry than is the human cancellous bone data.

Table VI - 1. Results of the linear log-log regression of the eigenvalue invariants against volume fraction ϕ for cancellous whale bone.

Eigenvalue	Λ_1	Λ_2	Λ_3	Λ_4	Λ_5	Λ_6
MPa	$2199E_t\,\phi^{1.75}$	$1004E_t\,\phi^{1.832}$	$341E_t\,\phi^{1.394}$	$340E_t\,\phi^{1.422}$	$792E_t\,\phi^{1.714}$	$1250E_t\,\phi^{1.982}$
R^2	0.982	0.935	0.948	0.913	0.946	0.964

VI – 6. Bounds on the Elastic Constants of Hardwoods and Softwoods by Isotropic and Transversely Isotropic Symmetries

The data on wood was taken from Hearmon (1948). It consisted of the orthotropic elastic coefficient matrices of 15 hardwoods and 8 softwoods specimens and the material density associated with each (Tables III - 1 and III - 2). We found, by employing the same procedures as those for cancellous bones, namely decomposing the elastic constant matrices into eigenvalues and eigenvectors, that the eigenvalues were strongly dependent upon density and the eigenvectors are almost independent of density. The eigenvalues of the orthotropic elastic matrices of hardwoods and softwoods regressed as functions of material density are shown in Tables III - 3. The isotropic bounds on the bulk and shear modulus of the hardwoods and the softwoods are shown in Figures 10 and 11. From these figures it is easy to see that the differences between the Voigt and Reuss bounds are significant (over 80%) in the case of isotropy. For the transversely isotropic bounds on the elastic constants (eigenvalues) of hardwoods (Figure 12), the first and third Voigt and Reuss eigenvalues are very close, but the second and the fourth eigenvalues differ by 20%. For the transversely isotropic bounds on the elastic constants (eigenvalues) of softwoods (Figure 13), the first, second and third Voigt and Reuss eigenvalues differ by less than 20%, but the differences of the fourth Voigt and Reuss eigenvalue are large.

VI – 7. Conclusion

Upon the basis of the data analyzed, we conclude that, although human and whale cancellous bones are orthotropic materials, there is only a small error in considering them to be transversely isotropic, especially for whale cancellous bone. A similar conclusion applies for hardwoods and softwoods. Although human and whale cancellous bone, hardwoods and softwoods are orthotropic materials, their degrees of orthotropy or anisotropy are different. These differences are reflected by the differences of Voigt and Reuss bounds for bulk and shear moduli. We conclude that human and whale cancellous bone has a lesser degree of orthotropy or anisotropy than hardwoods and softwoods because the differences of Voigt and Reuss bounds for human and whale cancellous bones are much smaller than those for hardwoods and softwoods. This may be verified by the inspection of Figures 6, 8, 10, and 11.

We also observe that the differences in Voigt and Reuss bounds increase with increasing the solid volume fractions for cancellous bones or density for woods. This suggests that the natural materials like cancellous bones and woods will become more anisotropic with increasing volume fraction or density. Human and whale cancellous bones are more isotropic at lower solid volume fractions.

VII. Summary

Over the last decade, the study of bone morphology has evolved into a new field of research. It has been proposed that it is possible to predict the macrostructural mechanical properties of bone tissue from microstructural parameters. In the most recent studies, the evaluation of bone mechanical competence from its architecture has been recognized as a reasonable approach for the determination of bone quality. In this dissertation it is suggested that the key factor controlling the mechanical properties of cancellous bone is the solid volume fraction or apparent density. In the second and the third chapters of this thesis we provide a theoretical basis and an analysis of experimental data to support this conclusion.

The method proposed in the second chapter for the averaging of elastic constant data treats each measurement data set systematically as a tensor instead of as a collection of individual elastic constant or matrix element measurements. This proposed method for averaging different measurements of the anisotropic elastic constants for a specific material has an advantage over the traditional method (e.g., Hearmon's) of averaging the individual matrix components of the elasticity or compliance matrices. Averaging invariants removes the effect of the reference coordinate system in the measurements. The traditional method of averaging the components may induce errors due to the various reference coordinate systems, thus distorting the nature of the symmetry.

The application of this result to several data bases showed that, for some materials with varied composition (softwoods, feldspar), the eigenvectors, but not the eigenvalues, were relatively independent of material composition. This result suggests a paradigm for extending the empirical method of regressing Young's modulus data against composition or porosity in an isotropic material to anisotropic materials. Our results suggest that one may be hopeful that the eigenvectors of a material of varied composition will not depend upon the varied composition, permitting all the compositional dependence to be represented only by the eigenvalues. The eigenvectors carry information on the material symmetry.

When the method mentioned above was applied to human and whale cancellous bones (chapter three), we found that the elasticity matrices of human and whale cancellous bone data had the properties expected: the eigenvectors of the elastic constant matrices are relatively independent of volume fraction, but the eigenvalues are strongly dependent on the volume fraction. It was shown that a knowledge of the volume fraction and the trabecular grain explained all but 5% of the variance in the Young's modulus, and all but 7% of the variance in shear modulus data. These results are superior to those results obtained in previous studies by other researchers. This study provided the first statistical proof that human and whale cancellous bones have orthotropic symmetry. The confidence level was 95%. It was concluded that, for these human and whale cancellous bone data, the volume fraction plus the trabecular grain are slightly better predictors of elastic constants than the fabric tensor models currently in use. The fabric tensors are elementary measures of the cancellous bone architectures.

It is shown in chapter four that it is possible to construct bounds on the effective elastic constants of any anisotropic elastic symmetry in terms of triclinic symmetry elastic coefficients. In this chapter the generalized Voigt and Reuss bounds on eigenvalues are developed, expanding the result of Hill (1952, 1963) who constructed bounds only on the effective isotropic elastic coefficients of a material with triclinic symmetry.

An application of these bounds is presented in chapter five. In this chapter we show that although human and whale cancellous bones are orthotropic materials, there is only a small error in considering them to be transversely isotropic. A similar conclusion applies for hardwoods and softwoods. We also show that the degrees of anisotropy for human and whale cancellous bones are lesser than those for hardwoods and softwoods. These conclusions are demonstrated by the differences in the Voigt and Reuss bounds on Young's moduli and shear moduli.

Figure 1. Trabecular grain

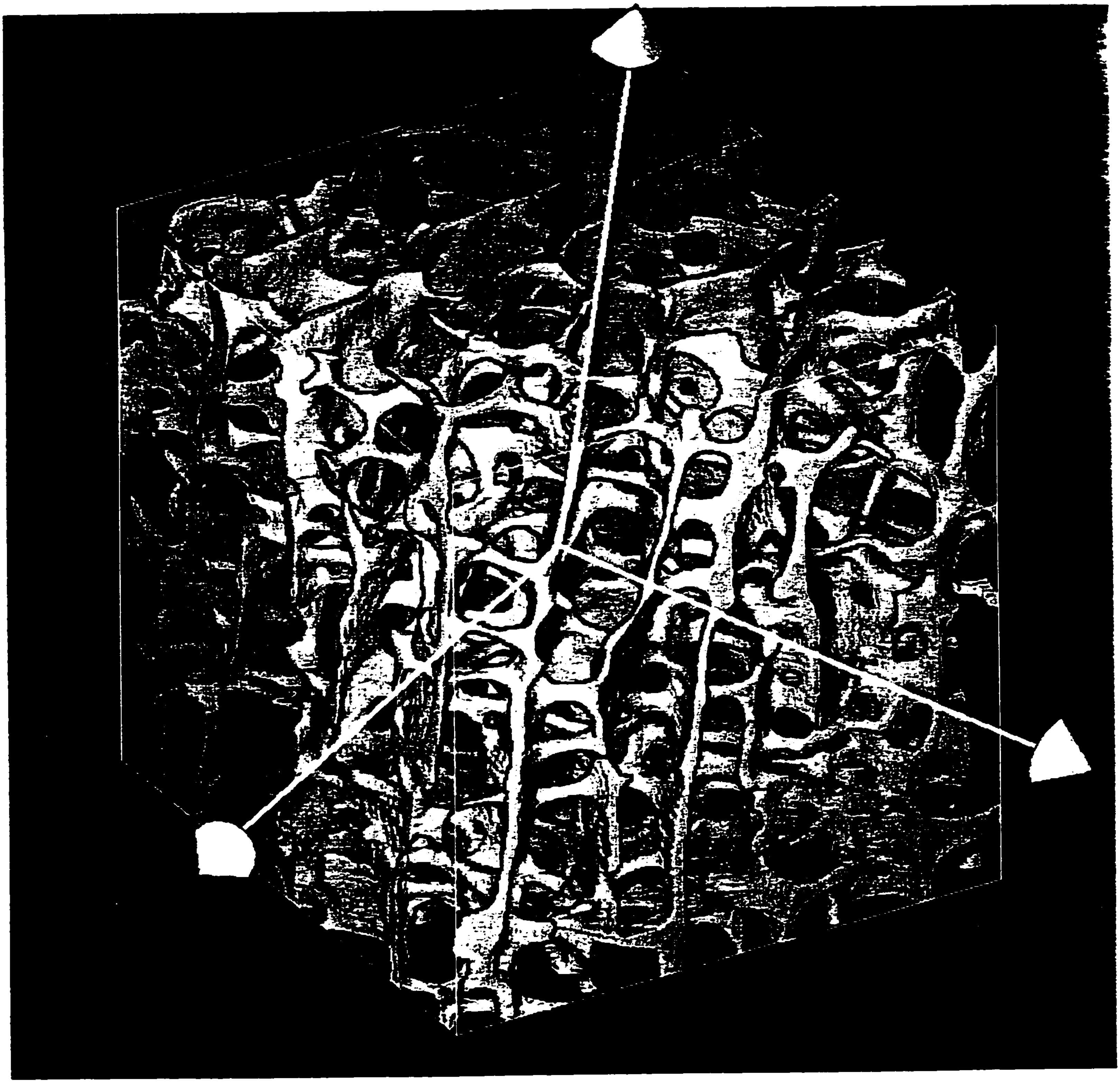

Figure 2. Human cancellous bone

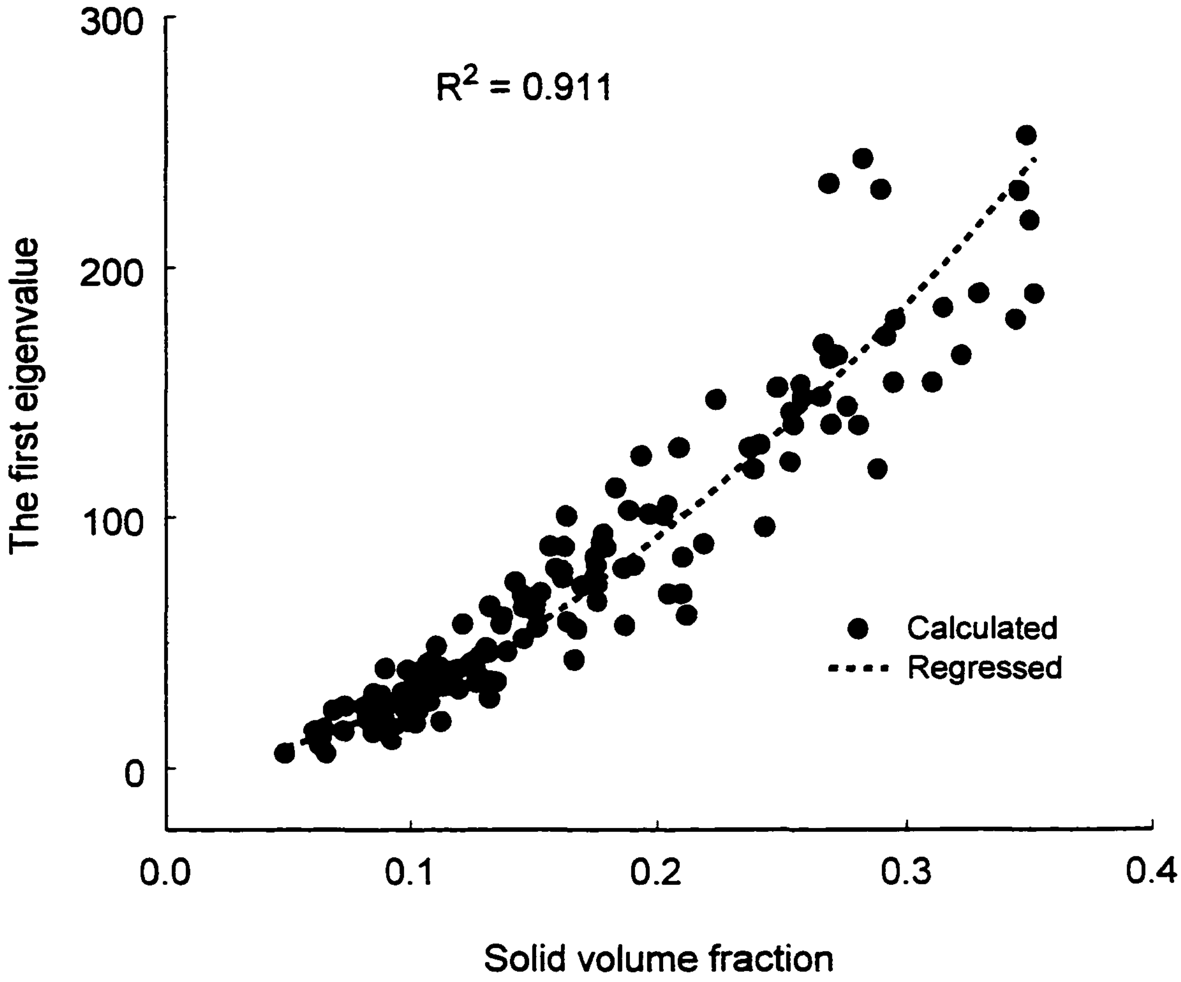

Figure 3. Young's modulus as a function of direction

Human bone (average) at $\phi = 0.35$

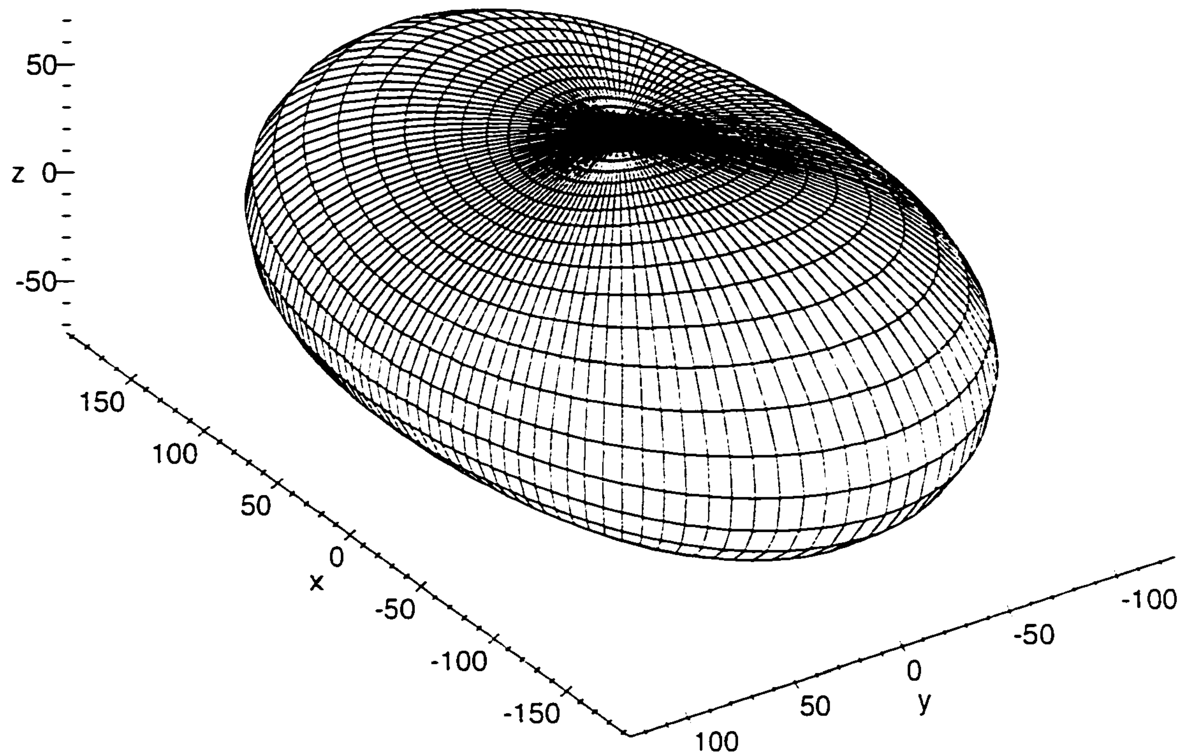

Figure 4. Young's modulus as a function of direction

Human bone (distal femur) at $\phi = 0.35$

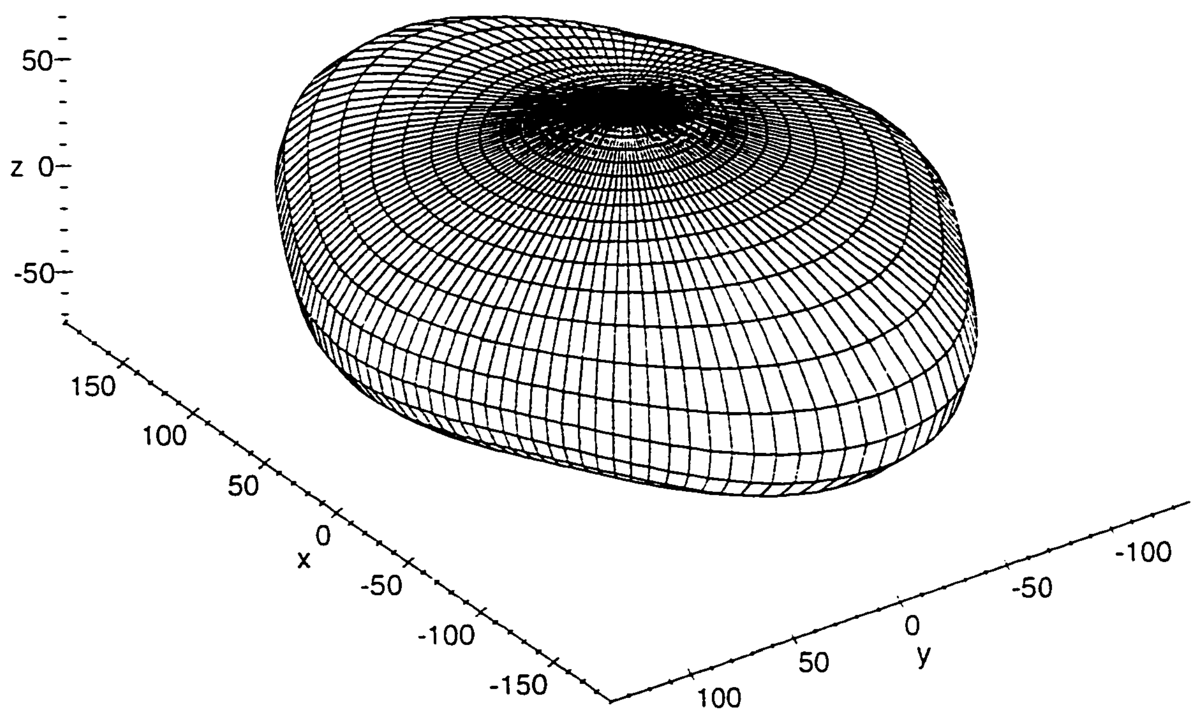

Figure 5. Human cancellous bone

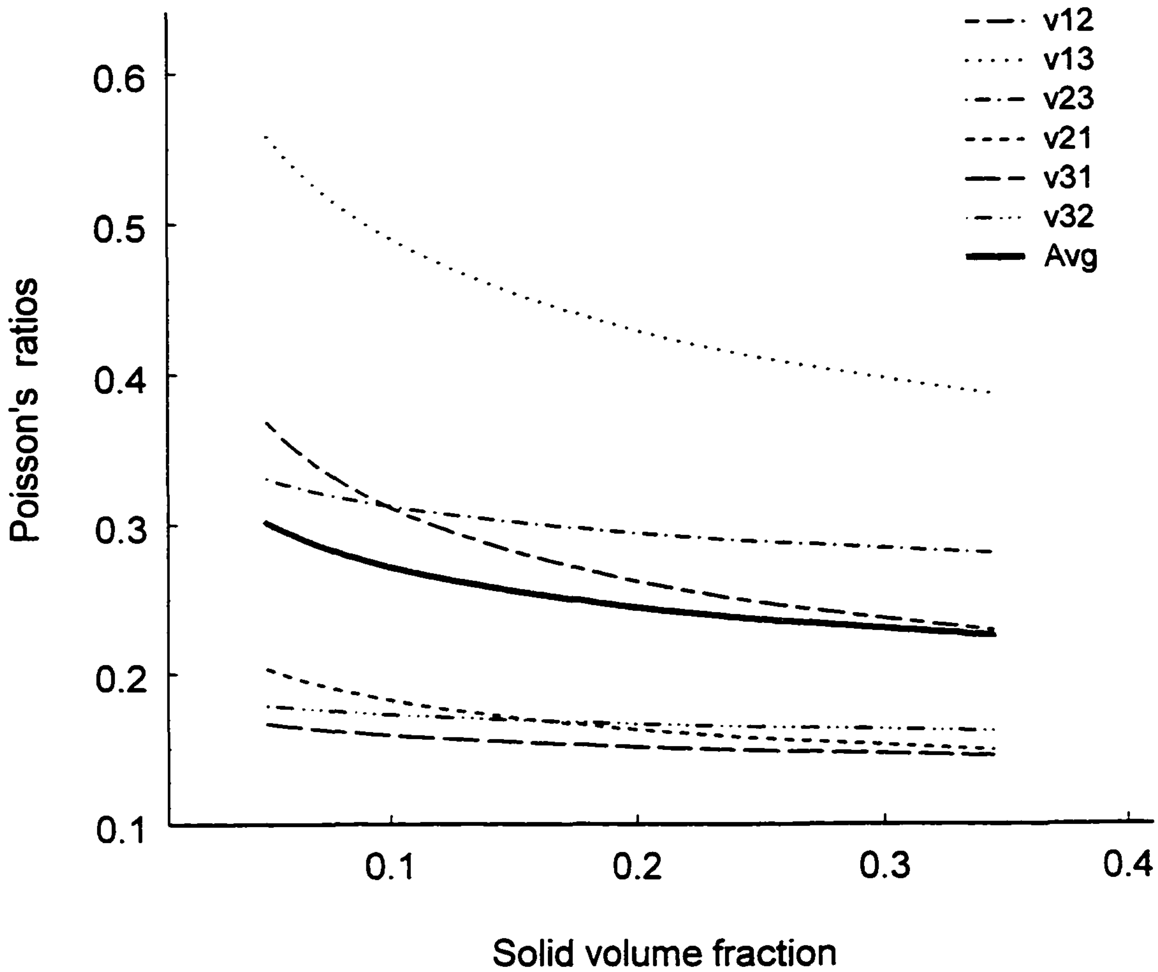

Figure 6. Human cancellous bone, isotropic bounds

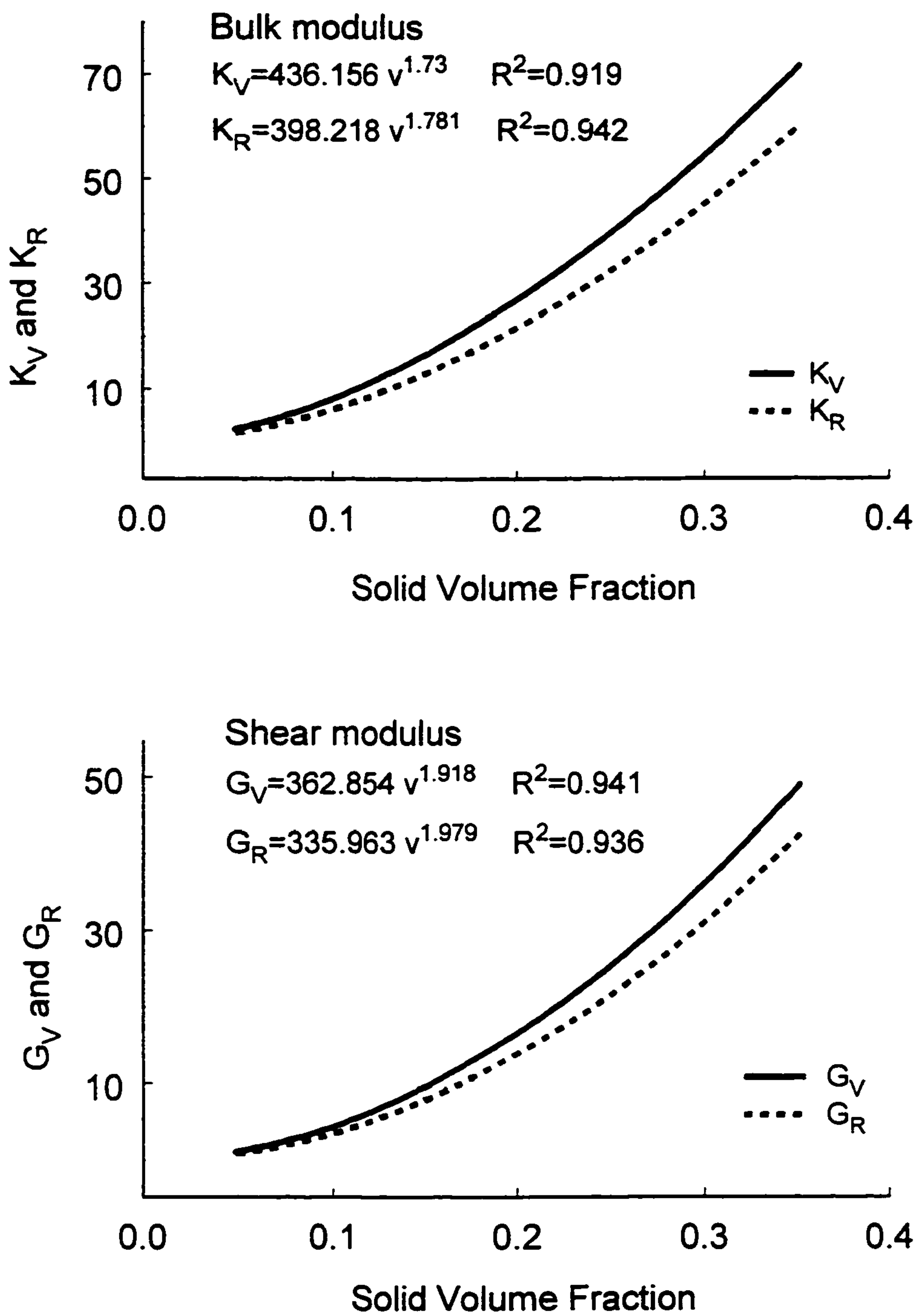

Figure 7. Human cancellous bone, transversely isotropic bounds

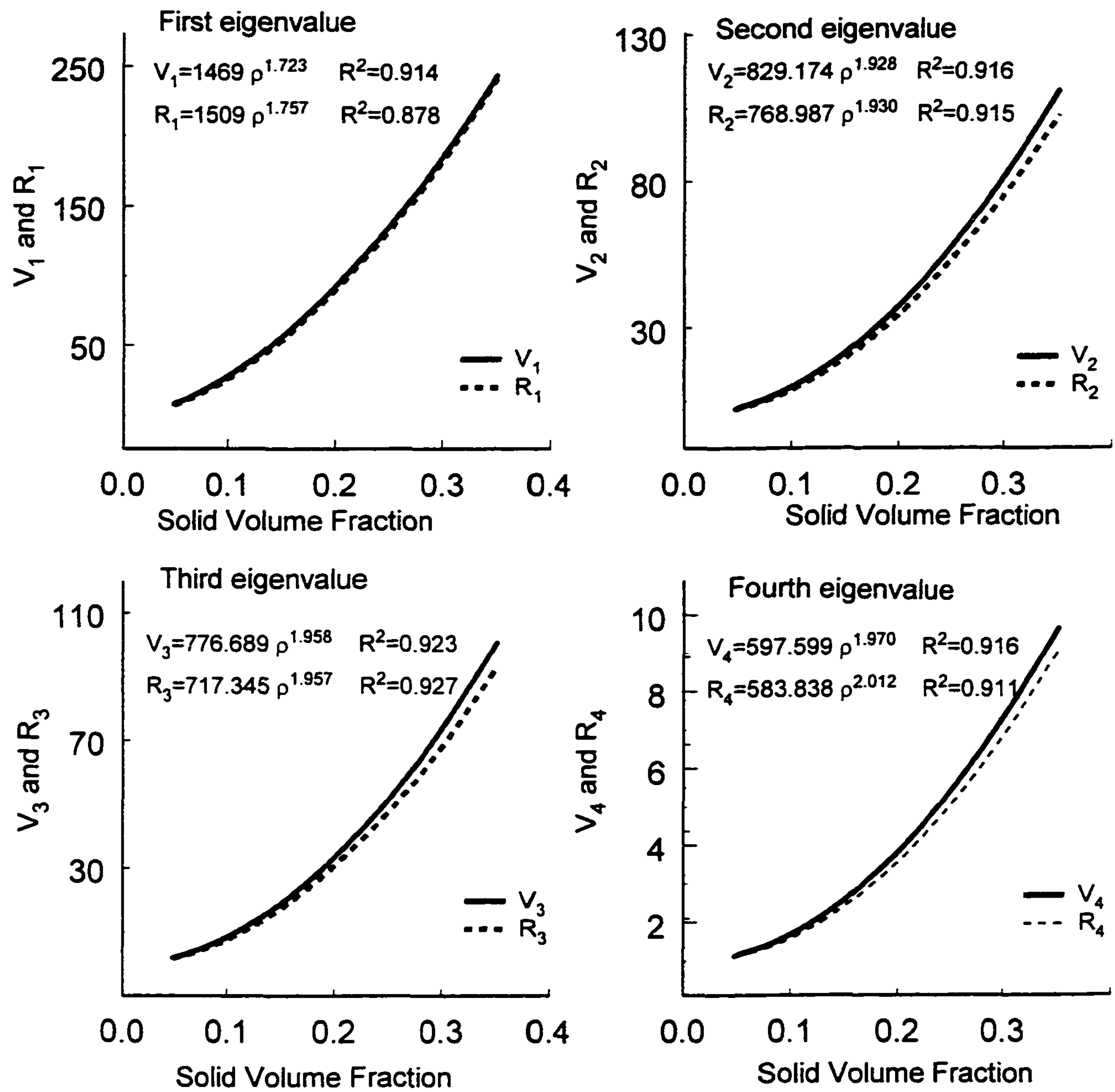

Figure 8. Whale cancellous bone, isotropic bounds

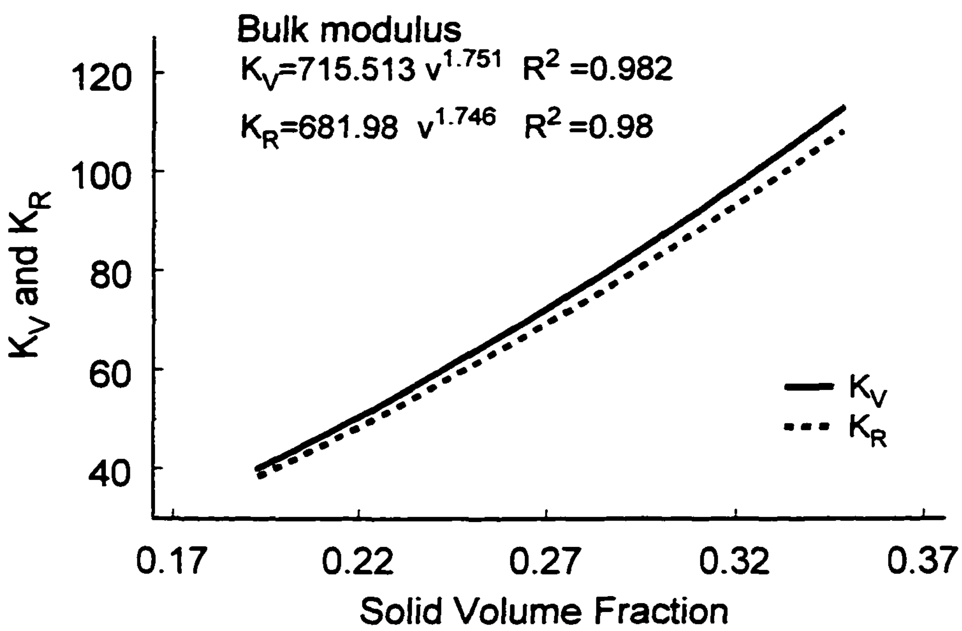

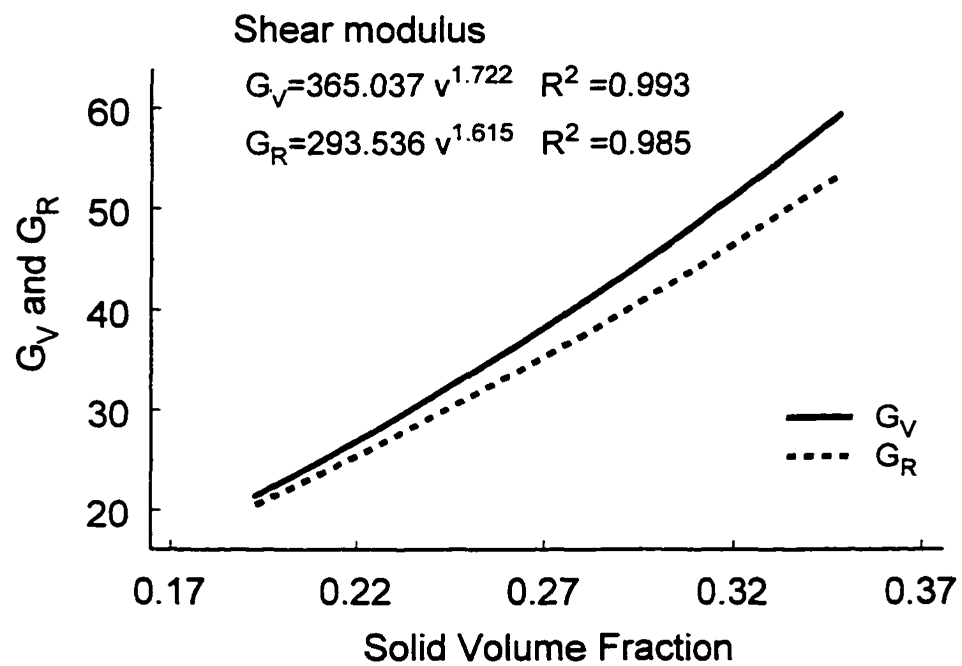

Figure 9. Whale cancellous bone, transversely isotropic bounds

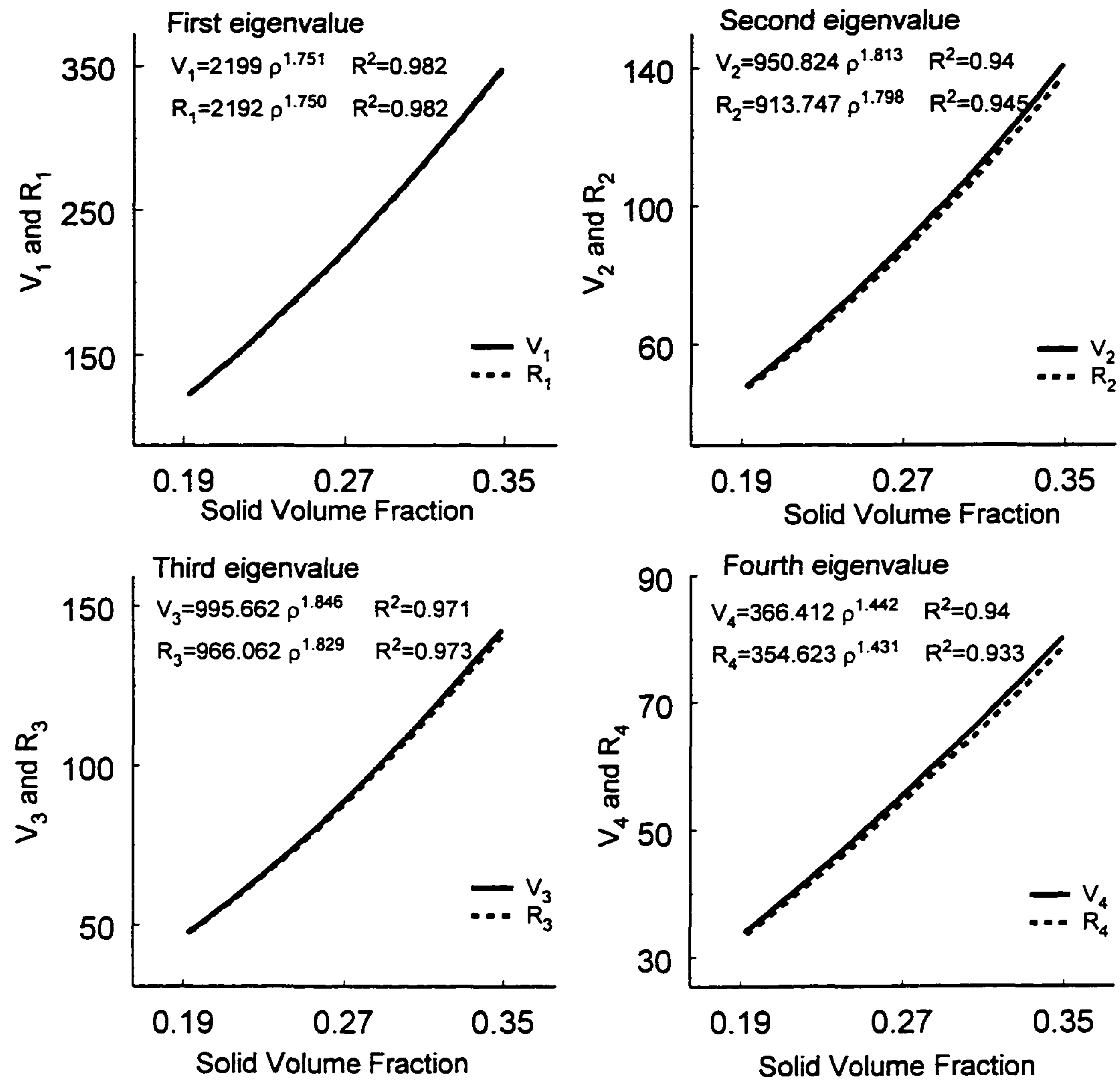

Figure 10. Hardwood, isotropic bounds

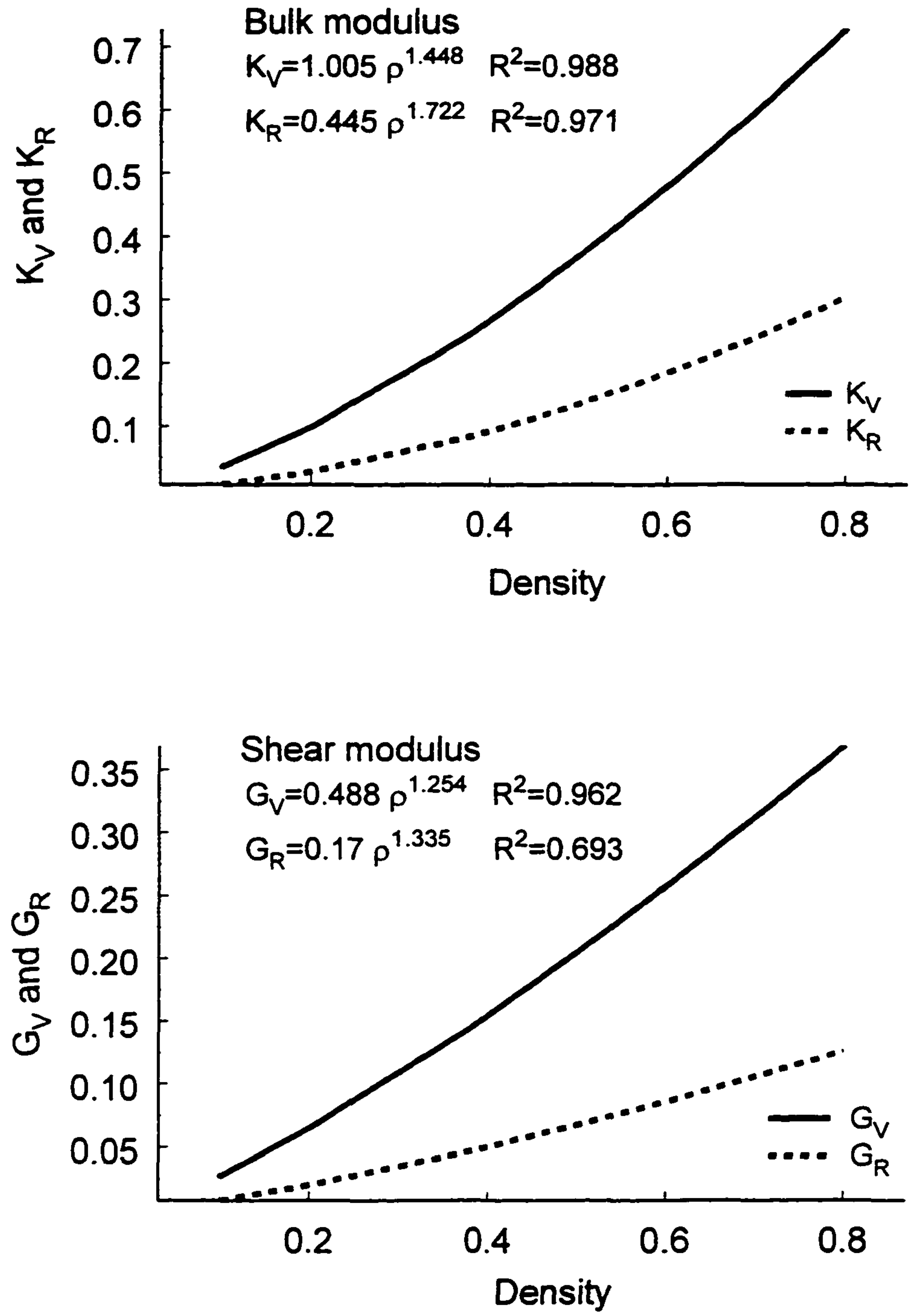

Figure 11. Softwood, isotropic bounds

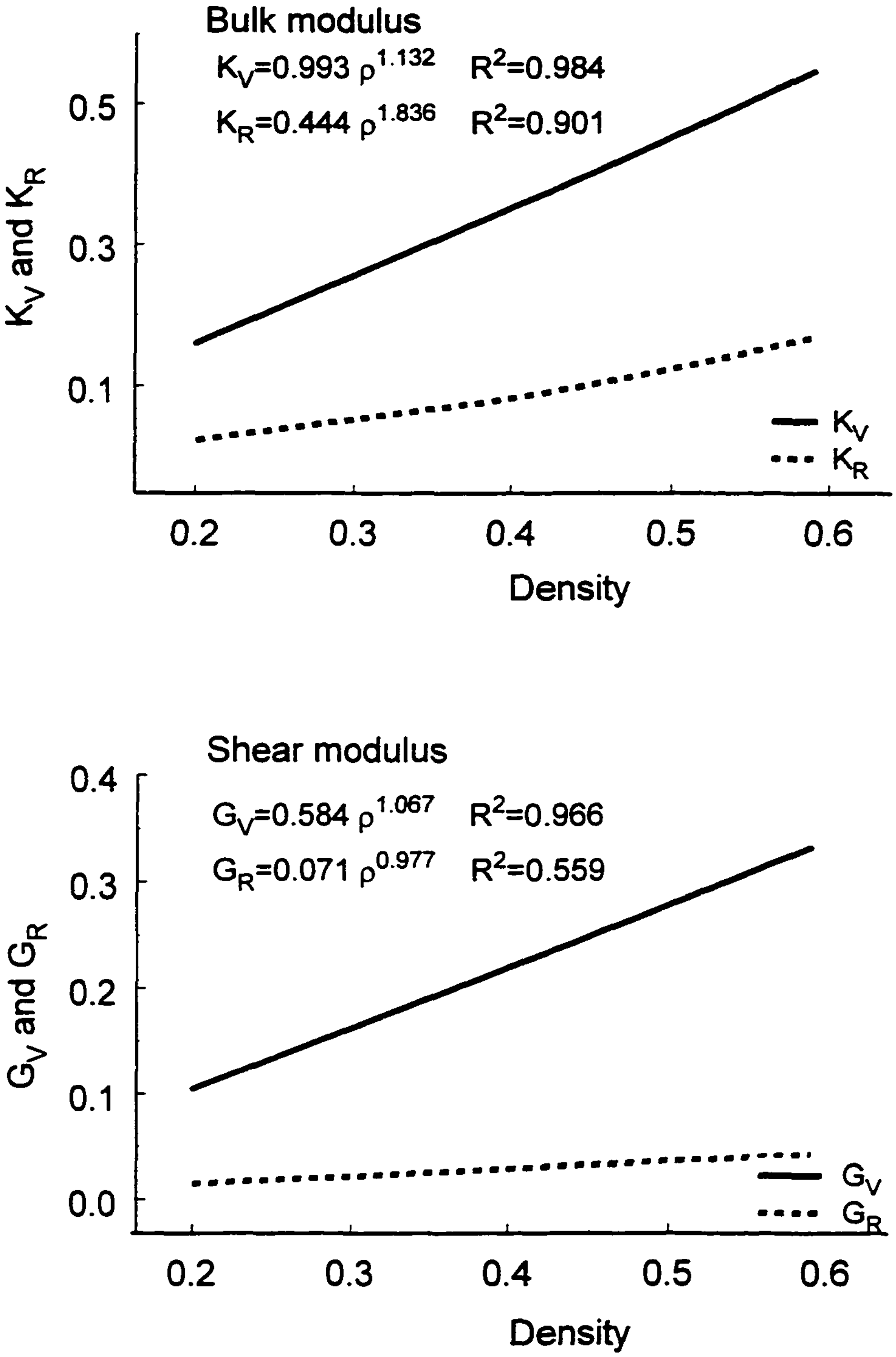

Figure 12. Hardwood, transversely isotropic bounds

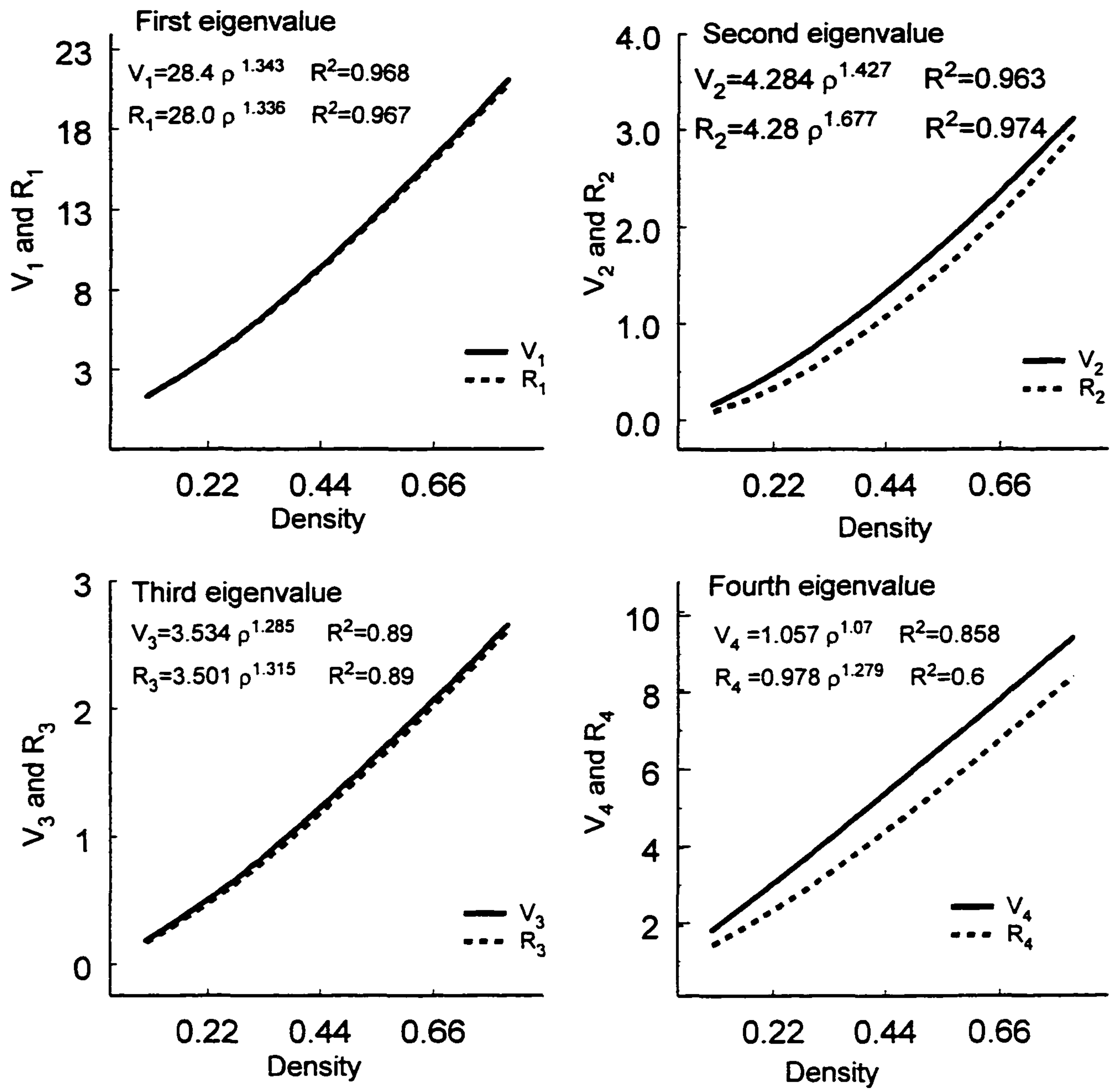

Figure 13. Softwood, transversely isotropic bounds

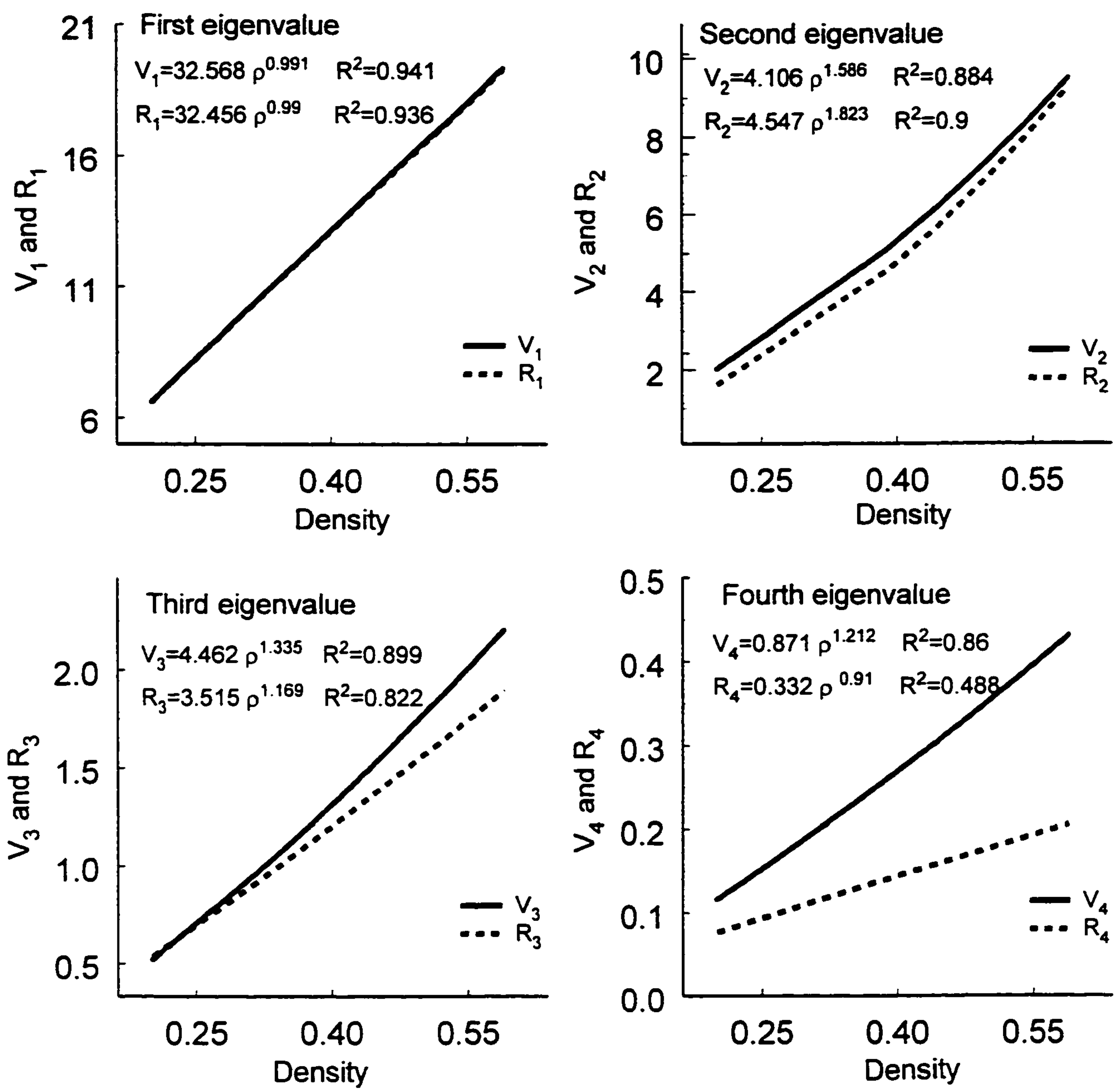

Appendix A. Eigenmodes for the Various Linear Elastic Symmetries

In this section the eigenmodes of the various linearly elastic symmetries will be summarized. The modes were determined by Kelvin (1856), Rychlewski (1984), Mehrabadi and Cowin (1990), Cowin and Mehrabadi (1992) and Cowin *et al.* (1991).

We begin with the eigenmodes for cubic symmetry, and those for isotropic symmetry will be obtained as a special case. The eigenproblem is expressed for cubic symmetry by using the representation for $\hat{\mathbf{c}}$ in a cubic symmetry coordinate system, thus

$$(\hat{\mathbf{c}} - \Lambda \mathbf{1})\hat{\mathbf{N}} = \begin{bmatrix} \hat{c}_{11} - \Lambda & \hat{c}_{12} & \hat{c}_{12} & 0 & 0 & 0 \\ \hat{c}_{12} & \hat{c}_{11} - \Lambda & \hat{c}_{12} & 0 & 0 & 0 \\ \hat{c}_{12} & \hat{c}_{12} & \hat{c}_{11} - \Lambda & 0 & 0 & 0 \\ 0 & 0 & 0 & \hat{c}_{44} - \Lambda & 0 & 0 \\ 0 & 0 & 0 & 0 & \hat{c}_{44} - \Lambda & 0 \\ 0 & 0 & 0 & 0 & 0 & \hat{c}_{44} - \Lambda \end{bmatrix} \begin{bmatrix} \hat{N}_1 \\ \hat{N}_2 \\ \hat{N}_3 \\ \hat{N}_4 \\ \hat{N}_5 \\ \hat{N}_6 \end{bmatrix} = \mathbf{0}. \qquad (A1)$$

The eigenvalues of $(A1)$ are of multiplicity one, two and three and are given by

$$\Lambda_{(1)} = \hat{c}_{11} + 2\hat{c}_{12}, \Lambda_{(2,3)} = \hat{c}_{11} - \hat{c}_{12}, \quad \Lambda_{(4,5,6)} = \hat{c}_{44}$$

or

$$\Lambda_{(1)}=c_{11}+2c_{12}\ , \ \Lambda_{(2,3)}=c_{11}-c_{12}\ , \ \Lambda_{(4,5,6)}=c_{44}, \qquad (A2)$$

respectively, and a set of eigentensors of $(A1)$ corresponding to these eigenvalues is

$$\mathbf{N}^{(1)} = \frac{1}{\sqrt{3}}\mathbf{1},\ \mathbf{N}^{(2)} = \frac{1}{\sqrt{6}}\begin{bmatrix} -1 & 0 & 0 \\ 0 & -1 & 0 \\ 0 & 0 & 2 \end{bmatrix}, \quad \mathbf{N}^{(3)} = \frac{1}{\sqrt{2}}\begin{bmatrix} -1 & 0 & 0 \\ 0 & 1 & 0 \\ 0 & 0 & 0 \end{bmatrix},$$

$$\mathbf{N}^{(4)} = \frac{1}{\sqrt{2}}\begin{bmatrix} 0 & 0 & 0 \\ 0 & 0 & 1 \\ 0 & 1 & 0 \end{bmatrix},\ \mathbf{N}^{(5)} = \frac{1}{\sqrt{2}}\begin{bmatrix} 0 & 0 & 1 \\ 0 & 0 & 0 \\ 1 & 0 & 0 \end{bmatrix},\ \mathbf{N}^{(6)} = \frac{1}{\sqrt{2}}\begin{bmatrix} 0 & 1 & 0 \\ 1 & 0 & 0 \\ 0 & 0 & 0 \end{bmatrix}, \qquad (A3)$$

respectively. These results for cubic symmetry readily reduce to those for isotropic symmetry when $\hat{c}_{44} = \hat{c}_{11} - \hat{c}_{12}$. The eigenvalues for isotropic symmetry are of multiplicity one and five and are given by

$$\Lambda_{(1)} = \hat{c}_{11} + 2\hat{c}_{12}, \Lambda_{(2,3,4,5,6)} = \hat{c}_{11} - \hat{c}_{12} = \hat{c}_{44}, \qquad (A4)$$

respectively.

The eigenproblem is expressed for tetragonal symmetry by using the representation for $\hat{\mathbf{c}}$ in a tetragonal symmetry coordinate system, thus

$$
(\hat{\mathbf{c}}-\Lambda\mathbf{1})\hat{\mathbf{N}} = \begin{bmatrix} \hat{c}_{11}-\Lambda & \hat{c}_{12} & \hat{c}_{13} & 0 & 0 & 0 \\ \hat{c}_{12} & \hat{c}_{11}-\Lambda & \hat{c}_{13} & 0 & 0 & 0 \\ \hat{c}_{13} & \hat{c}_{13} & \hat{c}_{33}-\Lambda & 0 & 0 & 0 \\ 0 & 0 & 0 & \hat{c}_{44}-\Lambda & 0 & 0 \\ 0 & 0 & 0 & 0 & \hat{c}_{44}-\Lambda & 0 \\ 0 & 0 & 0 & 0 & 0 & \hat{c}_{66}-\Lambda \end{bmatrix} \begin{bmatrix} \hat{N}_1 \\ \hat{N}_2 \\ \hat{N}_3 \\ \hat{N}_4 \\ \hat{N}_5 \\ \hat{N}_6 \end{bmatrix} = \mathbf{0}. \qquad (A5)
$$

The eigenvalues of ($A5$) are of multiplicity one, one, one, two and one are given by

$$
\begin{aligned}
&\Lambda_{(1)},\Lambda_{(2)} = \frac{1}{2}[(\hat{c}_{11}+\hat{c}_{12}+\hat{c}_{33}) \pm \sqrt{8\hat{c}_{13}^2+(\hat{c}_{11}+\hat{c}_{12}-\hat{c}_{33})^2}\,], \\
&\Lambda_{(3)} = \hat{c}_{11}-\hat{c}_{12}, \Lambda_{(4,5)} = \hat{c}_{44}, \ \Lambda_{(6)} = \hat{c}_{66} \ ,
\end{aligned} \qquad (A6)
$$

respectively, and the eigentensors corresponding to these eigenvalues are

$$
\mathbf{N}^{(1)} = \begin{bmatrix} \frac{1}{2}(\cos\alpha+\sin\alpha) & 0 & 0 \\ 0 & \frac{1}{2}(\cos\alpha+\sin\alpha) & 0 \\ 0 & 0 & \frac{1}{\sqrt{2}}(\cos\alpha-\sin\alpha) \end{bmatrix},
$$

$$
\mathbf{N}^{(2)} = \begin{bmatrix} \frac{1}{2}(\sin\alpha-\cos\alpha) & 0 & 0 \\ 0 & \frac{1}{2}(\sin\alpha-\cos\alpha & 0 \\ 0 & 0 & \frac{1}{\sqrt{2}}(\cos\alpha+\sin\alpha) \end{bmatrix}. \qquad (A7)
$$

$$\mathbf{N}^{(3)} = \begin{bmatrix} \frac{1}{\sqrt{2}} & 0 & 0 \\ 0 & -\frac{1}{\sqrt{2}} & 0 \\ 0 & 0 & 0 \end{bmatrix}, \quad \mathbf{N}^{(4)} = \frac{1}{\sqrt{2}} \begin{bmatrix} 0 & 0 & 0 \\ 0 & 0 & 1 \\ 0 & 1 & 0 \end{bmatrix},$$

$$\mathbf{N}^{(5)} = \frac{1}{\sqrt{2}} \begin{bmatrix} 0 & 0 & 1 \\ 0 & 0 & 0 \\ 1 & 0 & 0 \end{bmatrix}, \quad \mathbf{N}^{(6)} = \frac{1}{\sqrt{2}} \begin{bmatrix} 0 & 1 & 0 \\ 1 & 0 & 0 \\ 0 & 0 & 0 \end{bmatrix},$$

respectively, where

$$\tan 2\alpha = \frac{(\hat{c}_{11} + \hat{c}_{12} - \hat{c}_{33})}{2\sqrt{2}\hat{c}_{13}}. \qquad (A8)$$

This definition of the angle α is twice the angle α defined by Mehrabadi and Cowin (1990) in their equation (5.11).

In the case of trigonal symmetry the eigenproblem is expressed by using the representation for $\hat{\mathbf{c}}$ in a trigonal symmetry coordinate system, thus

$$(\hat{\mathbf{c}} - \Lambda \mathbf{1})\hat{\mathbf{N}} = \begin{bmatrix} \hat{c}_{11} - \Lambda & \hat{c}_{12} & \hat{c}_{13} & \hat{c}_{14} & 0 & 0 \\ \hat{c}_{12} & \hat{c}_{11} - \Lambda & \hat{c}_{13} & -\hat{c}_{14} & 0 & 0 \\ \hat{c}_{13} & \hat{c}_{13} & \hat{c}_{33} - \Lambda & 0 & 0 & 0 \\ \hat{c}_{14} & -\hat{c}_{14} & 0 & \hat{c}_{44} - \Lambda & 0 & 0 \\ 0 & 0 & 0 & 0 & \hat{c}_{44} - \Lambda & \sqrt{2}\hat{c}_{14} \\ 0 & 0 & 0 & 0 & \sqrt{2}\hat{c}_{14} & \hat{c}_{11} - \hat{c}_{12} - \Lambda \end{bmatrix} \begin{bmatrix} \hat{N}_1 \\ \hat{N}_2 \\ \hat{N}_3 \\ \hat{N}_4 \\ \hat{N}_5 \\ \hat{N}_6 \end{bmatrix} = \mathbf{0}. \qquad (A9)$$

The eignevalues of ($A9$) are of multiplicity one, one, two and two and are given by

$$\Lambda_{(1)}, \Lambda_{(2)} = \frac{1}{2}[(\hat{c}_{11} + \hat{c}_{12} + \hat{c}_{33}) \pm \sqrt{8\hat{c}_{13}^2 + (\hat{c}_{11} + \hat{c}_{12} - \hat{c}_{33})^2}\,],$$

$$\Lambda_{(3,6)} = \frac{1}{2}[(\hat{c}_{11} - \hat{c}_{12} + \hat{c}_{44}) + \sqrt{8\hat{c}_{14}^2 + (\hat{c}_{11} - \hat{c}_{12} - \hat{c}_{44})^2}\,],$$

$$\Lambda_{(4,5)} = \frac{1}{2}[(\hat{c}_{11} - \hat{c}_{12} + \hat{c}_{44}) - \sqrt{8\hat{c}_{14}^2 + (\hat{c}_{11} - \hat{c}_{12} - \hat{c}_{44})^2}\,], \qquad (A10)$$

respectively. The first two eigenvalues are the same as those for tetragonal symmetry given by ($A6$), the associated eigentensors $\mathbf{N}^{(1)}$ and $\mathbf{N}^{(2)}$ are given by ($A7$) and the value of the angle α by ($A8$). The eigentensors corresponding to the other eigenvalues are

$$\mathbf{N}^{(3)} = \frac{1}{\sqrt{2}}\begin{bmatrix} \cos\beta & 0 & 0 \\ 0 & -\cos\beta & \sin\beta \\ 0 & \sin\beta & 0 \end{bmatrix}, \quad \mathbf{N}^{(6)} = \frac{1}{\sqrt{2}}\begin{bmatrix} 0 & \cos\beta & \sin\beta \\ \cos\beta & 0 & 0 \\ \sin\beta & 0 & 0 \end{bmatrix},$$

$$\mathbf{N}^{(4)} = \frac{1}{\sqrt{2}}\begin{bmatrix} -\sin\beta & 0 & 0 \\ 0 & \sin\beta & \cos\beta \\ 0 & \cos\beta & 0 \end{bmatrix}, \quad \mathbf{N}^{(5)} = \frac{1}{\sqrt{2}}\begin{bmatrix} 0 & -\sin\beta & \cos\beta \\ -\sin s\beta & 0 & 0 \\ \cos\beta & 0 & 0 \end{bmatrix}, \qquad (A11)$$

where

$$\tan 2\beta = \frac{2\sqrt{2}\hat{c}_{14}}{(\hat{c}_{11} - \hat{c}_{12} - \hat{c}_{44})}. \qquad (A12)$$

The eigentensors and the eigenvalues for transversely isotropic or hexagonal symmetry are obtained from those of trigonal symmetry by allowing the elastic constant $\hat{c}_{14}$ vanish. As in the case of trigonal symmetry, there are four distinct

eigenvalues for transversely isotropic or hexagonal symmetry. Two are associated with different dilatational modes and two of multiplicity two are associated with different isochoric modes. The two dilatational modes, being identical to those of tetragonal or trigonal symmetry, are as described above or in
the section on tetragonal symmetry. However, since the elastic constant $\hat{c}_{14}$ and hence the angle β defined by ($A12$) vanishes, the third through sixth eigenvalues of ($A10$) reduce to

$$\Lambda_{(3,6)} = \hat{c}_{11} - \hat{c}_{12}, \quad \Lambda_{(4,5)} = \hat{c}_{44} . \qquad (A13)$$

The eigentensors are identical to those given by ($A7$) for tetragonal symmetry.

The details of the eigenmodes for the triclinic, monoclinic and orthotropic symmetries are not recorded here in detail but may be found in Mehrabadi and Cowin (1990) or Cowin and Mehrabadi (1992). Orthotropic symmetry has the three isochoric modes that are designated as $\mathbf{N}^{(4)}$, $\mathbf{N}^{(5)}$ and $\mathbf{N}^{(6)}$ in Equation ($A3$) as well as three dilatational modes like $\mathbf{N}^{(1)}$ and $\mathbf{N}^{(2)}$ in Equation ($A7$). Monoclinic symmetry has the two isochoric modes that are designated as, say $\mathbf{N}^{(5)}$ and $\mathbf{N}^{(6)}$ in Equation ($A7$) as well as four dilatational modes. Triclinic symmetry has, in ge neral, six dilatational modes, of which nothing can be said.

Appendix B. Derivation of the Formula for the Average Eigenbasis

We seek to define a basis $\hat{\mathbf{N}}_k^{AVG}$ that is, on the average, the closest to all the eigenvector bases $\hat{\mathbf{N}}_k^{I}, \hat{\mathbf{N}}_k^{II}, \ldots, \hat{\mathbf{N}}_k^{M}$, for each measurement determined from the given elastic constant data. Let the unknown $\hat{\mathbf{N}}_k^{AVG}$ be introduced by

$$\hat{\mathbf{N}}_k^{AVG} = \hat{Q}_{km}^{AI}\, \hat{\mathbf{N}}_m^{I}, \tag{B1}$$

and it is required to form an orthonormal basis:

$$\hat{\mathbf{N}}_k^{AVG} \cdot \hat{\mathbf{N}}_m^{AVG} = \delta_{km} = \hat{Q}_{ks}^{AI} \hat{\mathbf{N}}_s^{I} \cdot \hat{Q}_{mq}^{AI} \hat{\mathbf{N}}_q^{I} = \hat{Q}_{ks}^{AI} \hat{Q}_{mq}^{AI}. \tag{B2}$$

The vector difference between the average eigenbasis $\hat{\mathbf{N}}_k^{AVG}$ and the typical eigenbasis $\hat{\mathbf{N}}_k^{Y}$ is given by

$$\hat{\mathbf{N}}_k^{Y} - \hat{\mathbf{N}}_k^{AVG} = (\hat{Q}_{km}^{YI} - \hat{Q}_{km}^{AI})\, \hat{\mathbf{N}}_m^{I}\,. \tag{B3}$$

The sum over all k vectors of the square of the distance between the kth vector of the Y measurement and the kth vector of the average eigenbasis is

$$(\hat{\mathbf{N}}_k^{Y} - \hat{\mathbf{N}}_k^{AVG}) \cdot (\hat{\mathbf{N}}_k^{Y} - \hat{\mathbf{N}}_k^{AVG}) = \hat{Q}_{km}^{YI} \hat{Q}_{km}^{YI} + \hat{Q}_{km}^{AI} \hat{Q}_{km}^{AI} - 2\, \hat{Q}_{km}^{AI} \hat{Q}_{km}^{YI}\,. \tag{B4}$$

The sum over all measurements Y of the sum over all k vectors of the square of the distance between the kth vector of the Y measurement is

$$\sum_{Y=1}^{M}(\hat{\mathbf{N}}_k^Y - \hat{\mathbf{N}}_k^{AVG})\cdot(\hat{\mathbf{N}}_k^Y - \hat{\mathbf{N}}_k^{AVG}) = \sum_{Y=1}^{M}\hat{Q}_{km}^{YI}\hat{Q}_{km}^{YI} + M\hat{Q}_{km}^{AI}\hat{Q}_{km}^{AI} - 2\hat{Q}_{km}^{AI}\sum_{Y=1}^{M}\hat{Q}_{km}^{YI}. \qquad (B5)$$

This sum may be rewritten as

$$\sum_{Y=1}^{M}(\hat{\mathbf{N}}_k^Y - \hat{\mathbf{N}}_k^{AVG})\cdot(\hat{\mathbf{N}}_k^Y - \hat{\mathbf{N}}_k^{AVG}) = MC - 2M\hat{\mathbf{N}}_k^{AVG}\cdot\hat{\mathbf{N}}_k^{NA} + M\hat{\mathbf{N}}_k^{AVG}\cdot\hat{\mathbf{N}}_k^{AVG}. \qquad (B6)$$

or

$$\sum_{Y=1}^{M}(\hat{\mathbf{N}}_k^Y - \hat{\mathbf{N}}_k^{AVG})\cdot(\hat{\mathbf{N}}_k^Y - \hat{\mathbf{N}}_k^{AVG}) = MC - 2M\hat{Q}_{km}^{AI}\hat{A}_{km} + M\hat{Q}_{km}^{AI}\hat{Q}_{km}^{AI}.$$

where we have introduced the definitions

$$C \equiv \frac{1}{M}\sum_{Y=1}^{M}(\hat{\mathbf{N}}_k^Y\cdot\hat{\mathbf{N}}_k^Y)\ ,\ \hat{A}_{km} \equiv \hat{\mathbf{N}}_k^{NA}\cdot\hat{\mathbf{N}}_m^I\ , \qquad (B7)$$

where

$$\hat{\mathbf{N}}_k^{NA} = \hat{A}_{km}\hat{\mathbf{N}}_m^I\ .$$

In order to minimize the square of the distance between the sum of the *k*th vectors of all the measurements and the *k*th vectors of the average eigenbasis, an objective function ψ, equal to the sum over all measurements of the square of the distance between the two sets of six vectors and constrained by Lagrange multipliers $\hat{\Lambda}_{km}$ contracted with the constraint condition (*B*2), is introduced:

$$\psi = \sum_{Y=1}^{M} (\hat{\mathbf{N}}_k^Y - \hat{\mathbf{N}}_k^{AVG}) \cdot (\hat{\mathbf{N}}_k^Y - \hat{\mathbf{N}}_k^{AVG}) + M\, \hat{\Lambda}_{km} (\hat{Q}_{mq}^{AI} \hat{Q}_{mq}^{AI} - \delta_{km}). \tag{B8}$$

It is important to note that, since the constraint $\hat{Q}_{kq}^{AI} \hat{Q}_{mq}^{AI} = \delta_{km}$ is a symmetric matrix equation, the Lagrange multipliers $\hat{\Lambda}_{km}$ contracted with the constraint condition (*B*2) will necessarily be symmetric ($\hat{\Lambda}_{km} = \hat{\Lambda}_{km}$) to effect the constraint. An alternative expression for the objective function ψ is obtained when (*B*6) is substituted into (*B*8):

$$\psi = MC - 2M\, \hat{Q}_{km}^{AI}\, \hat{A}_{km} + M\, \hat{Q}_{km}^{AI} \hat{Q}_{km}^{AI} + M\, \hat{\Lambda}_{km} (\hat{Q}_{kq}^{AI} \hat{Q}_{mq}^{AI} - \delta_{km}) \ . \tag{B9}$$

The condition that the first derivative of (*B*9) with respect to $\hat{Q}_{nt}^{AI}$ vanish leads to the following relation between the matrix $\hat{\mathbf{A}}$, $\hat{\mathbf{Q}}^{AI}$ and $\hat{\Lambda}$:

$$\hat{A}_{nt} = \{\delta_{nm} + \hat{\Lambda}_{nm}\} \hat{Q}_{mt}^{AI} \qquad \text{or} \qquad \hat{A}_{nt}\, \hat{Q}_{rt}^{AI} = \delta_{nr} + \hat{\Lambda}_{nr} \ . \tag{B10}$$

Since the skew-symmetric part of the Lagrange multiplier $\hat{\Lambda}$ must be zero, it follows that

$$\hat{A}_{nt}\hat{Q}^{AI}_{rt} = \hat{A}_{rt}\hat{Q}^{AI}_{nt} \ , \ \hat{\mathbf{A}}(\hat{\mathbf{Q}}^{AI})^{T} = \hat{\mathbf{Q}}^{AI}(\hat{\mathbf{A}})^{T} \ , \qquad (B11)$$

and , from $(B11)$,

$$\hat{A}_{nt}\hat{Q}^{AI}_{rt} = \hat{A}_{rt}\hat{Q}^{AI}_{nt} = \delta_{nr} + \hat{\Lambda}_{nr} \ , \ \hat{\mathbf{A}}(\hat{\mathbf{Q}}^{AI})^{T} = \hat{\mathbf{Q}}^{AI}(\hat{\mathbf{A}})^{T} = \mathbf{I} + \hat{\Lambda} \qquad (B12)$$

In order to formally solve $(B12)$ to obtain the matrix $\hat{\mathbf{Q}}^{AI}$ as a function of the matrix $\hat{\mathbf{A}}$, we recall the polar decomposition theorem for matrices (cf., e. g., Ogden, 1984). For any non-singular second order tensor $\hat{\mathbf{A}}$ there exist unique positive definite second order tensors $\hat{\mathbf{U}}$ and $\hat{\mathbf{V}}$, and an orthogonal second order orthogonal tensor $\hat{\mathbf{R}}$ such that

$$\hat{\mathbf{A}} = \hat{\mathbf{R}}\hat{\mathbf{U}} = \hat{\mathbf{V}}\hat{\mathbf{R}}, \qquad (B13)$$

where

$$\hat{\mathbf{U}}^{2} = \hat{\mathbf{A}}^{T}\hat{\mathbf{A}}, \ \ \hat{\mathbf{V}}^{2} = \hat{\mathbf{A}}\hat{\mathbf{A}}^{T}, \ \hat{\mathbf{R}} = \hat{\mathbf{A}}\hat{\mathbf{U}}^{-1} = \hat{\mathbf{V}}^{-1}\hat{\mathbf{A}}. \qquad (B14)$$

Substituting $(B13)$ into $(B12)$, we obtain the condition

$$\hat{\mathbf{V}}\hat{\mathbf{R}}(\hat{\mathbf{Q}}^{AI})^T = \hat{\mathbf{Q}}^{AI}(\hat{\mathbf{R}})^T\hat{\mathbf{V}} = \mathbf{1}+\hat{\Lambda}, \qquad (B15)$$

which may be uniquely satisfied by the selection

$$\hat{\mathbf{Q}}^{AI} = \hat{\mathbf{R}} = \hat{\mathbf{A}}\hat{\mathbf{U}}^{-1} = \hat{\mathbf{V}}^{-1}\hat{\mathbf{A}}, \quad \hat{\mathbf{V}} = \mathbf{1}+\hat{\Lambda}, \qquad (B16)$$

a result that is a matrix prescription for the determination of $\hat{\mathbf{Q}}^{AI}$:

$$\hat{\mathbf{Q}}^{AI} = (\hat{\mathbf{A}}\hat{\mathbf{A}}^T)^{-(1/2)}\hat{\mathbf{A}}, \quad \hat{\mathbf{A}} \equiv \frac{1}{M}\sum_{Y=1}^{M}\hat{\mathbf{Q}}^{YI}. \qquad (B17)$$

The result of this section, the value of $\hat{\mathbf{N}}_k^{AI\mathcal{G}}$ for any symmetry, is obtained by substituting $\hat{\mathbf{Q}}^{AI}$ given by (B17) into (B1). Rewriting that result in terms of vectors, we obtain (B16) and (B17) with the inverse square root term given by the second of (B17).

It is fair to show that $\hat{\mathbf{Q}}^{AI}$ given by (B17) is a minimizer of the objective function ψ. The second derivative ψ is given by

$$\frac{\partial^2\psi}{\partial\hat{Q}_{rs}^{AI}\partial\hat{Q}_{nt}^{AI}} = 2M\,\delta_{st}(\delta_{rn}+\hat{\Lambda}_{nr}), \qquad (B18)$$

which, from ($B18$) and ($B16$) , has the form

$$\frac{\partial^2 \psi}{\partial \hat{Q}_{rs}^{AI} \partial \hat{Q}_{nt}^{AI}} = 2\, M\, \delta_{st} \hat{V}_{rn} \,. \tag{B19}$$

Since the matrix $\hat{\mathbf{V}}$ is positive definite , it follows from ($B19$) that

$$\frac{\partial^2 \psi}{\partial \hat{Q}_{rs}^{AI} \partial \hat{Q}_{nt}^{AI}} \geq 0 \,. \tag{B20}$$

Appendix C. Representation Theorem for Small Rotations

It is known that if $\mathbf{A}$ is a skew-symmetric matrix, $\mathbf{A}+\mathbf{A}^T=0$, then the matrix given by the exponential function of matrices

$$e^{\mathbf{A}} = \sum_{n=1}^{\infty} \frac{\mathbf{A}^n}{n!} \tag{C1}$$

Is orthogonal, $e^{\mathbf{A}}[e^{\mathbf{A}}]^T=\mathbf{1}$ (Mehrabadi *et al.,*1995). Note that since $\mathbf{A}$ is skew-symmetric, then $\mathbf{A}\mathbf{A}^T=-\mathbf{A}^2$, $tr[\mathbf{A}\mathbf{A}^T]$ is nonnegative and $tr[\mathbf{A}^2]$ is nonpositive. We specialize this result to six dimensions and introduce ξ and $\hat{\mathbf{W}}$ such that

$$\xi = \sqrt{tr[\mathbf{A}\mathbf{A}^T]}, \quad \mathbf{A} = \xi \hat{\mathbf{W}}; \tag{C2}$$

Then $tr[\mathbf{W}\mathbf{W}^T]=1$ and we can write ($C1$) in the form

$$\hat{\mathbf{Q}} \equiv e^{\xi\hat{\mathbf{W}}} = \hat{\mathbf{1}} + \frac{\xi}{1!}\hat{\mathbf{W}} + \frac{\xi^2}{2!}\hat{\mathbf{W}}^2 + \cdots + \frac{\xi^n}{n!}\hat{\mathbf{W}}^n + \cdots. \qquad (C3)$$

$$tr\hat{\mathbf{Q}} = 6 - \frac{\xi^2}{2} + tr[\mathbf{W}^4]\frac{\xi^4}{24} - \cdots, \qquad (C4)$$

Note that the trace of ($C3$) is given by

Since $tr[\hat{\mathbf{W}}^n]=0$ for odd n, $tr[\hat{\mathbf{W}}^n]=1$ and $tr[\hat{\mathbf{W}}^2]=-tr[(\hat{\mathbf{W}}\hat{\mathbf{W}}^T)]=-1$. Using the fact that $tr[\hat{\mathbf{W}}^n]=1$ requires the sum of the squares of the off diagonal terms of $\hat{\mathbf{W}}$ be equal one half, a not very sharp upper bound on $tr[\hat{\mathbf{W}}^n]/24$ of 4 1/16 may be established. Thus if terms of the order $4\xi^4$ are small compared to $\xi^2/2$, then

$$\xi^2 = 2(6 - tr(\hat{\mathbf{Q}})). \qquad (C5)$$

We conclude that if a six-dimensional orthogonal tensor $\hat{\mathbf{Q}}$ satisfies the condition that 4 times $2(6 - tr\hat{\mathbf{Q}})$ squared is a small quantity compared to $(6 - tr\hat{\mathbf{Q}})$, then $\hat{\mathbf{Q}}$ has the representation

$$\hat{\mathbf{Q}} \approx \mathbf{1} + \xi\,\hat{\mathbf{W}} \qquad (C6)$$

where

$$\hat{\mathbf{W}} + \hat{\mathbf{W}} = 0, \quad tr[\hat{\mathbf{W}}\hat{\mathbf{W}}^T\} = 1. \qquad (C7)$$

Appendix D. Analysis of the data of human cancellous bone

The purpose of this appendix is to present a step-by-step summary of the numerical analysis performed on the human cancellous bone data by describing the analysis performed on one specimen. The specimen selected was the sixth specimen, a vertebral specimen. The specimen was imaged, a finite element model of the trabecular structure was constructed (van Reitbergen, 1996,1998), and, by the analysis of the response of the model to various loading situations, the matrix of elastic constants (i.e., the elasticity matrix) for that particular specimen was determined. The actual specimen is shown in Figure 1. For the sixth specimen this compliance matrix of Voigt notation is given in the original coordinate system by:

$$\mathbf{s} = \frac{1}{E_t}\begin{bmatrix} 0.141 & -0.041 & -0.035 & -0.018 & 0.027 & 0.076 \\ -0.041 & 0.219 & -0.033 & 0.05 & -0.0093 & 0.05 \\ -0.035 & -0.033 & 0.129 & 0.026 & -0.0058 & -0.013 \\ -0.018 & 0.05 & 0.026 & 0.429 & 0.113 & -0.036 \\ 0.027 & -0.0093 & -0.0058 & 0.113 & 0.309 & 0.016 \\ 0.076 & 0.05 & -0.013 & -0.036 & 0.016 & 0.408 \end{bmatrix} \qquad (D1)$$

where E_t is the tissue modulus and equal to 1 Gpa. The elasticity matrix in Voigt notation is obtained from ($D1$) by inversion, thus

$$\mathbf{c} = \mathbf{s}^{-1} = E_t \begin{bmatrix} 9.86 & 2.773 & 3.147 & -0.115 & -0.581 & -2.072 \\ 2.773 & 5.952 & 2.346 & -0.926 & 0.382 & -1.267 \\ 3.147 & 2.346 & 9.35 & -0.851 & 0.315 & -0.662 \\ -0.115 & -0.926 & -0.851 & 2.805 & -1.08 & 0.399 \\ -0.581 & 0.382 & 0.315 & -1.08 & 3.712 & -0.168 \\ -2.072 & -1.267 & -0.662 & 0.399 & -0.168 & 3.016 \end{bmatrix} . \qquad (D2)$$

The double index Voigt notation employed in these two equations does not produce a tensor and the analysis to be performed requires tensors. The elasticity matrix as a second rank tensor in six dimensions may be obtained from the matrix above by multiplying the three-by-three matrices in the upper right and lower left corners of the six-by-six matrix by $\sqrt{2}$ and the three-by-three matrix in the lower right hand corner of the six-by-six matrix by 2 (Mehrabadi and Cowin, 1990; Cowin and Mehrabadi, 1995; Cowin and Yang, 1997), thus

$$\hat{\mathbf{c}} = E_t \begin{bmatrix} 9.86 & 2.773 & 3.147 & -0.162 & -0.821 & -2.93 \\ 2.773 & 5.952 & 2.346 & -1.309 & 0.54 & -1.791 \\ 3.147 & 2.346 & 9.35 & -1.204 & 0.445 & -0.936 \\ -0.162 & -1.309 & -1.204 & 5.61 & -2.159 & 0.798 \\ -0.821 & 0.54 & 0.445 & -2.159 & 7.425 & -0.335 \\ -2.93 & -1.791 & -0.936 & 0.798 & -0.335 & 6.032 \end{bmatrix} \qquad (D3)$$

This elasticity matrix is the matrix of components of a second rank tensor in six dimensions rather than the elasticity matrix in the Voigt notation and follows the conversion rules outlined above. The elasticity matrix was sorted so that $\hat{c}_{11} > \hat{c}_{22} > \hat{c}_{33}$. This was accomplished by a sequence of coordinate transformations that permuted the axes' labels, e.g., 1->2, 2->3, 3->1, etc. For the sixth specimen the permutation was 1->1, 2->3, 3->2, thus

$$\hat{\mathbf{c}} = E_t \begin{bmatrix} 9.86 & 3.147 & 2.773 & -0.162 & -2.93 & -0.821 \\ 3.147 & 9.35 & 2.346 & -1.204 & -0.936 & 0.445 \\ 2.773 & 2.346 & 5.952 & -1.309 & -1.791 & 0.54 \\ -0.162 & -1.204 & -1.309 & 5.61 & 0.798 & -2.159 \\ -2.93 & -0.936 & -1.791 & 0.798 & 6.032 & -0.335 \\ -0.821 & 0.445 & 0.54 & -2.159 & -0.335 & 7.425 \end{bmatrix} \qquad (D4)$$

Step 1. Find the eigenvalues and eigenvectors:

Using standard contemporary mathematical analysis programs such as MathCad, the eigenvalues and eigenvectors of (A4) are calculated:

$\Lambda_1 = 15.75$, $\Lambda_2 = 6.958$, $\Lambda_3 = 3.69$, $\Lambda_4 = 4.515$, $\Lambda_5 = 3.922$, $\Lambda_6 = 9.396$,

$$\hat{N}^{(1)} = \begin{bmatrix} 0.64 \\ 0.542 \\ 0.396 \\ -0.162 \\ -0.333 \\ 0.047 \end{bmatrix}, \hat{N}^{(2)} = \begin{bmatrix} -0.278 \\ 0.773 \\ -0.117 \\ -0.11 \\ 0.5 \\ -0.223 \end{bmatrix}, \hat{N}^{(3)} = \begin{bmatrix} -0.238 \\ 0.0068 \\ 0.602 \\ 0.712 \\ -0.039 \\ 0.268 \end{bmatrix}$$

$$\hat{N}^{(4)} = \begin{bmatrix} 0.472 \\ 0.036 \\ -0.511 \\ 0.398 \\ 0.242 \\ 0.546 \end{bmatrix}, \hat{N}^{(5)} = \begin{bmatrix} 0.313 \\ -0.287 \\ 0.441 \\ -0.216 \\ 0.76 \\ 0.019 \end{bmatrix}, \hat{N}^{(6)} = \begin{bmatrix} -0.368 \\ 0.157 \\ 0.106 \\ -0.499 \\ 0.026 \\ 0.761 \end{bmatrix} \qquad (D5)$$

After this sorting operation the eigenvectors for this specimen were similar in structure to the eigenvectors calculated for other specimens. By similar we mean that each set of eigenvectors followed a similar pattern. The typical pattern was that the first three components of the first eigenvector are all positive, the second component of the second eigenvector and the third component of the third eigenvector are positive and greater in magnitude than any of the other components of that eigenvector. For the fourth, fifth and sixth eigenvectors the fourth, fifth and sixth components, respectively, are the nearest to the value 1 and the other components are quite small. In a few cases these pattern guidelines were not satisfied and some judgment was needed in the arrangement of the eigenvectors.

Step 2. Find the average eigenvectors:

The nominal average (NA) of the eigenvectors, $\hat{N}_k^{NA}$, associated with a particular eigenmode, is the sum of all 141 eigenvectors associated with that particular eigenmode divided by 141, $\hat{N}_k^{NA} \equiv \frac{1}{141}\sum_{Y=1}^{141} \hat{N}_k^{Y}$.

The results for all six eigenmodes are:

$$\hat{N}_{(1)}^{NA} = \begin{bmatrix} 0.791 \\ 0.396 \\ 0.237 \\ 0.0017 \\ 0.031 \\ 0.0067 \end{bmatrix}, \quad \hat{N}_{(2)}^{NA} = \begin{bmatrix} -0.365 \\ 0.703 \\ 0.144 \\ 0.026 \\ -0.035 \\ -0.032 \end{bmatrix}, \quad \hat{N}_{(3)}^{NA} = \begin{bmatrix} -0.137 \\ -0.238 \\ 0.759 \\ 0.011 \\ 0.033 \\ -0.0006 \end{bmatrix}$$

$$\hat{N}_{(4)}^{NA} = \begin{bmatrix} 0.0018 \\ -0.0064 \\ -0.015 \\ 0.797 \\ 0.014 \\ -0.0064 \end{bmatrix}, \quad \hat{N}_{(5)}^{NA} = \begin{bmatrix} -0.039 \\ 0.028 \\ -0.05 \\ -0.029 \\ 0.753 \\ -0.003 \end{bmatrix}, \quad \hat{N}_{(6)}^{NA} = \begin{bmatrix} -0.032 \\ 0.02 \\ 0.0048 \\ -0.026 \\ 0.0008 \\ 0.773 \end{bmatrix} \qquad (D6)$$

The nominal average $\hat{N}_k^{NA}$ of eigenvectors given above is not, in general, an orthonormal basis. To obtain the average orthonormal eigenbasis, $\hat{N}_k^{AVG}$, nearest in a least squares sense, to the eigenbases of all individual 141 specimens, Cowin and Yang (1997) (equation 16) show the nominal average must be multiplied by a tensor which is the inverse square root of the tensor or open product of $\hat{N}_k^{NA}$ with itself $\hat{N}_k^{AVG} \equiv (\sum_{q=1}^{6} \hat{N}_q^{NA} \otimes \hat{N}_q^{NA})^{-\frac{1}{2}} \hat{N}_k^{NA}$;

thus from (*D*6) the $\hat{N}_k^{AVG}$ are given by

$$\hat{N}_{(1)}^{AVG} = \begin{bmatrix} 0.867 \\ 0.417 \\ 0.269 \\ 0.0035 \\ 0.04 \\ 0.015 \end{bmatrix}, \hat{N}_{(2)}^{AVG} = \begin{bmatrix} -0.468 \\ 0.863 \\ 0.181 \\ 0.022 \\ -0.044 \\ -0.041 \end{bmatrix}, \hat{N}_{(3)}^{AVG} = \begin{bmatrix} -0.16 \\ -0.282 \\ 0.944 \\ 0.014 \\ 0.053 \\ -0.0027 \end{bmatrix},$$

$$\hat{N}_{(4)}^{AVG} = \begin{bmatrix} 0.0078 \\ -0.015 \\ -0.02 \\ 0.999 \\ 0.028 \\ 0.021 \end{bmatrix}, \hat{N}_{(5)}^{AVG} = \begin{bmatrix} -0.047 \\ 0.036 \\ -0.052 \\ -0.028 \\ 0.996 \\ -0.0042 \end{bmatrix}, \hat{N}_{(6)}^{AVG} = \begin{bmatrix} -0.033 \\ 0.029 \\ 0.0061 \\ -0.021 \\ 0.0014 \\ 0.999 \end{bmatrix}. \tag{D7}$$

Step 3. Determine the type of elastic symmetry of these bone specimens:

There are eight possible types of linear elastic material symmetry (Cowin and Mehrabadi, 1995). To find the type of elastic symmetry characteristic of these 141 specimens we compare the eight eigenbases of these symmetries with the average eigenbasis (*D*7). The result of this comparison of the eight candidate eigenbases of these symmetries given in Mehrabadi and Cowin (1990), or Cowin *et al.* (1991), showed that elastic material symmetry with the closest eigenbasis is orthotropy. In fact the eigenbasis ($D7$) is so close to that of orthotropic symmetry that any further mathematical quantification of this result is unnecessary; it would be easy and trivial to justify this result statistically. The fact is that the eigenbases for the other linear elastic symmetries are very different from ($D7$) so there is no subjectivity in this section. The eigenbasis for orthotropic symmetry has the form (Mehrabadi and Cowin, 1990);

$$\hat{N}_{(1)}^{ORTH} = \begin{bmatrix} \hat{N}_{(1)}^{1} \\ \hat{N}_{(1)}^{2} \\ \hat{N}_{(1)}^{3} \\ 0 \\ 0 \\ 0 \end{bmatrix}, \quad \hat{N}_{(2)}^{ORTH} = \begin{bmatrix} \hat{N}_{(2)}^{1} \\ \hat{N}_{(2)}^{2} \\ \hat{N}_{(2)}^{3} \\ 0 \\ 0 \\ 0 \end{bmatrix}, \quad \hat{N}_{(3)}^{ORTH} = \begin{bmatrix} \hat{N}_{(3)}^{1} \\ \hat{N}_{(3)}^{2} \\ \hat{N}_{(3)}^{3} \\ 0 \\ 0 \\ 0 \end{bmatrix},$$

$$\hat{N}_{(4)}^{ORTH} = \begin{bmatrix} 0 \\ 0 \\ 0 \\ 1 \\ 0 \\ 0 \end{bmatrix}, \quad \hat{N}_{(5)}^{ORTH} = \begin{bmatrix} 0 \\ 0 \\ 0 \\ 0 \\ 1 \\ 0 \end{bmatrix}, \quad \hat{N}_{(6)}^{ORTH} = \begin{bmatrix} 0 \\ 0 \\ 0 \\ 0 \\ 0 \\ 1 \end{bmatrix}, \qquad (D8)$$

where

$$(\hat{N}_{(m)}^{1})^2 + (\hat{N}_{(m)}^{2})^2 + (\hat{N}_{(m)}^{3})^2 = 1 \quad \text{For m = 1,2,3.}$$

Comparison of ($D7$) with (D 8) shows that, in order for the average eigenbasis (D 7) to be orthotropic, we may neglect components in ($D7$) whose values are very small to obtain the following estimate of the average ($AVGEST$):

$$\hat{N}^{AVGEST}_{(1)} = \begin{bmatrix} 0.867 \\ 0.417 \\ 0.269 \\ 0 \\ 0 \\ 0 \end{bmatrix}, \hat{N}^{AVGEST}_{(2)} = \begin{bmatrix} -0.468 \\ 0.863 \\ 0.181 \\ 0 \\ 0 \\ 0 \end{bmatrix}, \hat{N}^{AVGEST}_{(3)} = \begin{bmatrix} -0.16 \\ -0.282 \\ 0.944 \\ 0 \\ 0 \\ 0 \end{bmatrix},$$

$$\hat{N}^{AVGEST}_{(4)} = \begin{bmatrix} 0 \\ 0 \\ 0 \\ 1 \\ 0 \\ 0 \end{bmatrix}, \hat{N}^{AVGEST}_{(5)} = \begin{bmatrix} 0 \\ 0 \\ 0 \\ 0 \\ 1 \\ 0 \end{bmatrix}, \hat{N}^{AVGEST}_{(6)} = \begin{bmatrix} 0 \\ 0 \\ 0 \\ 0 \\ 0 \\ 1 \end{bmatrix}. \qquad (D9)$$

The neglect of these small terms to obtain the eigenbasis for orthotropic symmetry is justified by use of a one-sided student z test, with known standard deviation, at the 95% confidence level. This test was applied to rotational difference measures described in Cowin and Yang (1997). This result is of considerable significance because the type of elastic symmetry was not assumed *a priori*; the type of elastic symmetry was obtained by matching the eigenbasis obtained from the data to the typical form of the eigenbasis for orthotropic symmetry. This demonstrates that these 141 specimens of human cancellous bone have elastic orthotropic symmetry at the 95% confidence level.

Step 4.Transformation of the matrix of elasticity tensor components to the canonical coordinate system for orthotropic symmetry:

The matrix of elasticity tensor components ($D4$) for the sixth specimen will be transformed to the average eigenbasis $\hat{N}_k^{AVG}$ given by ($D7$) by the tensor transformation rule for a Cartesian second rank tensor, a transformation rule that employs the orthogonal transformation from the original basis used for specimen six to the basis $\hat{N}_k^{AVG}$ given by ($D6$). The tensor transformation rule is $\hat{c}' = \hat{Q}\hat{c}\hat{Q}^T$, where the orthogonal tensor $\hat{Q}$ is obtained from the open or tensor product of the bases $\hat{N}_k^{NA}$, given by (D 5) and $\hat{N}_k^{AVG}$ given by ($D7$), thus

$$\hat{Q} = \begin{bmatrix} 0.725 & 0.088 & -0.131 & 0.458 & 0.355 & -0.338 \\ 0.116 & 0.884 & 0.307 & 0.065 & -0.296 & 0.136 \\ 0.272 & -0.078 & 0.643 & -0.523 & 0.471 & 0.101 \\ -0.275 & -0.202 & 0.648 & 0.429 & -0.176 & -0.498 \\ -0.552 & 0.329 & -0.079 & 0.223 & 0.73 & 0.0006 \\ 0.083 & -0.235 & 0.219 & 0.528 & 0.031 & 0.781 \end{bmatrix} \qquad (D10)$$

and $\hat{c}'$ is given by

$$\hat{c}' = E_t \begin{bmatrix} 13.477 & 3.034 & 2.533 & -0.006 & 0.472 & 0.032 \\ 3.034 & 8.228 & 1.867 & 0.064 & 0.088 & 0.125 \\ 2.533 & 1.867 & 4.668 & 0.0041 & 0.093 & 0.058 \\ -0.006 & 0.064 & 0.0041 & 4.521 & 0.024 & -0.104 \\ 0.472 & 0.088 & 0.093 & 0.024 & 3.946 & 0.033 \\ 0.032 & 0.125 & 0.058 & -0.104 & 0.033 & 9.395 \end{bmatrix} \qquad (D11)$$

Neglecting the elements with small values in the three-by-three matrices in the upper right and lower left hand corners of the six-by-six matrix ($D11$) as well as the off-diagonal elements in the three-by-three matrix in the lower right hand corner of the six-by-six matrix ($D11$), the transformed elastic matrix in the canonical coordinate system for orthotropic symmetry is given by

$$\hat{\mathbf{c}}^{EST} = \begin{bmatrix} 13.477 & 3.034 & 2.533 & 0 & 0 & 0 \\ 3.034 & 8.228 & 1.867 & 0 & 0 & 0 \\ 2.533 & 1.867 & 4.668 & 0 & 0 & 0 \\ 0 & 0 & 0 & 4.521 & 0 & 0 \\ 0 & 0 & 0 & 0 & 3.946 & 0 \\ 0 & 0 & 0 & 0 & 0 & 9.395 \end{bmatrix} \qquad (D12)$$

This result could also have been obtained by calculating the value of the eigenvalues referred to the $\hat{N}_k^{AVGEST}$ eigenbasis and then employing the spectral representation of in terms of its eigenvalues and eigenvectors,

$\hat{\mathbf{c}}^{EST} = \sum_{k=1}^{6} \Lambda_k \hat{N}_k^{AVEST} \otimes \hat{N}_k^{AVEST}$, to obtain the result ($D12$) .

In order to evaluate the accuracy of the representation ($D12$) for ($D11$) we investigate the difference

$$\hat{\mathbf{D}} = \sum_{k=1}^{6} \Lambda_k \hat{N}_k^{AVGEST} \otimes \hat{N}_k^{AVGEST} - \sum_{k=1}^{6} \Lambda_k \hat{N}_k^{AVG} \otimes \hat{N}_k^{AVG} \qquad (D13)$$

The criterion we employ to evaluate the accuracy of the representation (*D*12) for (*D*11) is to say that (*D*12) is a good representation for (*D*11) if the largest component of $\hat{\mathbf{D}}$ divided by the largest eigenvalue of (*D*11) is small. The value of $\hat{\mathbf{D}}$ for specimen six is given by:

$$\hat{\mathbf{D}} = \begin{bmatrix} -0.02 & 0.017 & -0.0066 & 0.006 & -0.472 & -0.032 \\ 0.017 & -0.014 & 0.004 & -0.064 & -0.088 & -0.125 \\ -0.0066 & 0.004 & -0.012 & -0.0041 & -0.093 & -0.058 \\ 0.006 & -0.064 & -0.0041 & -0.0063 & -0.024 & 0.104 \\ -0.472 & -0.088 & -0.093 & -0.024 & -0.024 & -0.033 \\ -0.032 & -0.125 & -0.058 & 0.104 & -0.033 & 0.0012 \end{bmatrix} \qquad (D14)$$

The biggest number in this matrix is 0.472. If we divide this number by the largest eigenvalue, 15.75, the estimate of error is 3%. Employing the same method we found that the maximum error for all 141 specimens was 4.4% and it occurred in the data for specimen 36. The error for the data from most of the specimens was less than 3.5%. The calculation of error has presented a problem because it can be done in many different ways. For example, the estimate of maximum error for this specimen is 12.8% if we consider the error relative to the smallest eigenvalue. Thus, a statement about error only has meaning relative to the method of calculation. It appears reasonable to us to base our estimate of error on the largest eigenvalue because that number will likely be the most significant in most situations. Another method of calculating the error was employed by van Rietbergen *et al.* (1996). Using van Rietbergen's method we found that the maximum error is 47% and occurred for specimen 39, although for all but 5 of the 141 specimens, the error was less than 25%. Van Rietbergen's method employs a matrix norm which includes

Step 5. Analysis of the eigenvalue dependence upon volume fraction and the final representation:

The six compositionally dependent invariants were regressed against their volume fractions using linear log-log relationships. The results of this analysis, the dependence of the eigenvalues upon the solid volume fraction, are shown in Table III - 3. Then using the spectral representation of the matrix of elastic coefficients in terms of the eigenvalues and eigenvectors, $\hat{\mathbf{c}}^{EST} = \sum_{k=1}^{6} \Lambda_k \hat{N}_k^{A|EST} \otimes \hat{N}_k^{A|EST}$, where the eigenvalues are compositionally dependent and the eigenvectors are not, the strain-stress relations were constructed. These relations reflect the explicit dependence upon volume fraction. The squared correlation coefficients (R^2) for the orthotropic elastic coefficients are as follows: for $1/E_1$, $R^2 = 0.934$; for $1/E_2$, $R^2 = 0.917$; for $1/E_3$, $R^2 = 0.879$; for $1/(2G_{23})$, $R^2 = 0.870$; for $1/(2G_{13})$, $R^2 = 0.887$; for $1/(2G_{12})$, $R^2 = 0.876$; for $-\nu_{12}/E_1$, $R^2 = 0.740$; for $-\nu_{13}/E_1$, $R^2 = 0.841$; for $-\nu 12/E_1$, $R^2 = 0.666$.

Appendix E. Extended Voigt and Reuss Averages

The purpose of this appendix is to record the values of the matrices $\hat{\mathbf{c}}^{V,Grp}$ for the crystalline elastic symmetries. Recall that *Crp* indicates either the Cub(ic), Hex(agoanl), Tri(gonal), Tet(ragonal), Ort(hotropic), Mon(oclinic) or T(riclinic) symmetry greoup. The values of the corresponding $\hat{\mathbf{s}}^{R,Grp}$ matrices are obtained from the associated $\hat{\mathbf{c}}^{V,Grp}$ matrices by replacing the kernel letter $\mathbf{c}$ by $\mathbf{s}$ and superscript V by R (it is to e noted that the ability to do this is a distinct advantage of the present notation over that of Voigt, 1928). The formulas of $\hat{\mathbf{c}}^{V,Grp}$ for the various crystalline elastic symmetries are calculated by averaging a matrix $\hat{\mathbf{c}}^{T}$ representing the $\hat{\mathbf{c}}$ matrix for a triclinic material over the finite set of orthogonal transformations in the associated crystalline group, as indicated by (IV-9). The finite set of orthogonal transformations in each crystalline symmetry group employed in obtaining the results listed below are those given by Cowin and Mehrabadi (1995). For example, by averaging a matrix $\hat{\mathbf{c}}^{T}$ representing the $\hat{\mathbf{c}}$ matrix for a triclinic material over the group of twenty-four orthogonal transformations associated with cubic symmetry (given by Cowin and Mehrabadi, 1995) $\hat{\mathbf{c}}^{V,Cub}$ is found to be given by

$$\hat{\mathbf{c}}^{V,Cub} = \begin{bmatrix} \hat{c}_{11}^{V,Cub} & \hat{c}_{12}^{V,Cub} & \hat{c}_{12}^{V,Cub} & 0 & 0 & 0 \\ \hat{c}_{12}^{V,Cub} & \hat{c}_{11}^{V,Cub} & \hat{c}_{12}^{V,Cub} & 0 & 0 & 0 \\ \hat{c}_{12}^{V,Cub} & \hat{c}_{12}^{V,Cub} & \hat{c}_{11}^{V,Cub} & 0 & 0 & 0 \\ 0 & 0 & 0 & \hat{c}_{44}^{V,Cub} & 0 & 0 \\ 0 & 0 & 0 & 0 & \hat{c}_{44}^{V,Cub} & 0 \\ 0 & 0 & 0 & 0 & 0 & \hat{c}_{44}^{V,Cub} \end{bmatrix} \qquad (E1)$$

where

$$\hat{c}_{11}^{V,Cub} = \frac{1}{3}(\hat{c}_{11}^{T} + \hat{c}_{22}^{T} + \hat{c}_{33}^{T}) \, , \, \hat{c}_{12}^{V,Cub} = \frac{1}{3}(\hat{c}_{12}^{T} + \hat{c}_{23}^{T} + \hat{c}_{31}^{T}) \, ,$$

$$\hat{c}_{44}^{V,Cub} = \frac{1}{3}(\hat{c}_{44}^{T} + \hat{c}_{55}^{T} + \hat{c}_{66}^{T}) \, , \qquad (E2)$$

For isotropic symmetry, the result for $\hat{\mathbf{c}}^{V,Iso}$ was given by Voigt (1928) and the associated $\hat{\mathbf{s}}^{V,Iso}$ was given by Reuss (1929). The $\hat{\mathbf{c}}^{V,Iso}$ for isotropic symmetry is a special case of the result for cubic symmetry given by (E1) when $\hat{c}_{44}^{V,Cub} = \hat{c}_{11}^{V,Cub} - \hat{c}_{12}^{V,Cub}$.

In the case of tetragonal symmetry $\hat{\mathbf{c}}^{V,Tet}$ is given by

$$\hat{\mathbf{c}}^{V,Tet} = \begin{bmatrix} \frac{1}{2}(\hat{c}_{11}^{T} + \hat{c}_{22}^{T}) & \hat{c}_{12}^{T} & \frac{1}{2}(\hat{c}_{13}^{T} + \hat{c}_{23}^{T}) & 0 & 0 & 0 \\ \hat{c}_{12}^{T} & \frac{1}{2}(\hat{c}_{11}^{T} + \hat{c}_{22}^{T}) & \frac{1}{2}(\hat{c}_{13}^{T} + \hat{c}_{23}^{T}) & 0 & 0 & 0 \\ \frac{1}{2}(\hat{c}_{13}^{T} + \hat{c}_{23}^{T}) & \frac{1}{2}(\hat{c}_{13}^{T} + \hat{c}_{23}^{T}) & \hat{c}_{33}^{T} & 0 & 0 & 0 \\ 0 & 0 & 0 & \frac{1}{2}(\hat{c}_{44}^{T} + \hat{c}_{55}^{T}) & 0 & 0 \\ 0 & 0 & 0 & 0 & \frac{1}{2}(\hat{c}_{44}^{T} + \hat{c}_{55}^{T}) & 0 \\ 0 & 0 & 0 & 0 & 0 & \hat{c}_{66}^{T} \end{bmatrix} , \qquad (E3)$$

and for orthotropic symmetry $\hat{\mathbf{c}}^{V,Ort}$ is given by

$$\hat{\mathbf{c}}^{V,On}=\begin{bmatrix} c_{11}^T & c_{12}^T & c_{13}^T & 0 & 0 & 0 \\ c_{12}^T & c_{22}^T & c_{23}^T & 0 & 0 & 0 \\ c_{13}^T & c_{23}^T & c_{33}^T & 0 & 0 & 0 \\ 0 & 0 & 0 & c_{44}^T & 0 & 0 \\ 0 & 0 & 0 & 0 & c_{55}^T & 0 \\ 0 & 0 & 0 & 0 & 0 & c_{66}^T \end{bmatrix}. \qquad (E4)$$

For trigonal symmetry $\hat{\mathbf{c}}^{V,Tn}$ is given by

$$\hat{\mathbf{c}}^{V,Tn}=\begin{bmatrix} c_{11}^{Tn} & c_{12}^{Tn} & c_{13}^{Tn} & c_{14}^{Tn} & 0 & 0 \\ c_{12}^{Tn} & c_{22}^{Tn} & c_{23}^{Tn} & -c_{14}^{Tn} & 0 & 0 \\ c_{13}^{Tn} & c_{23}^{Tn} & c_{33}^{Tn} & 0 & 0 & 0 \\ c_{14}^{Tn} & -c_{14}^{Tn} & 0 & c_{44}^{Tn} & 0 & 0 \\ 0 & 0 & 0 & 0 & c_{44}^{Tn} & \sqrt{2}c_{14}^{Tn} \\ 0 & 0 & 0 & 0 & \sqrt{2}c_{14}^{Tn} & c_{11}^T - c_{12}^T \end{bmatrix}. \qquad (E5)$$

where

$$\hat{c}_{11}^{V,Tn}=\frac{1}{8}(3\hat{c}_{11}^T+2\hat{c}_{12}^T+3\hat{c}_{22}^T+2\hat{c}_{66}^T)\ ,\ \hat{c}_{12}^{V,Tn}=\frac{1}{8}(\hat{c}_{11}^T+6\hat{c}_{12}^T+\hat{c}_{22}^T-2\hat{c}_{66}^T)$$

$$\hat{c}_{13}^{V,Tn}=\frac{1}{2}(\hat{c}_{13}^T+\hat{c}_{23}^T),\ \hat{c}_{14}^{V,Tn}=\frac{1}{4}(\hat{c}_{14}^T-\hat{c}_{24}^T-\sqrt{2}\hat{c}_{56}^T),$$

$$\hat{c}_{33}^{V,Tn}=\hat{c}_{33}^T,\ \ \hat{c}_{44}^{V,Tn}=\frac{1}{2}(\hat{c}_{44}^T+\hat{c}_{55}^T). \qquad (E6)$$

The result for hexagonal symmetry may be obtained by setting $\hat{\mathbf{c}}^{V.Trn} = \hat{\mathbf{c}}^{V.Hex}$ in ($E5$) and ($E6$) and then setting $\hat{c}_{14}^{Hex} = 0$. For monoclinic symmetry $\hat{\mathbf{c}}^{V.Mon}$ is given by

$$\hat{\mathbf{c}}^{V.Mon} = \begin{bmatrix} c_{11}^T & c_{12}^T & c_{13}^T & c_{14}^T & 0 & 0 \\ c_{12}^T & c_{22}^T & c_{23}^T & c_{24}^T & 0 & 0 \\ c_{13}^T & c_{23}^T & c_{33}^T & c_{34}^T & 0 & 0 \\ c_{14}^T & c_{24}^T & c_{34}^T & c_{44}^T & 0 & 0 \\ 0 & 0 & 0 & 0 & c_{55}^T & c_{56}^T \\ 0 & 0 & 0 & 0 & c_{56}^T & c_{66}^T \end{bmatrix}. \qquad (E7)$$

Appendix F. The Weaker Coaxiality Theorem

Theorem: Given two symmetric $\mathbf{N}$ by $\mathbf{N}$ matrices $\mathbf{A}$ and $\mathbf{B}$ such that

(a) $\mathbf{x}\cdot\mathbf{A}\mathbf{x} \le \mathbf{x}\cdot\mathbf{B}\mathbf{x}$ for all vectors $\mathbf{x}$ in the $\mathbf{N}$-dimensional space and

(b) The principal axes (i.e., the orthonormalized eigenvectors) of $\mathbf{B}$ are rotated from the principal axes of $\mathbf{A}$ by a small amount given by the orthogonal transformation ($C6$) where $\mathbf{W}=-\mathbf{W}^T$, $\mathrm{tr}(\mathbf{W}\mathbf{W}^T)=1$, $\xi^2 \ll 1$, then the eigenvalues of $\mathbf{A}$ and $\mathbf{B}$, $\Lambda_\alpha^{\mathbf{A}}$ and $\Lambda_\alpha^{\mathbf{B}}$, $\alpha=1,2,\ldots,\mathbf{N}$ respectively, satisfy the inequalities

$$\Lambda_\alpha^{\mathbf{A}} \le \Lambda_\alpha^{\mathbf{B}},\ \alpha=1,2,\ \ldots,\ \mathbf{N}\ . \qquad (F1)$$

Proof: The spectral decompositions of $\mathbf{A}$ and $\mathbf{B}$,

$$\mathbf{A}=\sum_{\alpha=1}^{N}\Lambda_{\alpha}^{\mathbf{A}}(\mathbf{a}^{\alpha}\otimes\mathbf{a}^{\alpha}),\ \ \mathbf{B}=\sum_{\alpha=1}^{N}\Lambda_{\alpha}^{\mathbf{B}}(\mathbf{b}^{\alpha}\otimes\mathbf{b}^{\alpha}), \tag{F2}$$

are representation of $\mathbf{A}$ and $\mathbf{B}$ in terms of their eigenvalues, $\Lambda_\alpha{}^{\mathbf{A}}$ and $\Lambda_\alpha{}^{\mathbf{B}}$, $\alpha=1,2,\ldots,\mathbf{N}$, respectively, and their orthonormalized eigenvectors, $\mathbf{a}^\alpha$ and $\mathbf{b}^\alpha$, $\alpha=1,2,\ldots,\mathbf{N}$, respectively. Since the principal axes of $\mathbf{B}$ are rotated from the principal axes of $\mathbf{A}$ by a small amount given by the orthogonal transformation $\mathbf{Q}=\mathbf{1}+\xi\mathbf{W}$, where $\mathbf{W}=-\mathbf{W}^{T}$, $\mathrm{tr}(\mathbf{W}\mathbf{W}^{T})=1$, $\xi^2<<1$, it follows that

$$\mathbf{b}^{\alpha}=\mathbf{Q}\mathbf{a}^{\alpha}=\mathbf{a}^{\alpha}+\xi\mathbf{W}\,\mathbf{a}^{\alpha},\ \alpha=1,2,\ldots,\mathbf{N}\,. \tag{F3}$$

Substituting this representation for $\mathbf{b}^\alpha$ into the spectral representation ($F2$) for $\mathbf{B}$, it follows that

$$\mathbf{B}=\sum_{\alpha=1}^{N}\Lambda_{\alpha}^{\mathbf{B}}(\mathbf{a}^{\alpha}\otimes\mathbf{a}^{\alpha})+\xi\sum_{\alpha=1}^{N}\Lambda_{\alpha}^{\mathbf{B}}(\mathbf{a}^{\alpha}\otimes\mathbf{W}\mathbf{a}^{\alpha}+\mathbf{W}\mathbf{a}^{\alpha}\otimes\mathbf{a}^{\alpha})+$$
$$\xi^{2}\sum_{\alpha=1}^{N}\Lambda_{\alpha}^{\mathbf{B}}(\mathbf{a}^{\alpha}\otimes\mathbf{a}^{\alpha}), \tag{F4}$$

thus

$$\mathbf{x}\cdot\mathbf{B}\mathbf{x}=\sum_{\alpha=1}^{N}\Lambda_{\alpha}^{\mathbf{B}}(\mathbf{x}\cdot\mathbf{a}^{\alpha})^{2}+\xi\sum_{\alpha=1}^{N}\Lambda_{\alpha}^{\mathbf{B}}(\mathbf{x}\cdot\mathbf{a}^{\alpha})(\mathbf{x}\cdot\mathbf{W}\mathbf{a}^{\alpha})+\xi^{2}\sum_{\alpha=1}^{N}\Lambda_{\alpha}^{\mathbf{B}}(\mathbf{x}\cdot\mathbf{W}\mathbf{a}^{\alpha})^{2}. \tag{F5}$$

Employing ($F2$) and ($F4$) the inequality $\mathbf{x}\cdot\mathbf{Ax} \le \mathbf{x}\cdot\mathbf{Bx}$ (for all vectors $\mathbf{x}$ in the $\mathbf{N}$-dimensional space) may be written in the form

$$\sum_{\alpha=1}^{N} \Lambda_{\alpha}^{A}(\mathbf{x}\cdot\mathbf{a}^{\alpha})^{2} \le \sum_{\alpha=1}^{N} \Lambda_{\alpha}^{B}(\mathbf{x}\cdot\mathbf{a}^{\alpha})^{2} + \xi\sum_{\alpha=1}^{N} \Lambda_{\alpha}^{B}(\mathbf{x}\cdot\mathbf{a}^{\alpha})(\mathbf{x}\cdot\mathbf{W}\mathbf{a}^{\alpha}) + \xi^{2}\sum_{\alpha=1}^{N} \Lambda_{\alpha}^{B}(\mathbf{x}\cdot\mathbf{W}\mathbf{a}^{\alpha})^{2}. \qquad (F6)$$

Finally, since this result must hold for all $\mathbf{x}$, it must hold when $\mathbf{x} = \mathbf{a}^{\alpha}$, $\alpha=1,2,\ldots,\mathbf{N}$, and since $\mathbf{a}^{\alpha}\cdot\mathbf{a}^{\alpha}=1$, $\alpha=1,2,\ldots,\mathbf{N}$ and $\mathbf{a}^{\alpha}\cdot\mathbf{W}\,\mathbf{a}^{\alpha}=0$, $\alpha=1,2,\ldots,\mathbf{N}$ (which follows from $\mathbf{W}=-\mathbf{W}^{T}$) the inequality ($F1$) follows.

References

Balendran, B. and Nemat-Nasser, S. 1995
Bounds on the elastic moduli of composites.
J. Mech. Phys. Solids **43**, 1852-1853.

Blank, L. 1980
Statistical Procedures for Engineering, Management, and Science.
McGraw Hill, New York

Carter, D. R. and Hayes, W. C. 1977
The compressive behavior of bone as a two-phase porous structure
J. Bone Jt. Surg, 59, pp. 954-962

Cowin, S. C. 1985
The Relationship Between the Elasticity Tensor and the Fabric Tensor
Mechanics of Materials, **4**, 137-147.

Cowin, S. C. 1986
Wolff's Law of Trabecular Architecture at Remodeling Equilibrium
Biomechanical Engineering, **108**, 83-88.

Cowin, S. C. and M. M. Mehrabadi, 1987
On the Identification of Material Symmetry for Anisotropic Elastic Materials
Quart. J. Mech. Appl. Math., **40**, 451-476

Cowin, S. C. 1989
The mechanical properties of cortical bone
Bone Mechanics, CRC Press, Boca Raton, FL

Cowin, S. C.,Mehrabadi, M. M. and Sadegh, A.M. 1991
Kelvin formulation of the anisotropic Hooke's law
In *Modern Theory of Anisotropic Elasticity and Applications*
(Ed. J. J. Wu, T. C. T.Ting and D. M. Barnett), pp. 340-356, SIAM, Philadelphia, PA

Cowin, S. C. and Mehrabadi, M. M. 1992
On the structure of the linear anisotropic elastic symmetries.
J. Mech. Phys. Solids **40**, 1459-1472

Cowin, S. C. and Mehrabadi, M. M. 1995
Anisotropic symmetries of linear elasticity.
Appl. Mech. Rev. **48**, 247-285.

Cowin, S. C. and Yang, G.1997
Averaging anisotropic elastic constant data.
J. Elasticity, **46**,151-180

Currey, J. D. 1969
The relationship between the stiffness and the mineral content of bone

J. Biomechanics **2**, 477-484
Currey, J. D. 1984
The Mechanical Adaptations of Bone
Princeton University Press, Princeton
Daniel, W. W., 1978
Biostatistics: A Foundation for Analysis in the Health Sciences.
Wiley, New York
Fedorov, F. I., 1968
Theory of Elastic Waves in Crystals.
Plenum Press, New York
Fyhrie, D. P., Lang, S. M. and Kuo, R. F. 1992
The three-dimensional morphology of human vertebral cancellous bone
Trans Orthop. Res. Soc. **17**, p.112
Fyhrie, D. P., Fazzalari, N. L., Goulet, R. and Goldstein, S. A. 1993
Direct calculation of the surface-to-volume ratio for human cancellous bone
J. Biomechanics **26**, 955-967
Guitin, M. E. 1972
The linear theory of elasticity
Handbuch der Physik, pp 1-296, Berlin, Springer Verlag.
Harrigan, T. And Mann, R. W. 1984
Characterization of microstructural anisotropy in orthotropic materials using a second rank tensor.
J. Mat. Sci., **19**, 761-767
Hearmon, R. F. S., 1946
The elastic constants of anisotropic materials.
Rev. Mod. Phys. **18**, 409-415
Hearmon, R. F. S., 1948
The Elasticity of Wood and Plywood.
Forest Products Research Special Report
#9, Dept. Sci. Inds. Res., HMSO, London.
Hearmon, R. F. S., 1952
The elastic constants of piezoelectric crystals.
Brit. J. Appl. Phys. **3**, 120-123
Hearmon, R. F. S., 1956
The elastic constants of anisotropic media-II.
Phil. Mag. Suppl., **5**, 323-382.
Hearmon, R. F. S., 1961
An Introduction to Applied Anisotropic Elasticity.

Oxford University Press, Oxford.
Hill, R. 1952
The elastic behavior of crystalline aggregate.
Proc. Phys. Soc. A65, 349-354.
Hill, R. 1963
Elastic properties of reinforced solids: some theoretical principles.
J. Mech. Phys. Solids **11**, 357-372.
Hodgskinson, R. and Currey, J. D. 1990a
Effects of structural variation on Young's modulus of non-human cancellous bone,
Journal of Engineering in Medicine, Proc. Instn. Mech. Engrs., **204**, 43-52
Hodgskinson, R. and Currey, J. D. 1990a
The Effects of structural variation on Young's modulus of cancellous bone:
A comparison of human and non-human material,
Journal of Engineering in Medicine, Proc. Instn. Mech. Engrs., **204**, 115-121
Hollister, S. J. Fyhrie, D. P.,Jepsen, K. J. And Goldstein, S. A. 1991
Application of homogenization theory to the study of trabecular bone mechanics,
J. Biomechanics **24**, 825-839
Kabel, J., van Rietbergen, B., Dalstra, M., Odgaard, A., Huiskes, R. 1999a
The mechanical properties of trabecular bone can be predicted from its architecture and its effective isotropic tissue properties , submitted to *J. Biomechanics*.
Kabel, J., van Rietbergen, B., Odgaard, A., Huiskes, R. 1999b
The relation between trabecular architecture and mechanical properties of cancellous bone , submitted to *Bone*.
Katz, J. L. 1984
The Structure and Anisotropic Mechanical Properties of Bone
IEEE Transaction on Biomedical Engineering, Vol. BME-31, No. 12

Keaveny, T. M., Pinilla, T. P. Crawford, R. P., Kopperdahl, D. L. And Lou, A. 1997a
Systematic and Random Errors in the Testing of Trabecular Bone
J. Orth. Res., 15, 101-110, 1997.
Kollmann, F. F. P. and Cote, W. A. Jr. 1968
Principal of Wood Science and Technology
I Solid Wood, Springer Verlag.
Mehrabadi, M. M. and Cowin, S. C. 1990
Eigentensors of linear anisotropic elastic materials
Quart J Mech. Appl. Math. **43**, 15-41
Mehrabadi, M. M., Cowin, S. C. and Horgan, C.O., 1993
Strain energy bounds for linear anisotropic materials.

J. Elasticity **30**, 191-196
Mehrabadi, M. M. and Cowin, S. C. and Jaric, J., 1995
Six-dimensional orthogonal tensor representation of the rotation about an axies in three dimensions.
Int. J. Solids Structure **32**, 439-449.
Mirsky, L. 1990
An introduction to linear algebra
Dover, New York.
Odgaard, A.,Kabel, J., van Rietbergen, B., Dalsrea, M. and Huiskes, R. 1997
Fabric and elastic principal directions of cancellous bone are closely related
J. Biomechanics **30**, 487-495
Phillips S., Fox N., Jacob J., Wright W. 1988
The direct medical costs of osteoporosis for American women aged 45 and older
Bone 1988; 9:271-279.
Reuss, A. 1929
Berechnung der Fliegrenze von Mischkristallen auf Grund der Plastizitatsbedingung Fur Einkristalle
ZAMM, **9**, 49-58.
Rice, J. C., Cowin, S.C. and Bowman,J. A. 1988
On the dependence of the elasticity and the strength of cancellous bone on apparent density
J. Biomechanics, **22**, pp. 155-168
Rychlewski,J. 1984
On Hooke's law
Prikl Matem Mekhan **48**, 303-314
Snyder, B. D. and Hayes, W. C. 1990
Multiaxial Structure-Property Relations in Trabecular Bone
Biomechanics of Diarthrodial Joints (ed. V. C. Mow, A.Ratcliffe, S.L.Y.Woo)
pp. 31-59, Springer, New York.
Snyder, B. D. 1991
Anisotropic Structure-Property Relations for Trabecular Bone
Ph.D. Dissertation, University of Pennsylvania.
Thomson (Lord Kelvin), W. K., 1856
Elements of a mathematical theory of elasticity.
Phil. Trans. R. Soc. **166**, 481-498
Thomson (Lord Kelvin), W. K., 1878
Elasticity In: *Encyclopadia Britannica*
Adam and Charles Black, Edinburgh

Turner, C. H., Cowin, S. C., Rho, J. Y., Ashman, R.B. and Rice, J. C. 1990
The Fabric Dependence of the Orthotropic Elastic Properties of Cancellous Bone
J. Biomechanics, **23**, 549-561
van Rietbergen, B., Odgaard, A., Kabel, J. and Huiskes, R 1996
Direct mechanical assessment of elastic symmetries and properties of trabecular bone architecture.
J. Biomechanics **29**, 1653-1657.
van Rietbergen, B., Odgaard, A., Kabel, J. and Huiskes, R. 1998
Relationships between bone morphology and bone elastic properties can be Accurately quantified using high-resolution computer reconstructions
J. Orthop. Res., **16**, 23-28
Voigt, W., 1928
Lehrbuch der Kristallphysik.
Teubner, Leipzig.
Whitehouse, W. J. 1974
The quantitative morphology of anisotropic trabecular bone.
J. Microsc., **101**, 153-168.
Wu, E. M., Jerina, K. L., and Lavengood, R. E. 1973
Data Average of Anisotropic Composite Material Constants
Analysis of Test Method for High Modulus Fibers and Composites
ASTM STP 521, American Society for Testing and Materials, pp 229-252
Wolff, J. 1892
Das Gesetz der Transformation der Knochen.
Hirschwald, Berlin.
Translated as: The law of bone remodeling, Springer-Verlag, Berlin, 1986.

IMAGE EVALUATION TEST TARGET (QA-3)

150mm

6"